DOCTORAL DISSERTATION

A STUDY ON CHANNEL CAPACITY ENHANCEMENT BASED ON BEAM PATTERN WITH POLARIZATION DIVERSITY

ビームパターン及び偏波ダイバーシチによる
チャネル容量の改善に関する研究

ROHANI BINTI BAKAR

Graduate School of Engineering

YOKOHAMA NATIONAL UNIVERSITY

MARCH 2016

DOCTORAL DISSERTATION

A STUDY ON CHANNEL CAPACITY ENHANCEMENT BASED ON BEAM PATTERN WITH POLARIZATION DIVERSITY

ビームパターン及び偏波ダイバーシチによる
チャネル容量の改善に関する研究

ROHANI BINTI BAKAR

Submitted in Partial Fulfillment of the Requirements

for the degree of

Doctor of Philosophy in Engineering

March 2016

This dissertation was reviewed and approved by the following:

Hiroyuki Arai
Professor
Research Advisor
Chair of Committee

Takehiko Adachi
Professor
Review Committee Member

Toshihiko Baba
Professor
Review Committee Member

Nobuhiro Kuga
Associate Professor
Review Committee Member

Koichi Ichige
Associate Professor
Review Committee Member

ABSTARCT

There is an increasing demand in communication system today as to provide a wireless mobile data services that has the capability of empowering higher voice and data rates but at the same times managed to accommodate higher capacity users. A few years ago “stay connected” might be one of the key choices for network users to choose which wireless provider to subscribe with. The demand back then was to have and maintain an internet access anywhere anytime. But today, stay connected is more of a must than a choice because what we want is not just an access but an access with higher voice and data rates with higher capacity users in a channel. As mobile voice service is already part of our lives by most, mobile voice with data and video services are fast becoming an important and necessity part as well. Thus, backhaul capacity must be increased so that mobile broadband, data access and video services can effectively support user usage trends while keeping mobile infrastructure costs in check.

Most of the mobile data traffic is being generated indoors where the services provided are including high-performance computing and delivering real-time video and multimedia. However, indoor performance is significantly poorer compared to outdoor performance due to propagation problems such as signals distortion, attenuation and redirection by floors, ceilings, walls, and etc. Thus the advanced cellular architecture such as LTE is very suitable in designing a system for small indoor base station as it can provide satisfactory end-user experiences while the current cellular architecture won’t be able to meet the anticipated growth in mobile data traffic. However, the advance environment itself is not enough to cope with the growing demand. An antenna with channel capacity enhancement capability operating in LTE environment is one of the solutions to this challenge. A large number of low costs, small base station installed to cover a large area is expected can increase the channel capacity significantly and expend the coverage. Thus, it is almost required to

not just design an antenna, but with channel capacity enhancement especially for indoor communication system where access is expected.

Higher capacity can be achieved by improving the antenna system itself. MIMO system is a multiple antenna system entwined in LTE standard that gives significant enhancement in data rate and channel capacity. In multi antenna environment, optimizing the radiation pattern and polarization are very effective especially for enhancing the channel capacity. Thus, it is important to encompass these factors into antenna design so that we can produce an antenna with good radiation pattern and polarization that will help improving the channel capacity as a whole. Chapter 1 and 2 described in details on the technology behind the LTE and MIMO especially and the focusing is put on channel capacity specifically.

Chapter 3 discussed MIMO system performance which evaluated in the means of channel capacity where the discussion revolved around the relationship between channel capacity and spatial correlation and modeling by ray tracing method for channel response. As the main objective is to improve the capacity in a channel by utilizing the beam radiation pattern, various simulations were done in various conditions and arrangements with comparison between common pattern and beam pattern with the target that the channel capacity can be improved using beam pattern utilizing the polarization diversity. Among the results, it is proven that multi antenna system gives higher capacity than single antenna system. The correlation between each antenna in one point for both transmit and receive antenna presents an important factor in channel capacity as lower correlation provides higher channel capacity. As a summary, the channel capacity can be enhanced using multi antenna system employing beam pattern antenna with higher capacity than dipole antenna.

Chapter 4 presented a low profile directional antenna intended for small base station operating at 3.5 GHz as an antenna that can produce directional and dual polarization patterns that will enhance the capacity in a channel. This antenna was designed with an emphasis on radiation pattern where our priority was to produce a more directive pattern in both vertical and horizontal polarization plane. In this study, we utilized dipole antenna as the horizontal element and loop antenna as the vertical element with a total height of 18 mm. The antenna was fed independently where the vertical and horizontal polarization can be chose freely, which eradicated the need for complex feeding circuit such as phase shifter. The tilt angle relative to the horizontal

plane which is downward elevation angle is equals to 30° while the HPBW of the radiation characteristic is less than 80° in both vertical and horizontal polarization. The design also provided a space in the center of the structure where it can be utilized according to desirable applications.

Chapter 5 introduced smart antenna system combines with multiple antenna elements where it signal processing capability can optimized its radiation pattern automatically in response to signal environment. Switched beam antenna system forms multiple fixed beams with heightened sensitivity in particular direction. The proposed antenna has dual polarization pattern which can be switched from one to another and this capability can optimized the propagation characteristics, therefore increases the channel capacity. This antenna also was intended for small base station operation as the other design, with a bandwidth that is wide enough for LTE environment. The operating frequency was realized at 2.6 GHz with bandwidth of 100 MHz where the antenna array provides three-beams switching in both E- and H-plane, with tilted angle of ±15°. The antenna was fed through two ports simultaneously thus there was a need to design a phase shifter circuit in which the microstrip switched-line phase circuit was proposed that can provide 0, ±90° and ±180° phase difference for input phase excitation.

In the last section of Chapter 4 and 5, we presented channel capacity calculation using the beam-patterns produced by the proposed antenna respectively. The simulation environment for channel capacity calculation was similar as in Chapter 3, but the position of each transmit antenna was adjusted according to the actual configuration as described in their respective chapters. The results confirmed that directional beam pattern with polarization diversity antenna enhanced the overall channel capacity in a small base station as compared with omni direction pattern antenna. The conclusion was discussed in Chapter 6 as a closure for the research done of the study on channel capacity enhancement based on beam pattern with polarization diversity.

CONTENTS

LIST OF ABBREVIATIONS

3GPP	Third Generation Partnership Project
AMPS	Advanced Mobile Phone System
ANDSF	Automatic Network Discovery and Selection Function
BPSK	Binary Phase-Shift Keying
BS	Base Station
CA	Carrier aggregation
CDD	Cyclic Delay Diversity
CDF	Cumulative Density Function
CDMA	Code Division Multiple Access
CoMP	Coordinated Multi-Point
CQI	Channel Quality Indicator
CRE	Cell Range Expansion
C-RNTI	Cell Radio Network Temporary Identifier
CSI	Channel State Information
D2D	Device to Device
D-BLAST	Diagonal-Bell Laboratories Layered Space-Time
DOA	Direction of Arrival
EDGE	Enhanced Data GSM Environment
eICIC	Enhanced Inter-Cell Interference Coordination
E-MBMS	Enhanced-MBMS
eNodeB	Enhanced NodeB
EPC	Evolved Packet Core
EPS	Evolved Packet System
E-UTRA	Evolved UMTS Terrestrial Radio Access
E-UTRAN	Evolved UMTS Terrestrial Radio Access Network
EVDO	Evolution-Data Optimized

FDD	Frequency division duplex
feICIC	Further eICIC
FFT	Fast Fourier Transform
GERAN	GSM/EDGE Radio Access Network
GPRS	General Packet Radio Service
GSM	Global System for Mobile Communication
HetNets	Heterogeneous Network
HSPA	High Speed Packet Access
IFFT	Inverse Fast Fourier Transform
IMT-Advanced	International Mobile Telecommunication-Advanced
IP	Internet Protocol
ITU	International Telecommunication Union
LOS	Line of Sight
LTE	Long Term Evolution
MAC	Medium Access Control
MANET	Mobile Ad Hoc Networks
MBMS	Multimedia Broadcast Multicast Services
MCS	Modulation Coding Scheme
MIMO	Multiple Input Multiple Output
MISO	Multiple Input single Output
MME	Mobility Management Entity
MRC	Maximal Ratio Combining
MU-MIMO	multi user MIMO
NCT	New Carrier Type
NMT	Nordic Mobile Telephone
OFDM	Orthogonal Frequency Division Multiple Access
PARP	Peak to Average Power Ratio
PCB	Printed Circuit Board
PDCCH	Physical Downlink Control Channel
PHY	Physical
PMI	Precoding Matrix Indicator
PRB	Physical Resource Blocks
PUCCH	Physical Uplink Control Channel
PUSCH	Physical Uplink Shared Channel

QAM	Quadrature Amplitude Modulation
QoS	Quality of Service
QPSK	Quadrature Phase-Shift Keying
RAT	Radio Access Technology
RF	Radio Frequency
RI	Rank indication
RLC	Radio Link Control
RNC	Radio Network Controller
RRC	Radio Resource Control
SAE	System Architecture Evolution
SAP	Service Access Point
SC-FDMA	Single Carrier Frequency Division Multiple Access
SDMA	Spatial Division Multiple Access
SDU	Service Data Unit
SIMO	Single Input Multiple Output
SISO	Single Input Single Output
STC	Space Time Coding
SU-MIMO	single user MIMO
TACS	Total Access Communication System
TDD	Time Division Duplex
TFT	Traffic Flow Templates
UMTS	Universal Mobile Telecommunications System
UTRA	Universal Terrestrial Radio Access
UTRAN	Universal Terrestrial Radio Access Network
V-BLAST	Vertical-Bell laboratories Layered Space-Time
VoIP	Voice over Internet Protocol
WLAN	Wireless Local Area Network
WMAN	Wireless Metropolitan Area Network

LIST OF FIGURES

LIST OF TABLE

CHAPTER 1

INTRODUCTION

1.1 Overview

There is an increasing demand in communication system today as to provide a wireless mobile data services that has the capability of empowering higher voice and data rates but at the same times managed to accommodate higher capacity users. A few years ago “stay connected” might be one of the key choices for network users to choose which wireless provider to subscribe with. The demand back then was to have and maintain an internet access where ever we go. But today, stay connected is more of a must than a choice because what we want is not just an access but an access with higher voice and data rates with higher capacity users in a channel.

Overall data traffic is expected to grow tent fold from year 2014 to 2019 driven by the burst of smart devices such as smart phones and tablets which by 2019, it is expected to outgrow non-smart devices by 59 percent [1]. Figure 1.1 shows that the overall mobile data traffic is expected to grow to 24.3 Exabyte per month by 2019. As mobile voice service is already part of our lives by most, mobile voice with data and video services are fast becoming an important and necessity part as well. In 2014, the total mobile-connected devices have exceeded the world population and it is expected to continue growing. Thus, an increment in backhaul capacity is a must so that mobile broadband, data access and video services can efficaciously support user usage trends while at the same time keeping mobile infrastructure costs in check.

Figure 1.1: Mobile data traffic forecasts by 2019.

Most of the mobile data traffic is being generated indoors where the services including delivering real-time video and multimedia and high-performance computing. However, indoor performance is significantly poorer compared to outdoor performance due to propagation problems such as signals distortion, attenuation and redirection by floors, ceilings, walls, and etc. Thus the advanced cellular architecture such as Long Term Evolution (LTE) is very suitable in designing a system for small indoor base station (BS) as it can provide satisfactory end-user experiences while the current cellular architecture won't be able to meet the anticipated growth in mobile data traffic.

However, the advance environment itself is not enough to cope with the growing demand. An antenna with channel capacity enhancement capability operating in LTE environment is one of the solutions to this challenge. A large number of low costs, small BS installed to cover a large area is expected can increase the channel capacity significantly and expend the coverage. Extremely low-cost indoor BS which can be installed by users themselves not only can be used at homes, offices, halls, shopping malls but also can be implemented by operators as hotspots deployed at highly concentrated traffic, both indoor and outdoor. Thus, it is almost required to not just design an antenna, but with channel capacity enhancement especially for indoor communication system where access is certainly expected.

One of the methods to develop a higher capacity in a channel is by using Multiple Input Multiple Output (MIMO) technology as reported in a handful of studies on maximizing channel capacity [2]–[4]. However, as we are using more than one antenna in MIMO, a low profile design with miniaturization is favorable because at the same time we want to produce an antenna that is low in cost and easy to install. On the

other hands, in [5] and [6], they discussed the channel capacity enhancement by utilizing the polarization diversity technique. Presently however, there are only a small number of researches that studied miniaturization for antenna design with considering of radiation pattern for channel capacity enhancement, especially one with a small size, low profile structure utilizing directive patterns.

1.2 Long Term Evolution (LTE)

LTE was first introduced in Third Generation Partnership Project (3GPP) which was produced out of Global System of Mobile Communication (GSM) cellular standard. The LTE project was initiated in 2004 and concentrated on improving Universal Terrestrial Radio Access (UTRA) and optimizing 3GPP radio access architecture building on GSM/UMTS family standards that dates from 1990. The Stage 2 of the standard was finished in 2007 while the final stage was completed in Release 8 which was frozen in December 2008. The LTE project was developed to assure the competitiveness of Universal Mobile Telecommunications System (UMTS) for the next 10 years and beyond. The aims were to provide higher data rates, lower latency with smooth internet protocol (IP) connection between the network provider and user especially during mobility. The description in this section is mainly referred from article [7].

The LTE standard was constructed as completely new standard where it does not referred from previous series. The previous elements were adopted only if there was imperative for them to exist in the new standard. The architecture may appear similar to the previous standard as they were created by similar standards bodies however, but in reality LTE operates in different spectrum using different physical layer and different coding technique. The entire LTE systems are described by a large number of 3GPP working groups which supervised every aspect such as air interface, infrastructure network and even the protocol stack. LTE has been designed to support only packet-switched network contrary to the previous cellular system which implemented the circuit-switched network. This complete transition allowed some simplifications and optimizations of the architecture. At the physical layer (PHY), a

circuit switched model is retained where here the continuous connection is maintained especially on the downlink. At Service Access Point (SAP) however, LTE completely supports a packet switched model.

Referred as Evolved UMTS Terrestrial Radio Access (E-UTRA) or Evolved UMTS Terrestrial Radio Access Network (E-UTRAN), LTE offers a migration path for 3GPP standardized technologies that can be viewed as the true mobile broadband technology. LTE is built on fresh technical principles where it applies new multiple access schemes on the air interface with Orthogonal Frequency Division Multiple Access (OFDM) in downlink and Single Carrier Frequency Division Multiple Access (SC-FDMA) in uplink. Moreover, MIMO antenna schemes also construct an imperative part of LTE. The existing UMTS protocol concepts underwent some major changes in LTE in favor of simpler protocol architecture.

LTE standard is completely integrated into the existing cellular infrastructure for 2G and 3G which differentiates the technology from other so called 4G technologies. This integration allows complete connectivity with seamless handoff to the previous standards. At the moment, LTE can be said as the latest generation of the 3GPP standards with the Internet Protocol (IP) only network and the data rates can supports up to 150 Mbps. This fact opens up new possibilities such as new applications and services such as multimedia streaming, Voice over Internet Protocol (VoIP), video conferring or even high-speed cellular modem.

The download rates for LTE standard is up to 150 Mbps for downlink while the uplink rates is 50 Mbps over a wide area. Although theoretically the highest speed is targeted, each user's bandwidth will depends on how the carriers deploy their network and the available bandwidth. And the challenge is to design a standard that support high data rates while minimizing power. The LTE standard is constructed for full-duplex operation where it enables transmission and reception at the same time. Not only just that, it physical layer is unique for its asymmetrical modulation and data rates for uplink and downlink.

1.2.1 LTE Requirements

The cellular system in LTE support fully packet switched services with the main specifications can be outline as follows [8]:

Data Rate: The maximum data rates for downlink targeting 100 Mbps and 50 Mbps for uplink with 20 MHz spectrum allocation, assuming one transmit antenna and two receives antennas.

Throughput: The target for downlink average user throughput per MHz is 3-4 times better than 3GPP Release 6 while the target for uplink average user throughput per MHz is 2-3 times better.

Spectrum Efficiency: The downlink target is 3-4 times better than 3GPP Release 6 while the uplink target is 2-3 times better. Table 1.1 below tabulates the requirement for data rates and spectrum efficiency.

Table 1.1: Data rate and spectrum efficiency requirements defined for LTE.

Downlink (20 MHz)			Uplink (20 MHz)		
Unit	Mbps	bps/Hz	Unit	Mbps	bps/Hz
Requirement	100	5.0	Requirement	50	2.5
2 x 2 MIMO	172.8	8.6	16QAM	57.6	2.9
4 x 4 MIMO	326.4	16.3	64QAM	86.4	4.3

User plane latency: The time it takes for one-way transmit between a packet being available at the IP layer in the E-UTRAN edge node and the availability of this packet at IP layer in the E-UTRAN node shall be less than 30 ms.

Control plane latency: Transferring period from a passive connection with the network (IDLE state) to an active connection (CONNECTED state) shall be further reduced to allow fast transition times.

Bandwidth: LTE allows a subset of bandwidths of 1.4, 3, 5, 10, 15 and 20 MHz.

Interworking: The interworking between LTE and the existing UTRAN/GERAN system and non-3GPP system was assured. Multimode terminals shall support

handover to and from UTRAN/GERAN with interruption time shall be less than 300 ms and 500 ms for real time and non-real time services respectively.

Multimedia Broadcast Multicast Services (MBMS): MBMS shall be further improved and referred as Enhanced-MBMS (E-MBMS).

Costs: Ensures a reasonable cost, power consumption as well as the complexity of system and terminal. Multi-vendor equipment interoperability is allowed at all the interfaces specified.

Mobility: The system optimizes for low mobile speed within 0-15 km/h as well as higher mobile speeds including high speed train for special case.

Spectrum allocation: Operation in paired and unpaired spectrum is possible.

Co-existence: Ensures co-existence in the same geographical area and co-location with UTRAN/GERAN. It is requires also to ensure co-existence between operators in adjacent bands and cross-border co-existence.

Quality of Service (QoS): Supports end-to-end QoS and VoIP also is allowed with at least as good as UMTS circuit switched networks.

Network synchronization: Does not allowed time synchronization of different network sites.

1.2.2 LTE Architecture

The LTE is constructed primarily duplex operation in paired spectrum. It can support Time Division Duplex (TDD) operation in unpaired spectrum, although it is not a main target of the design. The downlink channel runs as continuous stream. It PHY layer operates with interspersed sync continuously where multiple channels were provided with varying modulation at the same time. The actual Service Data Unit (SDU) packets are coming from the top of the protocol stack and it has no relation between the air interfaces.

Utilizing a concept of resource block, one slot has a block of 12 subcarriers. A transport block is defined as a group of resource blocks with a typical coding or

modulating. The PHY interface which is a transport block and it carries data for the particular user allocated in a period of time. Each radio frame has a period of 10 ms with each sub frame of 1 ms long. One transport block can serve multiple users at any particular time on the downlink and what to send is controlled by Medium Access Control (MAC).

Figure 1.2 describes a high-level view of LTE architecture where it shows the unit that most closely interacts with user or mobile device. Enhanced into enhanced NodeB (eNodeB) base station as to distinguish it from UMTS base station which is NodeB, eNodeB base station has removed Radio Network Controller (RNC) and transferred the functionality to eNodeB instead and partly to core network gateway. As eNodeB can communicate directly over X2 interface, it handles the handover itself where the gateway nodes located between radio network and core network is connected to the gateway nodes by S1 interface. The gateway is divided into two entities; System Architecture Evolved (SAE) at user plane and Mobility Management Entity (MME) at control plane. SAE is responsible for user plane. On the other hand MME is the control plane entity where it responsibility range from session management signaling, location tracking of mobile device, user mobility including gateway selection to the internet when user request for IP address from the network. Both SAE and MME can be applied either on the same hardware or separated.

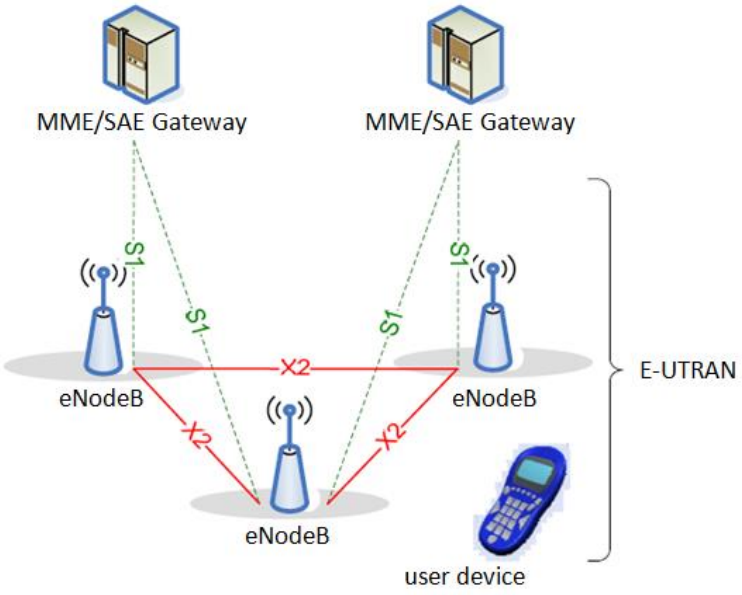

Figure 1.2: LTE architecture overview.

LTE Downlink Transmission Scheme

The download transmission scheme for LTE is referred upon conventional OFDM where the available spectrum is divided into multiple carriers named subcarriers. A low rate data stream independently modulates each of these subcarriers. Then the stream is transmitted via band subcarriers simultaneously. The subcarriers are spaced apart at fixed frequencies of 15 KHz apart which introduces orthogonality among carriers. The transmission speed of each subcarrier can be much slower than the overall data rate it is transmitted in parallel. Thus, the multipath fading can be keep to minimum and the effect delay spread as well as multipath fading itself become separate from the channel bandwidth used. The reason is because the bandwidth of each subcarrier stands the same and the only change is the number of subcarriers for different achievable overall bandwidth.

The most general modulation techniques in OFDM are binary phase-shift keying (BPSK), quadrature amplitude modulation (QAM) and quadrature phase-shift keying (QPSK). For OFDM downlink transmission, the Inverse Fast Fourier Transform (IFFT) converts the signal to time domain from frequency domain before it is modulated and amplified. The resulting signal is then transmitted through the air. At the receiver side, the signal is demodulated and amplified before is converted back by Fast Fourier Transform (FFT) into frequency domain. The data transmits in the downlink is received by several users simultaneously. This multiple access is managed by control messages which inform mobile devices, data waiting, which part of data is directed to them and which part is overlooked. On the PHY, the modulation schemes ranges from QPSK over 16QAM to 64QAM and to fulfill different reception conditions it can be quickly changed from different subcarriers.

LTE Uplink Transmission Scheme

The uplink transmission scheme for LTE uses a different transmission scheme which is SC-FDMA. It is because the OFDM inherently suffers from high peak to average power ratio (PARP) and this which regrettably drain the battery of mobile device quickly. It is highly desirable to produce mobile devices that use energy as low as possible resulting in other transmission technique for uplink instead. SC-FDMA

generally have similar scheme as OFDMA but with much lower PARP thus is chosen. Basically SC-FDMA also transmits data over the air interface using many subcarriers the additional processing steps are needed. First, a number of input bits are group together, then were passed through FFT. The output then is fed into IFFT block. Basically, many of the subcarriers are set to zero as only few will be used by mobile station. On the other hand, the signal on the receiver side is demodulated, amplified, and fed back into FFT block. The effect of additional step applied during the transmission is reserved by feeding the resulting signal into IFFT block. This process produce the time domain signal which then reconstruct the original signal bits by feeding into detector block.

1.2.3 LTE Protocol Operation

Scheduling

The PHY resource for both uplink and downlink shared channel is allocated by eNodeB. The resources are consisted of Modulation Coding Scheme (MCS) and Physical Resource Blocks (PRB) where MCS decides the bit rate, hence the capacity of PRB. LTE use semi-persistent scheduling because it reduces control channel signaling where it can avoid overhead overload. On the control channel, it will cause a lot of traffic if each downlink frame is signaled individually and then more bandwidth will be used than necessary. For both uplink and downlink, semi-persistence scheduling can be configured and an ongoing allocation can be set that maintains until it is changed.

The Physical Downlink Control Channel (PDCCH) carries Cell Radio Network Temporary Identifier (C-RNTI) which is the dynamic user identifier. First, the C-RNTI will announce that an upcoming downlink resource has been de-multiplexed by the MAC. This resource has been transmitted to higher layer and is now queued for a user. Semi-persistence scheduling periodicity is set up by RNC. Dynamic or semi-persistence scheduling is designated using different scrambling codes for C-RNTI on PDCCH. Compared to the downlink shared channel, the PDCCH is does not carry a lot of information where it is said as a very low-bandwidth channel.

The scheduling information for uplink is formed on the PDCCH too. The C-RNTI will announce that an upcoming uplink resource is queued for a user. The time when uplink slot is available and when it actually has to be sent is called delay, and this time provides user to de-queue, decides the appropriate priority and the best way to pack the transport block. The information is based on the QoS requirements of the scheduler that is functioning locally.

Quality of Service (QoS) Architecture

LTE architecture allows "hard QoS" with end-to-end QoS and the radio bearers are promised bit rate. According to applications, QoS with various levels can be applied to the LTE traffic. QoS is a natural fit because the LTE MAC is fully scheduled. The Evolved Packet System (EPS) bearers support one-to-one correspondence with Radio Link Control (RLC) radio bearers as well as support for Traffic Flow Templates (TFT).

Management and Control Functions

The user control and management in LTE is managed in the Radio Resource Control (RRC). The functions managed by the RRC are as the following:

- Process broadcast system information that gives information which provides decision to a device either to connect or not to the network.
- Incoming call paging to a device in idle mode.
- Manages RRC connection between user and eNodeB.
- Protects integrity and ciphers RRC messages.
- Control radio bearer.
- Mobility functions such as handover of active calls mode, and reselection cell of idle mode.
- Reports user management and controls the quality of the signal.
- Maintains the uplink queuing for QoS management as well as QoS requirements for other active radio bearers.

Handover and Roaming

When transferring from one BS to another, handover plays important function to provide seamless connectivity. There are two types of handover, intra-RAT and inter-RAT. The intra-RAT (Radio Access Technology) handles handover within one radio access technology for example within LTE from one eNodeB to another. On the other hand, inter-RAT handles handover between radio access technologies for example between LTE and WIMAX or 3GPP2 or even wireless LAN. Those handovers which are non-LTE are being characterized for LTE standard and involved not just higher layers but often different radio modems. However the call continuity with uplink is promised up to 100 ms of disruption and the technique used when transferring a call are such as operations in software layers above the modem stack or mobile IP.

Handover is controlled by the eNodeB and occurs in the active state. The knowledge of the network topology combines with the measurements from the user is used by eNodeB to decide the time for handover and to which eNodeB. However, re-selection of the cell is decides by the user and happens during idle state.

Power Saving Operation

Significant power uses by receiver in wireless data communication for the radio frequency (RF) transceiver, wideband signal processing, fast A/D converters, and etc. With wireless device battery maintain at the same size but LTE data rates increases by a factor of 50 over 3G, it is very important to improve the power usage at these very high data rates and wide bandwidth. The power saving comes from hardware, system architecture and protocol.

The objective of power saving mechanism employed by wireless standards is to turn off the radio as much as possible while staying connected to the network. Most of the time, radio modem can be turned off even though mobile device remains connected to the network with reduced throughput. At specific times, the receiver is turned on for updates and for full performance the device can quickly change to full mode.

1.2.4 LTE MIMO Concepts

In LTE, MIMO system forms a necessary unit in order to accomplish the requirements set for spectral efficiency and throughput. In the downlink side, a 2 x 2 MIMO configuration is considered as the base configuration. However, a 4 x 4 MIMO configuration also is predicted and included in specifications. Depending on the MIMO mode used, different gains also can be achieved.

LTE also conceives different downlink MIMO modes which can be adjusted according to channel conditions, traffic requirements and user capabilities. Table 1.2 shows the transmission modes that are possible in LTE.

Table 1.2: Transmission Modes in LTE as of 3GPP Release 8.

Transmission Mode	Description
TM1	Single Antenna Transmission (SISO)
TM2	Transmit Diversity
TM3	Open-loop spatial multiplexing, no user feedback on MIMO transmission provided
TM4	Closed-loop multiplexing, user provides feedback on MIMO transmission
TM5	Multi-user MIMO (MU-MIMO) where more than one user is assigned to the same resource block
TM6	Closed-loop precoding for rank=1
TM7	Single-layer beamforming

On the other hand, MU-MIMO can be used for the uplink transmission where signals may be transmitted on the same resource block by multiple user terminals simultaneously. This scheme is called as Spatial Division Multiple Access (SDMA) where only one transmit antenna and transmitter chain is needed at user side. This is the advantage as the user that share the same resource block will have to employ orthogonal pilot patterns mutually.

Transmit antenna selection can be used to exploit the benefit of two or more transmit antenna while at the same time still keeping the user at low cost. In this case, the user has two transmit antennas but only one transmitter chain and power amplifier. The antenna that gives the best channel to eNodeB is chosen by a switch

according to the feedback by the eNodeB. The transmit antenna selection is managed by a user.

MIMO schemes can function properly if each user reports the information to BS about mobile radio channel. This channel state information (CSI) consists of many types of reporting modes and formats which are determined depending on mode of network and operation choice. The channel quality report may consist of channel quality indicator (CQI), rank indication (RI) and precoding matrix indicator (PMI). CQI will indicate the quality of downlink mobile channel that the user experienced. RI shows the number of transmission layers that are useful when spatial multiplexing is used while PMI will tell the optimum precoding matrix for a given radio condition to be used in the base station. Radio network will configure the reporting process which can be periodic or aperiodic. CQI request contained in the uplink scheduling triggers aperiodic reporting where user will send report on physical uplink shared channel (PUSCH). In case of periodic reporting, physical uplink control channel (PUCCH) is used in case no PUSCH is available.

1.3 Long Term Evolution-Advanced (LTE-Advanced)

This section discuss the enhancement of LTE system which mainly referred from article [8]. After LTE standardization reached a mature state where the only changes in specifications reduced to corrections and fixing bugs, the 3GPP teams worked on improving the LTE according to International Mobile Telecommunication-Advanced (IMT-Advanced) requirement which capabilities go beyond IMT 2000. In order to support advanced services and applications, data rate requirement of 100 Mbps and 1 Gbps with low mobility scenarios must be realized. In September 2009 the 3GPP Partners made a formal submission to the International Telecommunication Union (ITU) proposing that LTE Release 10 and beyond (LTE-Advanced) should be evaluated as a candidate for IMT-Advanced. The evaluation process was successfully completed in October 2010 and acknowledged as 4G technology.

As the name suggested, LTE-Advanced is an evolution of LTE. Although the essential target is to address the anticipated increase in data rates, LTE-Advanced incorporates various enhancements including the aggregation of carriers and advanced antenna techniques. However, the most important benefit comes from optimizing HetNets where the performance in small cells is largely improved. For example, LTE-Advanced introduced Range Expansion where the overall network capacity is increased much more than just adding small cells can gives. The new interference management technique provides a possibility of adding more small cells without reducing the overall network performance. Figure 1.3 shows the overview of the enhanced LTE-Advanced components.

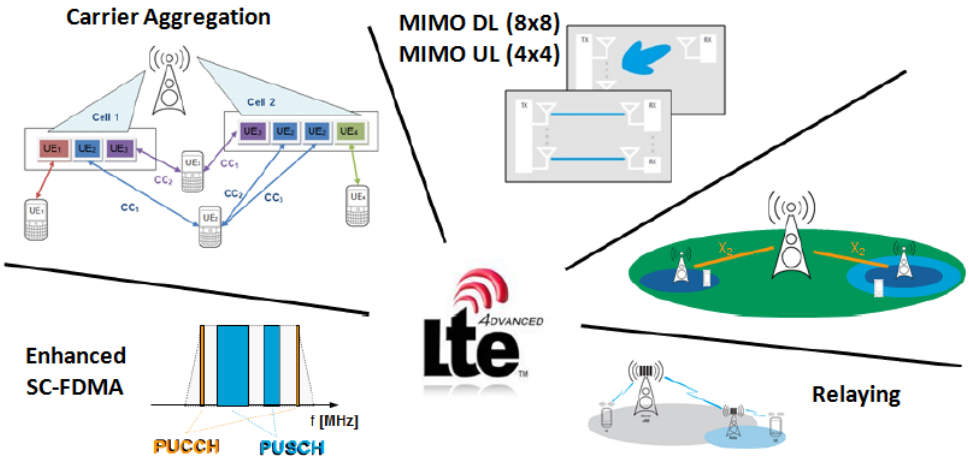

Figure 1.3: Overview of the main LTE-Advanced components.

1.3.1 LTE-Advanced Requirements

In general, LTE-Advanced needs to enhance the capacity in the channel to meet the aim targeted in IMT-Advanced by increasing the download and upload maximum data rated and spectral efficiency. The other specifications can be outlined as follows:

Data Rate: Maximum target data rate for downlink is 1 Gbps and for uplink is 500 Mbps.

Cell Edge User Throughput: Throughput for the system should be as high as possible. It is defined as 5% of the cumulative density function (CDF) of the user

throughput, normalized with the overall cell bandwidth. Table 1.3: shows the requirement for the cell edge performance.

Table 1.3: Targets for cell edge user throughput.

	Antenna configuration	Target [bps/Hz/cell/user]
Uplink	1 x 2 / 2 x 4	0.04 / 0.07
Downlink	2 x 2 / 4 x 2 / 4 x 4	0.07 / 0.09 / 0.12

Spectrum Efficiency: The downlink (8 x 8 mode) maximum spectrum efficiency supports 30 bps/Hz and uplink (4 x 4 mode) supports 15 bps/Hz. Moreover, Table 1.4 tabulates average spectrum efficiency targeted for the system. It is describes as the aggregate throughput of all users (the number of correctly received bits over a certain period of time) normalized by the overall cell bandwidth divided by the numbers of cells.

Table 1.4: Targets for average spectrum efficiency.

	Antenna configuration	Target [bps/Hz/cell]
Uplink	1 x 2 / 2 x 4	1.2 / 2.0
Downlink	2 x 2 / 4 x 2 / 4 x 4	2.4 / 2.6 / 3.7

User Plane Latency: User plane latency for LTE-Advanced is reduced less than in LTE Release 8.

Control Plane Latency: The target for transition time from idle mode with IP address allocated to connected mode should be less than 50 ms including the establishment of user plane. The target for the transition from a dormant state to connected mode should be less than 10 ms.

Mobility: LTE-Advanced allows mobility across the cellular network depending on the frequency band for various mobile speeds uplink, up to 350 km/h or even 500 km/h. The system performance shall be improved from 0 to 10 km/h compared to LTE Release 8.

Spectrum Flexibility: The allocated bands in LTE Release 8 plus additional bands give the initial frequency bands for the system as follows;

- 450 – 470 MHz band
- 698 – 862 MHz band

- 790 – 862 MHz band
- 2.3 – 2.4 GHz band
- 3.4 – 4.2 GHz band, and
- 4.4 – 4.99 GHz band

Spectrum allocations for LTE-Advanced operate in different sizes with wider allocations compared to LTE Release 8. The target is to provide bandwidth solutions wider than 20 MHz on consecutive spectrum. The complexity of user devise however should be considered during spectrum aggregation. The system also supports Time Division Duplex (TDD) and Frequency Division Duplex (FDD) for both existing paired and unpaired frequency bands.

VoIP Capacity: For all antenna configuration VoIP capacity is improved compared to LTE Release 8.

Other than above, LTE-Advanced targets also as follows:

- Assume 8 x 8 MIMO in downlink and 4 x 4 MIMO in uplink.
- Carrier aggregation (CA)
- MIMO enhancement
- Heterogeneous network enhancement
- Coordinated Multi-Point (CoMP)
- eNodeB Relays

1.3.2 LTE-Advanced Technology Components

User Categories for LTE-Advanced

New user categories are added into LTE Release 10 where these categories describe the device capabilities to certain extend. For example categories 6 and 7 support MIMO 2 x 2 and/or 4 x 4 with maximum data rates up to 300 Mbps. The highest category, 8 supports 8 x 8 MIMO with maximum data rate of 3 Gbps, if the maximum of five component carriers are aggregated. However, these categories are only just an indication of the user device capabilities where it serves as upper bound for achievable data rates.

Band Aggregation

High data rates can be achieve by aggregating the multiple LTE carrier. Two or more component carriers where each with a maximum of 110 resources blocks are aggregated in order to support wider transmission bandwidth uplink to 100 MHz. The initial maximum bandwidth of 40 MHz or even less will be used, where an operator network will allow diverse spectrum allocation that is more flexible due to the band aggregation feature. For an individual operator, spectrum fractions always occur in an existing band allocation for various frequency bands. Therefore the capability to aggregate frequency band is equally important as achieving higher data rate.

Frequency deployments of existing technology for the different regions in the whole world are different. Thus a large number of solution forms to move the existing technologies to LTE/LTE-Advanced. There was interest in large number of different band combinations that leads to a few carrier frequency scenarios. It was agreed then to work on these limited scenario first before adding another scenario. Frequency band are added to 3GPP specification whenever identified because the support for frequency bands is generally release independently. However, a user supporting frequency band in higher release may support frequency band of previous release.

Enhanced MIMO Technology

LTE-Advanced expends the MIMO capabilities to now supporting 8 downlink and 4 uplink layers. Downlink scheme for LTE-Advanced is extended from LTE while the uplink scheme for LTE-Advanced is upgraded to be as same as downlink scheme in LTE. Moreover, in addition to spatial multiplexing scheme, transmit diversity also is possible for both downlink and uplink.

LTE-Advanced also introduce the 3D MIMO concept where the beam can be adjusted in both horizontal and vertical dimensions. Previously, the eNodeB transmitter can only adjust the beam in horizontal dimension only with the down-tilt in vertical dimension was fixed for each user. The horizontal adjustment will allows the beam to be directed upward to floors in a building or perhaps over small cell to reduce interference.

New Carrier Type (NCT)

The other name for NCT is “lean carrier” where the new version will reduced the overhead of control channel and reference signal as well as energy consumption. Even though there is no data being transmitted, the current cell references signals are always on that induced interference.

LTE-Wi-Fi Integration

In a situation where both 3GPP and non-3GPP networks are available, users will need to choose which is the best network to use. Thus, a new function called Automatic Network Discovery and Selection Function (ANDSF) is introduced where it provides information to user on selecting the network.

Device to Device (D2D)

Rather than sending data through eNodeB, D2D function allows users to communicate using LTE spectrum directly. While the users are still under eNodeB control with the signaling sent to eNodeB, the EPC must be improved to support this function. One of the important functions of D2D is for public safety after a disaster where user to user communication may be required when the network is unavailable. D2D also can be applied for new social networking applications and services with proximity based where the exchange of data is possible because the device are closed to each other.

Enhanced Inter-Cell Interference Coordination (eICIC)

In a pure macro cell network, a user connected with its respective serving cell suffers at the cell edge interference from a neighboring cell. Additional users also create interferences on the uplink that cannot be eliminated although suitable transmission power is selected. The old solutions method use in LTE; interference coordination, interference cancellation on the receiver and randomization in the physical layer bit stream are no longer sufficient. Thus, LTE-Advanced introduced a new interference

coordination method named Heterogeneous Network (HetNets) to deal with interference problem.

HetNets are built up by macro cell (inter site distance ~ 1 km) to ensure coverage, and by small cell which is referred to micro cell (inter site distance ~ 200 m), pico cells (inter site distance ~ 100 m) and femto cells (home eNodeB) and relay station to highlight the shadowed regions or to increase the data rate in hot spots. Figure 1.4 shows an example of the cells layout of the HetNets. The same frequency is used by all cells which induce more severe interference problem as compared to single layer arrangements.

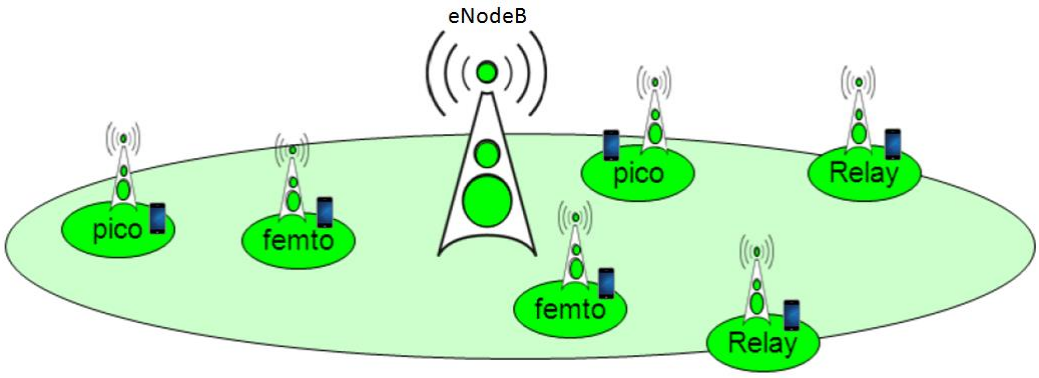

Figure 1.4: Example cells layout of Heterogeneous Network (HetNets).

eICIC uses time domain, frequency and power to alleviate the intra-frequency interference that overlap in HetNets. And the most challenging issue in the implementation of HetNets is the interference induced by sharing the carrier with the overlaid macro cells when the networks have limited spectrum for LTE deployment. The benefits of HetNets can be listed as following:

- Offload users and traffic from the macro home eNodeB
- Increase capacity at traffic hot spots
- Improved coverage and performance at cell edges
- Fill coverage holes
- Provide coverage when real estate constrains do not allow macro

The development of eICIC then is continued rapidly with under the new Further eICIC (feICIC) which includes the following development:

- Interference cancellation receiver in the terminal
- Ensures the weak cells can detected
- Ensure that remaining interference is removed
- Interference cancellation is done at both user and network side.

Cell Range Expansion (CRE)

CRE techniques is designed to address the issue when high power transmission from macro cells severely shrinks small cells coverage, resulting in underutilization of low-power nodes. Thus the small cells become unable to capture a number of traffic near the macro cells because of the limited power transmission. CRE is achieved through the use of user specific setting where the cell association bias is set in idle mode and the modification of handover parameters is set in active mode. CRE will bias the handoff boundaries in favor of small cells, inducing more users to be connected by the closest cells.

Coordinate Multipoint (CoMP)

Aside from bandwidth aggregation, CoMP also capable of boasting the data rates in LTE-Advanced to a new threshold. During handover, the signal coming from other eNodeB can interferes with the user from that particular eNodeB especially when the user is moving at high speed. During this time, the interference is very strong and the data rate will becomes very slow. CoMP will coordinate the transmission from multiple eNodeB to a single user to reduce interference and improve the performance at cell edge where the interference is very severe. CoMP can be considered a distributed MIMO system where eNodeB uses multiple antennas and cooperates to transmit to and/or receive from users. Both downlink and uplink can apply the CoMP technique.

Relaying

Relaying technique also is introduced to improve the coverage as well as the capacity. User will communicate with a relay node and relay node will communicates with a donor eNodeB. The donor eNodeB may serve one or several relay node and also communicate with non-relay user directly, creating its own cell. It transmits its own cell ID, reference signals and synchronization. However on user side, it communicates with relay node without realizing of the donor eNodeB. Figure 1.5 shows the Type 1 relay which is defined in Release 10.

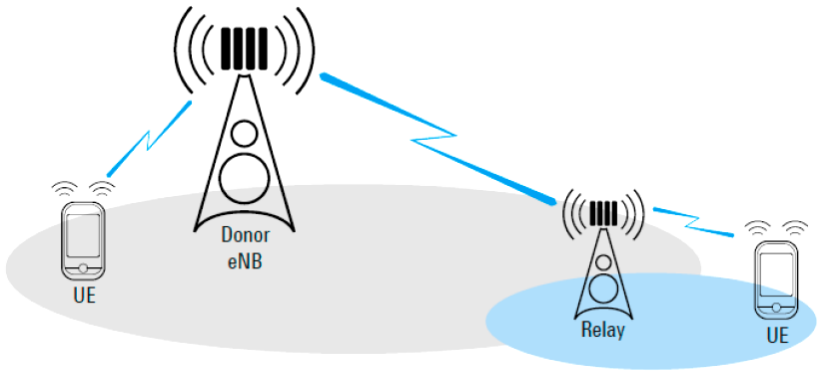

Figure 1.5: Type 1 relay as defined in Release 10.

1.4 5G and Beyond

The era of mobile communication network can be defined as generation starting from first generation (1G), second generation (2G), third generation (3G) and now is the era of fourth generation (4G). The revolution of the generation becomes more faster as of the late because of a surge of increase of user in wireless mobile. Each generation defines their own technologies with their own threshold speed, composing of many technologies, services as well as applications. Starting from 1G with Advanced Mobile Phone System (AMPS), Nordic Mobile Telephone (NMT) and Total Access Communication System (TACS), 2G gave GSM, General Packet Radio Service (GPRS), Enhanced Data GSM Environment (EDGE) and Code Division Multiple Access (CDMA) 2000 while 3G introduced UMTS, Code Division Multiple Access (CDMA), Evolution-

Data Optimized (EVDO) and High Speed Packet Access (HSPA). For 4G however, the technology has becomes closely entwined with the generation itself where LTE as the technology is considered as 4G. 4G networks are combined with one core network and a number of radio access networks. This integration which combines multiple radio access interfaces into a single core network produces a seamless roaming/handoff with a very high performance [9], [10].

The fifth generation, 5G is expected to be ready by year 2020 [9]. However, no specific technology is defined yet for 5G at current time. There is no firm 5G standard that has been agreed on as yet, and there may have multiple standards operating under 5G names. The expectation for 5G is that it will have access to different wireless technologies where it is supposed to combine the different flows from different technologies especially the current one. It includes all type of advanced features that interconnecting the world without limit.

As each generation defines higher speed, the 5G obviously is expected to go beyond 4G limits with data rates for downlink 1Gbps and higher. Some reckons that 5G will go 100 times faster than 4G with 1000 times in capacity although the official limit has not been announced yet. However, looking at this estimation means that there will be more capacity for users and the network does not need to throttle the access to their network. Other expectation is the reduced latency as the speed becomes faster. Also, 5G is expected to be able to reach the area where the current network incapable to. This is because it is expected that multiple antenna will be deployed, allowing signals to multiple directions.

A few key objectives that can be expected from 5G are superior QoS and user experience, reliable connectivity experience and ability to handle upsetting growth in network capacity. The increasing in user expectation of mobile applications and services grows an increase of usage and complexity in traffic that needs to be managed intelligently. High-quality service becomes a focus where a superior QoS will be induced to improve the user experience. As the connection becomes more complicated with many cells involve, a more reliable connectivity during handover will be needed to ensure a continuous connectivity experienced by user without dropping the data rates. As many techniques used and become more complicated, the server workload, network bandwidth demand, storage capacity and power cost will increase as well. Demanding more capacity is not an immediate solution instead but

optimizing capacity in a new direction may bring a logical solution to these growing demands.

5G will bring not only unbelievably fast broadband speeds but also enough capacity for users to perform the growing applications without dropping the data rates. As the user demand to be connected anytime anywhere, 5G should provide uninterrupted access to communication, information as well as entertainment that will open up a new world for user to experience.

1.5 Scope and Objectives

1.5.1 Scope

The study of channel capacity as well as antenna design in this research was done assuming LTE environment, the fourth generation (4G) of mobile communication. The study also included the study of MIMO concentrating on 4 x 4 MIMO as MIMO system implemented in LTE technology. The frequency resonance for all the experiments done in this study revolved around LTE frequency which is 2.6 GHz and 3.5 GHz while all the antenna design have dual polarization elements with the tilted radiation patterns. The study targets the hardware part which is antenna applied to multi antenna system and the discussions focused on small indoor base station which simply represented by small room. In other words, this dissertation focuses on indoor base station and describes the multi antenna technology that uses radiation pattern wisely to improve the capacity performance in a channel.

1.5.2 Objectives

There are 2 objectives in this study. The first one is to study the channel capacity in general view which implements the ideal condition of the base station as well as the radiation pattern. The channel capacity is studied with comparison between dipole

antenna pattern and beam pattern with the target to improve the channel capacity in the room by using the beam patterns with polarization diversity. The second objective is to design an antenna that can produce a tilted beam pattern and at the same time is capable of dual polarization. Generally, the objective of this dissertation is to show multi-antenna technology utilizing radiation pattern wisely than can improve the channel capacity in a small base station.

1.6 Dissertation Structure

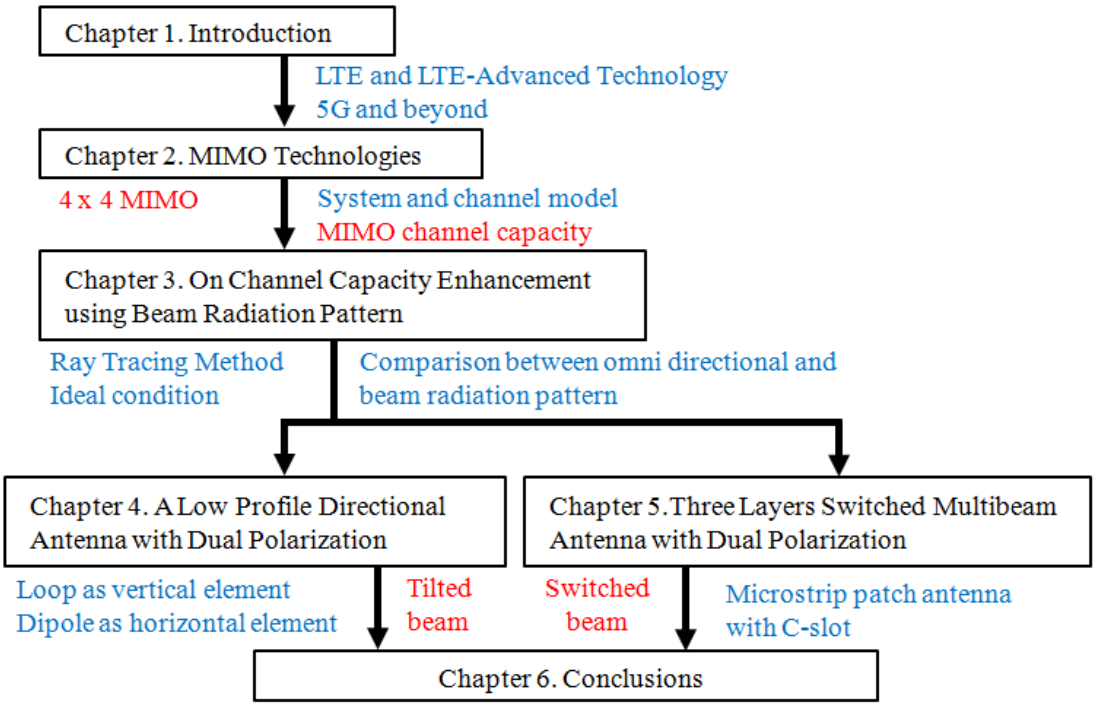

Figure 1.6: Organization of the dissertation.

Figure 1.6 illustrates the structure of the dissertation starting with Chapter 1 discussing the LTE technology namely the 4G technology which includes the LTE requirements, architecture, operation protocol and the most important is MIMO system implemented in LTE technology. The discussion is further revolving around LTE-Advance and 5G technology and beyond. Chapter 2 presents the overview of MIMO system that focusing on channel model for multiple antenna system that

includes the explanation about spatial diversity and spatial multiplexing, CSI and beamforming. The channel capacity for MIMO system also is discussed with regard the capacity in fading channel. Finally a few application of MIMO system also is presented.

In Chapter 3, MIMO system performance is evaluated in the means of channel capacity where the discussion revolve around the relationship between channel capacity and spatial correlation and modeling by ray tracing method for channel response. As the main objective is to improve the capacity in a channel by utilizing the beam radiation pattern, various simulations were done in various conditions and arrangements with comparison between dipole antenna pattern and beam pattern with the target that the channel capacity can be improved using beam pattern utilizing the polarization diversity. The discussion about channel capacity is further continued with Chapter 4 and Chapter 5 as these 2 chapters describe the antenna design capable of producing the tilted beams and dual polarization.

Chapter 4 describes a low profile directional antenna with dual polarization that can produce titled beam with dual polarization which introduces loop antenna as vertical polarization element and dipole antenna as horizontal polarization element. A reflector and director were added to the element array with the purpose to shape and direct the radiation pattern in a certain angle. In the later chapter, the antenna design was improved by replacing the dipole with printed dipole to improve the antenna characteristic. As the continuation from Chapter 3, the channel capacity calculation using radiation pattern obtained from this antenna configuration also is included in discussion.

Chapter 5 describes another antenna structure named three layers switched multi beam antenna with dual polarization where it produces switched tilted beam patterns with dual polarization. The discussion started with basic microstrip patch antenna and their parameter analysis, and further enhanced to two layers and with slot. The proposed antenna design that consists of dual-polarized orthogonal square patch array is discussed as well as the feeding circuit for the antenna structure which is microstrip switched-line phase shifter. As with Chapter 4, the channel capacity calculation using radiation pattern obtained from this antenna configuration also is included in discussion.

Finally, the conclusion of the study for every chapter is presented in Chapter 6.

CHAPTER 2

MIMO TECHNOLOGIES

2.1 Overview

In every generation of wireless mobile communication system, the main target is always to provide higher data rate as well as higher capacity in the channel. The expectation is increasing year after year leading to various advance techniques introduced for higher quality user experience. Aside from conventional methods, for example introducing higher modulation technique or providing larger bandwidth, higher data rate and capacity also can be achieve by improving the antenna system itself. MIMO is multiple antenna system entwined in LTE standard that gives significant enhancement in data rate and channel capacity. This chapter considers the introduction to basic MIMO concepts, the principle as well as the implementation in LTE [11], [12].

2.1.1 Definition

MIMO technology was formally introduced in the IEEE 802.11n protocol that brings wireless local area network (WLAN) technology into the multiple antennas era [13]. Akin to the name suggested, multiple antennas are used at both the transmit end and the receive end for transmitting and receiving signals. Even in a rich-scattering

propagation that usually degrades the quality of the signal, MIMO technology reduces error codes that will improve the data rate and channel capacity.

2.1.2 Purpose and Motivation

Fundamentally, only one antenna is used at both transmit and receive end in the traditional WLAN system where the signals are transmitted using the 802.11 a/b/g protocol. The maximum data rate is 54 Mbps and it is difficult to be increased anymore. However, with the increasing demand on wireless mobile services and applications, the speed of wireless transmission needs to be enhanced extensively. MIMO system is introduced as one of the solution in increasing the data rate for signal transmission and it accomplished the growing requirements on both bandwidth and signal quality.

The motivation for designing MIMO technology is to address issues arising in conventional wireless system especially the capacity constrain in the networks, the quality of the signals and the coverage area where the signals can reach. MIMO mainly exploits the space dimension which in turn improves the wireless system capacity, range and reliability. When it was first introduced, MIMO-OFDM system has set the corner stone of the future wireless broadband system.

2.1.3 History

The history of MIMO technology is very long dating back to 1908 where it was first used by Marconi[1] to reduce fading [13]. However, MIMO technology was finally recommended in communication system only in 1970s. In 1990s, scientists in the Bell Laboratories [2] set the foundation for MIMO application in wireless mobile communication system. In 1995, MIMO capacity was analyzed by Telatar [14] in a fading environment and in 1996, a new MIMO processing algorithm called Diagonal-Bell Laboratories Layered Space-Time (D-BLAST) is proposed by Foschini [15]. In

[1] Guglielmo Marconi (1874-1937)
[2] AT&T Bell Laboratories, founded by Alexander Graham Bell in 1925

1998, Tarokh et al. [16] analyzed space-time codes for high data rate while Wolniansky et al. [17] established a MIMO experimental system using Vertical-Bell laboratories Layered Space-Time (V-BLAST). The preceding work of MIMO technology continue to evolve as the system offers a wide range of capability that can still be explored as shown throughout the history.

2.2 MIMO Systems and Channel Model

2.2.1 Conventional Antenna System

In conventional antenna system, one antenna is used each at the transmitting and receiving end. In MIMO, this mode is called Single Input Single Output (SISO) and illustrated in Figure 2.1 below.

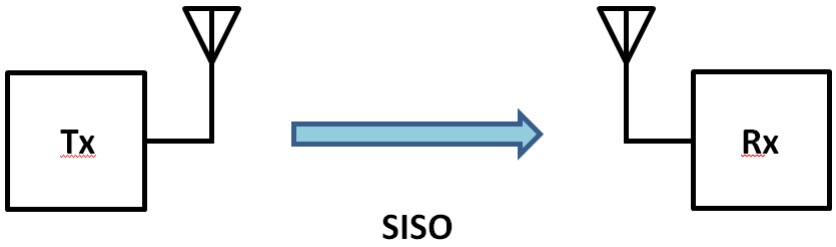

Figure 2.1: SISO antenna configuration.

Channel capacity in communication systems is defined by the famous Shannon[3]-Hartley[4] theorem that states; the maximum capacity (transmission bit rate) that can be achieved over a given channel bandwidth in the present of noise. Shannon proposed a formula to calculate channel capacity in SISO mode as follow;

$$C = B \log\left(1 + \frac{S}{N}\right)^2 \quad (2\text{-}1)$$

[3] Clause Elwood Shannon (1916-2001)
[4] Ralph Vinton Lyon Hartley (1888-1970)

where B stands for bandwidth, and S/N stands for signal-to-noise ratio [18]. As stated in the theorem, the formula calculates the maximum rate for the reliable communication in a channel with the existence of noise.

2.2.2 Multiple Antenna System

A MIMO system technically consists of ***m*** transmit and ***n*** receive antenna. All the antennas are considered independent of each other when the positions of the antennas are far away from each other. Similarly, multiple independent channels are then produced at transmit and receive end. Thus, each stream of the ***m*** x ***n*** data streams also independent of each other and this will increase the system capacity as the number of antenna increase. MIMO wireless channel can be describe as in Figure 2.2 below.

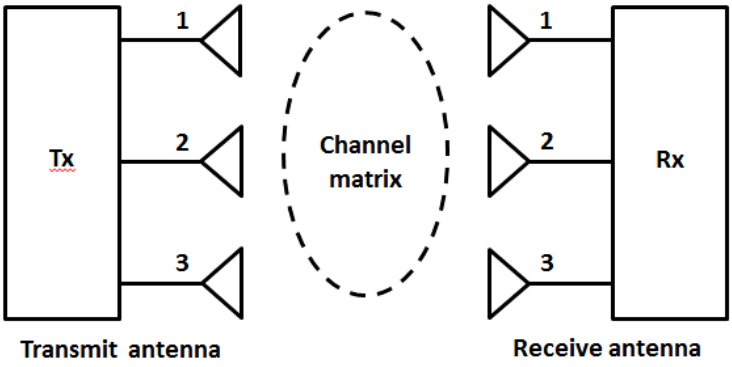

Figure 2.2: MIMO wireless channel.

Every antenna will receive not only the direct stream intended for it, but also indirect stream intended for other antennas the same channel is used. Assuming a time-independent, narrowband channel, the direct connection from antenna 1 to 1 is stated as h_{11}, h_{22} etc., while the indirect connection from antenna 1 to 2 is stated as cross component h_{21}, h_{12}, etc. Based on this formula the transmission matrix, H with the dimension of ***m*** x ***n*** is obtained as follow;

$$H = \begin{bmatrix} h_{11} & h_{12} & h_{..} & h_{1m} \\ h_{21} & h_{22} & h_{..} & h_{2m} \\ h_{...} & h_{...} & h_{...} & h_{.m} \\ h_{n1} & h_{n2} & h_{n.} & h_{nm} \end{bmatrix}$$

Based on this formula, the transmission vector can be written as;

$$y = Hx + n \tag{2-2}$$

where **y** is the receive vector, **x** is the transmit vector and **n** is the noise. A number of independent streams will be transmitted with the maximums stream are depending on the number of receive antenna, **n**. For example, for 4 x 4 MIMO mode, up to 4 streams will be transmitted while for asymmetrical mode as 3 x 2 MIMO, the maximum number of streams that can be transmitted is two or fewer. In theory, under the ideal condition, the capacity increases linearly with the number of streams ***n***. And if the number of antennas is not limited, MIMO system might be able to provide an infinite capacity in channel. Figure 2.3 below shows the comparison for channel capacity between different MIMO modes calculated using equation 2-1 against SNR.

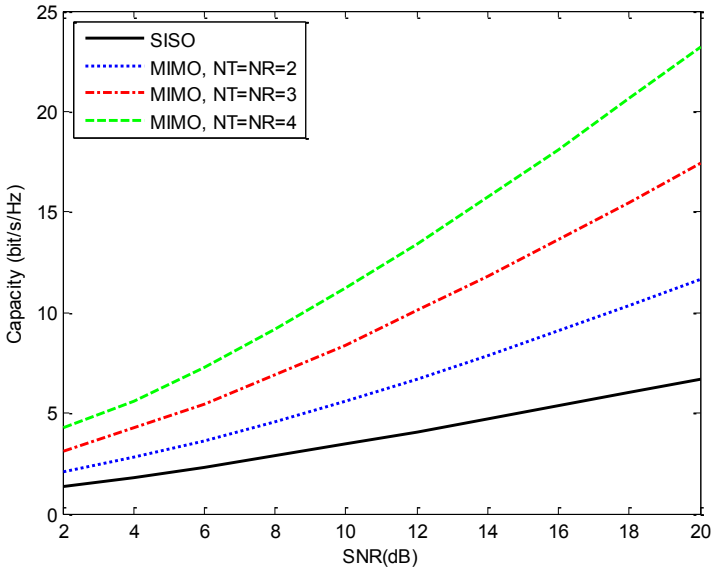

Figure 2.3: Comparison of channel capacity between different Tx and Rx antenna.

General operation for MIMO system started with a stream of input symbols that are encoded by a space-time encoding function into M_T x 1 discrete-time complex

baseband stream x[n]. The x[n] stream then is converted by pulse shaping filter into M_T x 1 continuous-time complex baseband stream x(t) and then the baseband signal is modulated with transmission carrier. After modulation, the stream is divided into **n** sub stream, and simultaneously transmitted through **m** antennas. The parallel sub streams are transmitted to the receiver from different paths because the transmission is scattered in wireless channels. The transmission channel H superposes the transmitted signal due to the distortion of the environment and are received by **n** receiving antenna. As synchronous sampling is assumed, the receive signal y(t) with additive noise is down converted to baseband and sampled to produce a discrete-time signal sequence. The estimated symbols are finally decoded by the space time coding decoding block which restores the original data stream. Figure 2.4 demonstrates the general operation for MIMO system as was explained. Sub streams are all transmitted at the same time using the same bandwidth without the need of extra bandwidth although the number of stream increases. Therefore, the total transmit power is also maintained providing the best power allocation in the system.

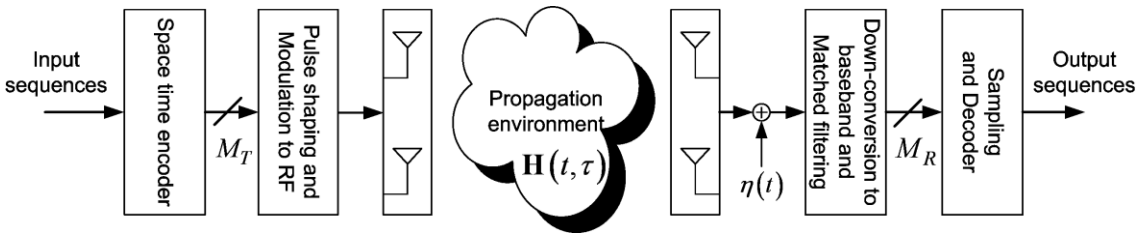

Figure 2.4: General operation for MIMO system.

There are few types of MIMO transmission that has been introduced [11], [19]. One of them is single user MIMO (SU-MIMO). Only one user is served in SU-MIMO transmission on a given time on a given time-frequency resource within a cell. If the out-of-cell interference is assumed as additional Gaussian noise, the channel model is reduced to point-to-point MIMO channel instead. Figure 2.5 describes SU-MIMO configuration where all the streams go to single user using multiple antenna.

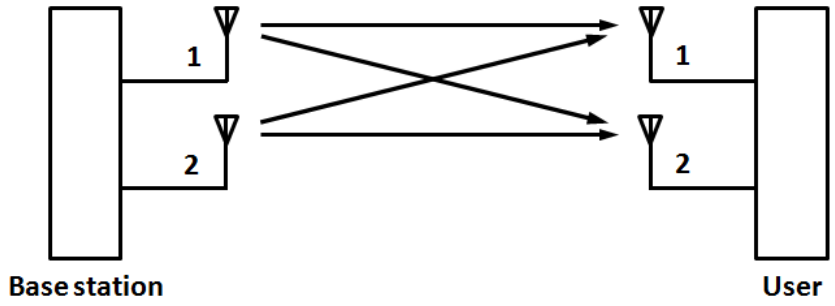

Figure 2.5: SU-MIMO configuration.

Opposite of SU-MIMO is multi user MIMO (MU-MIMO) whereas the name suggested, multiple users are served in parallels over a given time-frequency resources but by using spatial multiplexing instead. Figure 2.6 demonstrates MU-MIMO configuration. In MU-MIMO, the multiplexing gain proportions with the number of transmit antennas unlike in SU-MIMO whereas multiplexing gain is narrowed by the minimum number of transmit and receive antennas, provided that there are enough users in the cell. However, it is asymptotically optimal for single stream transmission per user even though multiple streams per user are possible, as shown in [20]. Boccardi in [21] also prove that only one stream is activated per selected user mostly for finite number of users. MU-MIMO is especially useful in the uplink because the complexity on the user side can be kept at a minimum by using only one transit antenna.

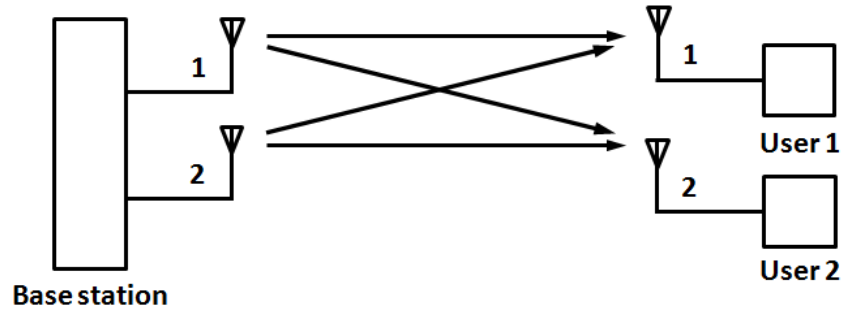

Figure 2.6: MU-MIMO configuration.

Another transmission that is employed in MIMO is cyclic delay diversity (CDD) where in this mode, streams are transmitted by the individual transmit antennas but with a time delay. When a signal is transmitted from multiple antennas and the channel is relatively flat, unwanted signal cancellation might occur. CDD is added to

the signal being transmitted to reduce the impact of possible cancellation of the signal. The delay, which depends on different bandwidth and conditions, is about a few microseconds which will introduce frequency dependent phase shift thus CDD will increase the frequency selectivity at the receiver.

2.2.3 Spatial Diversity and Spatial Multiplexing

The environment in wireless communication propagation path is actually very belligerent and hostile. The signal transmitted over a wireless communication link is vulnerable and exposed to propagation path problems such as fading, co-channel interference, scattering effects in time and frequency, path loss effect and many more. Thus, it is a challenge to design a system that will survive in this environment and maintain the original information in the signal. Moreover, the limited availability of the bandwidth also presents a significant challenge because it is important to design a system with higher spectral efficiency and higher quality of the signal but at a low cost.

MIMO implement techniques that can improve the spectral efficiency and offers high quality channel as compared to traditional communication system [22]. For example, spatial multiplexing techniques offer an increasing in data rates while fading can be alleviated by applying transmit and receive diversity [16], [23]. Coverage area also can be improve by employing coherent combining techniques which gives array gain and increases the signal to noise ration of the system. The description in this section is mainly referred from [11] and [13].

MIMO generally can be classified with respect to antenna configuration as discussed before which reflect the number of transit and receive antenna. There are four categories as listed below;

- SISO – Single Input Single Output system – 1 Tx, 1 Rx
- SIMO – Single Input Multiple Output system – 1 Tx, N_R Rx
- MISO – Multiple Input single Output system – M_T Tx, 1 Rx
- MIMO – Multiple Input Multiple Output – M_T Tx, N_R Rx

Apart from antenna configurations, MIMO also can be categorized with respect to how data is transmitted across the given channel. As there are multiple antennas in a

system, there will be multiple different propagation paths in the environment too. Depending on the output target of the system, there are two types of technique that is being implemented in MIMO which are spatial diversity and spatial multiplexing. Diversity technique is implemented to improve the reliability of the system where it is possible to send same data over different propagation paths thus provides the diversity gain. Spatial multiplexing is implemented to improve the data rate of the system where it is possible to place different portions of the data on different propagation paths thus provides degrees of freedom or multiplexing gain.

Spatial diversity or space diversity one of the wireless diversity schemes where it uses two or more antenna to improve the quality and reliability of a wireless link. In the environment where the multipath situation can deteriorate the receive signal, spatial diversity especially effective at mitigating these multipath situations. If one signal becomes severely deteriorate, another signal might have sufficient signal to recover the original signal. MIMO system provides two types of spatial diversity for wireless channels transmit diversity and receive diversity. The purpose of the spatial diversity implemented in the system is to make the transmission more robust although the data rate is maintained.

In diversity technique, the same information is transmitted across the independent fading channels as to encounter the fading problem. As a result, the amount of fading experienced by each copy of data will be different ensuring that at least one of the copies suffers less fading compared to the other copies. Hence, the chance of the original data information is properly received will increase and the reliability of the entire system will improved as well. The technique also significantly reduces the co-channel interference.

Transmit Diversity

In transmit diversity, the system uses more transmit antennas than receive antennas, $m>n$. The simplest form of transmit diversity which is known as MISO for multiple input single output consist of two transmit antennas and one receive antenna as shown in Figure 2.7. In this configuration, the same data is transmitted via two antennas using different path. The redundant signals are generated using space time

coding (STC) where it integrates the characteristics of modulating, coding and diversity.

STC achieves SDMA by combining matrix and coding technologies which can improve the capability of the system to avoid signal attenuation and thus increase the channel capacity. High quality data transmission at high rate for both transmit and receive diversity is achieved by STC. Unlike non-STC coding system, the STC system offers other benefits such as anti-noise capabilities, improving anti-interference and high coding gain while ensuring bandwidth. The fact that the antenna and redundancy coding is moved from mobile user to the base station also provide benefit because these technologies are less in cost and much simpler to implement.

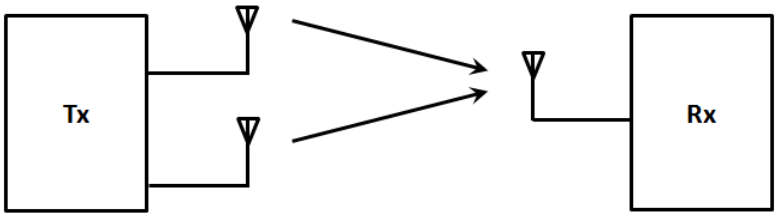

Figure 2.7: MISO antenna configuration.

Receive Diversity

In receive diversity, the system uses more receive antennas instead, $m<n$. The simplest configuration which consist of two receive antennas and one transmit antenna is called single input multiple output (SIMO) as shown in Figure 2.8. SIMO is really easy to implement as it requires no special coding technique. Basically the receiver end only needs two antennas for receiving two independent loss signals transmitted. Since two different transmission paths are used, the receiver sees the incoming signal as two differently faded signals with low SNR value. However, using methods such as maximal ratio combining (MRC) and diversity selection, the SNR of the received signals can be increased. In diversity selection, the strongest signal transmitted from the two antennas will be selected because it contains higher SNR while MRC will combine two signals and produces a stronger signal instead. The received signals are weighted with respect to their SNR value and the summed.

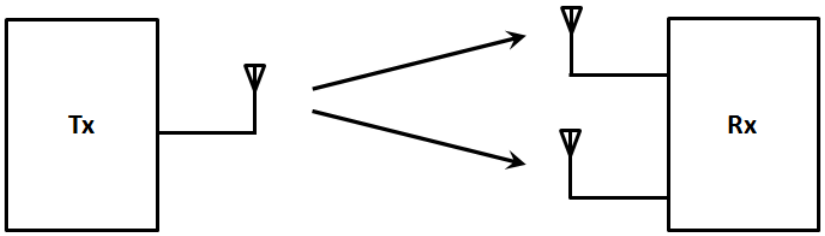

Figure 2.8: SIMO antenna configuration.

As diversity technique aims to improve the reliability of the transmission channel, spatial multiplexing technique is implemented to increase the data rate instead. The data is split into separate streams where these streams then are transmitted via separate antenna independently. The technique is similar to OFDM technique where different frequencies of the sub-channels carry different sections of the modulated date. In spatial multiplexing however, several independent sub-channels are formed in the same allocated bandwidth in the scattering by the environment is rich enough. The multiplexing gain is also described as degrees of freedom where it number is equal to minimum number or transmit antenna or receive antenna. The degree of freedom in MIMO arrangement controls the total capacity of the system.

Figure 2.9 presents the difference between spatial diversity technique and spatial multiplexing technique, assuming 3 x 1 MISO configurations. In the transmit diversity technique, three different transmit antenna is used to transmit the same information across different independent spatial channels. The diversity gain here is 3 while the multiplexing gain is 0. On the other hand, spatial multiplexing technique multiplexed each bit of the data stream on three different spatial channels, resulting in the increment in data rate. Contrary to before, the multiplexing gain here is 3 while the diversity gain is 0 instead.

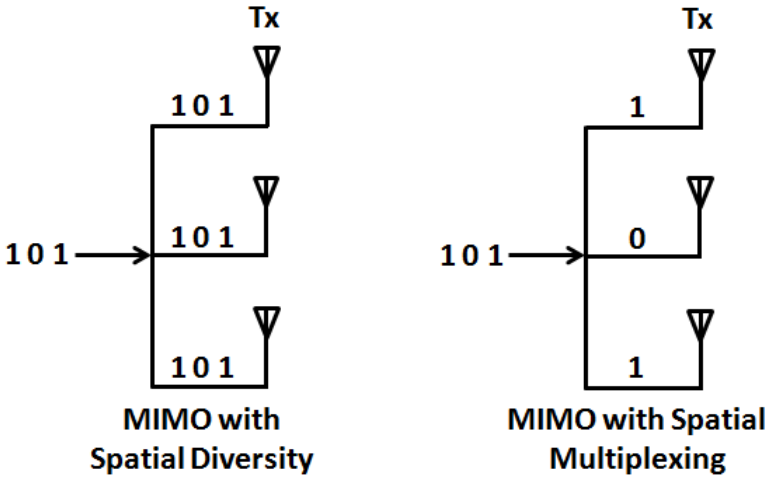

Figure 2.9: Comparison between spatial diversity technique and spatial multiplexing technique.

2.2.4 Channel State Information (CSI) and Condition Number

Although various techniques are implemented in MIMO, in reality the effectiveness of transmitting multiple streams of data over multiple antennas depends on the actual geometry of the antenna systems. Transmission of independent data streams over multiple antennas depends on the correlation factor which measures the influence of the spatially separated signals over each other. One way to eliminate the mutual influence of spatially separated signals is by using orthogonally polarized antennas that sufficiently separate the signals in spatial dimension [24].

The transmission matrix, also called CSI determines the suitability of MIMO techniques and influences the capacity to a great extent. CSI indicates the known channel properties for a communication link. The information in CSI defines the way a signal travels from transmitter to receiver and portrays the mixed effect of propagation effect such as fading, scattering and power decay with distance. The CSI allows the transmission to adapt to current channel conditions, which is very critical to get a high data rate, reliable communication in multiple antenna system. Estimation of CSI needs to be done at the receiver and this estimation is usually quantized and sent back to the transmitter. Hence, it is possible to have different CSI for the transmitter and receiver [25].

In SISO channel, the CSI is constant and does not change from bit to bit. Thus, the knowledge of CSI in SISO channel is often not needed as it is characterized by steady state of SNR. In the case of rapid fading channels, the CSI varies rapidly and MIMO is employed to break the channel variations into spatially separated sub channels. Thus, the knowledge of CSI at both transmit and receive end will open uplink the possibility of incorporating this information in intelligent system design.

A typical CSI matrix is formed in by transmitting a symbol from each Tx antenna and its response from Rx antenna are recorded. For example for 3 x 3 MIMO configurations, if Tx_1 sent voltage value '1', the Rx antenna might pick up the voltage values as shown in figure. Simultaneously, the process I repeated for Tx_2 and Tx_3 and the response from all Rx might be as shown in Figure 2.10. From that result it can be said that the transmission through Tx_2 is not effective as the voltage values recorded for it is very low. Thereby, the Rx may feedback that CSI matrix to the Tx and the Tx may decide not to transmit signal from Tx_2 and this will save power for the system. If Tx transmits data blindly and Rx just constructs the CSI matrix, the method is called open loop transmission and generally is not very effective. If Rx feedback the CSI matrix to Tx, the method is called closed loop diversity scheme and this opens up the possibility for intelligent communication. Figure 2.10 shows the real value of CSI matrix which describes both the amplitude and phase variation of the channel.

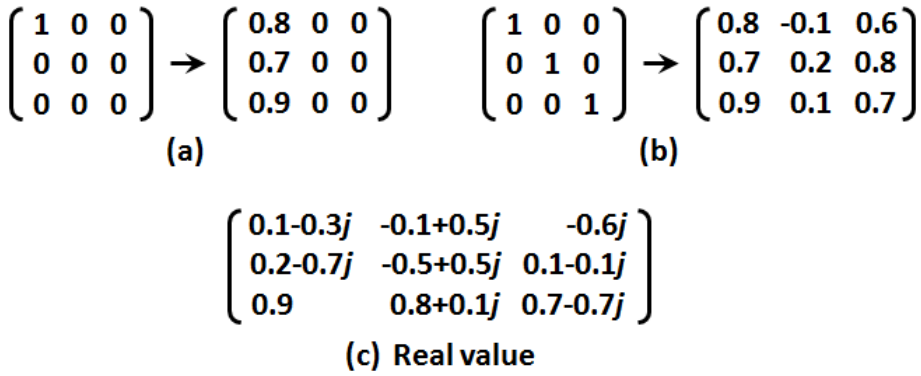

Figure 2.10: Example of CSI matrix by 3 x 3 MIMO configuration.

As multiple antennas are used in MIMO configuration for both transmitter and receiver, each receiver receives not only the direct signal intended for it, but also receives a fraction of signal from other streams. The direct path from Tx_1 to Rx_1 is

expressed as channel response h_{11} while the channel response of the path forms between Tx_1 and Rx_2 is h_{21} and so on. The channel matrix dimension will be N x M. The response of the MIMO channel is expressed as a set of linear equations. As example for 2 x 2 MIMO configurations, the received vector derived from equation 2.2 is expressed as

$$\begin{bmatrix} y_1 \\ y_2 \end{bmatrix} = \begin{bmatrix} h_{11} & h_{12} \\ h_{21} & h_{22} \end{bmatrix} \begin{bmatrix} x_1 \\ x_2 \end{bmatrix} + \begin{bmatrix} n_1 \\ n_2 \end{bmatrix}$$
$$y_1 = h_{11}x_1 + h_{12}x_2 + n_1$$
$$y_2 = h_{21}x_1 + h_{22}x_2 + n_2$$

The receiver has to solve this set of equation to find out what was transmitted (x). The stability of the solution depends on the condition number of the transmission H (CSI).

A small change in input can cause a drastic difference in solution where in MIMO system, the variations to solution can be affected by the noise term. The solution should be robust against variation in the noise at least to certain extent. The sensitivity of the solution to small changes in the input data is measured by condition number of the transmission matrix, H. It indicates the stability of the solution (x) to small change in incoming data (y).

At the receiver, the received data is known and is often corrupted by noise. From the system linear equation y=Hx+n, the received vector that is corrupted by noise **n** can be wrote as $\bar{y}$=y-n=Hx. Also, as the channel transmission matrix H is usually estimated approximately, the solution for x is obtained as $x=H^{-1}\bar{y}$ where the solution may or may not exist and may or may not be unique. If a symmetric transmission matrix N x N is considered, and if the input $\bar{y}$ is arbitrary, a unique solution is possible only if the matrix H is non-singular. The condition number of a non-singular matrix is given as $k(\mathrm{H}) = \|H\|\|H^{-1}\|$ where ||H|| denotes the matrix norm. The condition number measures the relative sensitivity of the solutions to the changes in the changes in the input data ($\bar{y}$). The changes to the solution can be expressed as

$$\frac{\|\Delta x\|}{\|x+\Delta x\|} \leq k(H)\frac{\|\Delta\bar{y}\|}{\|\bar{y}\|} \qquad (2\text{-}3)$$

where Δx represents the change in the solution, $\Delta\bar{y}$ represent a change in the observed or received samples and k(H) denotes the condition number of the transmission matrix.

In other words, a small change in the input data gets multiplied by the condition number and produces changes in the output or solution. This indicates that a high condition numbers is not desirable and is regarded as ill-condition matrix. It will behave similarly as a singular matrix where it will not render any solution or will give infinite non-unique solutions. Therefore in MIMO transmission, the ability to transmit multiple data across a MIMO channel relies on the ability of the receiver to solve the systems of linear equations in an unambiguous and stable way. Thus the condition number of the transmission matrix affects the suitability of spatial multiplexing in MIMO channel. A well-conditioned matrix which is a low condition number of matrix allows reliable transmission of spatially multiplexed signal, whereas an ill-conditioned matrix makes it difficult to do so. Additionally, the rank of the transmission matrix which is rank (H) indicates how many data streams can be multiplexed spatially on a MIMO channel. Thus, the rank and the condition number of the transmission matrix present a crucial part in a MIMO system design.

2.2.5 Beamforming

As one of the main targets for MIMO technology is to increase the channel capacity in the wireless network, various forms of technology that capable of improving the capacity can be considered to be implemented into the system. For many years antenna technology has been used to improve the system performance in increasing the network capacity [11], [26]. Signal levels can be improved and interference can be reduced by implementing directive antenna. Directive antenna started from sectorized antennas where a cell site is split into sector of 60° and 120° and operated as one cell. The capacity in GSM can be tripled by 120° antennas [11], [26].

Adaptive antenna arrays use narrow beams to intensify spatial multiplexing. Belong to adaptive antenna arrays, smart antenna has a smart, different direction of arrival (DOA) estimation. It can construct a user-specific beam where the complexity of the array system can be reduced by optional feedback. Smart antenna is divided into two groups;

- Phased array systems: Also called switched beamforming where it has a number of pre-defined patterns than can be switched. The required beam will be switched according to the required direction.
- Adaptive array systems: Also called adaptive beamforming with infinite number of patterns that can fixed in real time according to the requirements.

Beamforming is the method used to construct a radiation pattern of an antenna array that have a certain direction and capable to perform a required performance or conditions. It can be applied not just in MIMO technology but in all antennas arrays systems as well. MIMO beamforming using phased array systems have to first determine the DOA of the incoming signal before switching to the most appropriate beam. Unfortunately however, it is not guaranteed that the fixed beam is able to match exactly to the direction as intended. Adaptive array systems can direct the beam in the exact direction as required while at the same time move the beam in real time. This procedure particularly gave advantage for moving systems as with mobile telecommunications.

2.3 MIMO Channel Capacity

The use of multiple antennas at both sides of the transmission channel can tremendously increase channel capacities provided that the propagation medium is rich scattering and at the same time increase the quality of the transmission. It was first being proved by Bell Labs works at the end of 1990s [12], [15], [27]–[30]. Increased capacity is obtained by spatial multiplexing while increased quality is obtained by diversity technique without any need for either extra bandwidth or extra transmission power. The discussion in this section is mainly referred from [12].

2.3.1 Capacity of a Fading Channel

The capacity, C in a time-varying channel is a random variable where the instantaneous value lies upon the channel realization. In this situation, the Shannon

capacity of the channel can be zero in value. There are two types of channel capacity that mostly defined which are ergodic capacity and outage capacity. Ergodic capacity is defined as the statistical average of mutual information where the expectation is taken over H. It is the expected value of C which is appropriate for fast varying channels. On the other hand, the outage capacity is defined as the information rate below which the instantaneous mutual information falls below a prescribed value of probability express as percentage. Usually, it is used when the packet-based transmission system is considered and the channel is properly described by block-fading model. However, a channel outage may occur if the pre-assumed channel capacity is larger than the instantaneous capacity.

In the following discussion, general assumptions are made which are mostly valid for indoor applications [31], [32]. In communication channel, it is essential to assume the effect of transmit and receive antennas as well as the propagation medium. The effect of the antenna patterns is neglected and the far field which is dominant reflectors is assumed to be sufficiently far from transmit and receive antenna. One simple case that is considered is a non-selective frequency flat fading channel where this is valid for narrow-band communications. Represents to other equivalent baseband, a complex circularly-symmetric random variable with normalized power characterizes each sub-channel. The whole MIMO channel is defined by a channel matrix H that has a dimension m x n. While Pt assumes the total transmit power at each sample time.

CSI known to Rx but unknown to Tx

This is the classic case that is usually considered as reference. The channel is assumed to be known and can be perfectly estimated at the receiver but unknown to the transmitter. Since the transmitter does not know the channel, the available power is distributed uniformly between the transmit antennas and this is considered the optimal way of power allocation. The total average SNR at the receiver array can be expressed as $\rho_T = P_T/\sigma_n^2$ where σ_n^2 is the variance of the addictive white Gaussian complex noise. The definition of MIMO channel capacity in units of bps/Hz is;

$$C = \log_2 det\left[I + \frac{\rho_T}{T_x} HH^T\right] \quad (2\text{-}4)$$

where $\boldsymbol{I}$ is the identity matrix. If we consider the singular value decomposition of H, the above equation can also be written as;

$$H = U_H \Lambda_H V_H^T \tag{2-5}$$

where $.^T$ denotes complex conjugate transpose, U_H and V_H are defined as unitary matrices with dimension (N x N) and (M x M) respectively, and Λ_H is an (N x M) matrix that has singular values of H. If $M = min\{M, N\}$ and $\lambda_{H,i}, i = 1, \cdots\cdots, M$, the new definition of MIMO capacity is;

$$C = \log_2 det\left[I_N + \frac{\rho_T}{M}\Lambda_H \Lambda_H^T\right] = \sum_{i=1}^{M} \log_2\left(1 + \frac{\rho_T}{M}\lambda_{H,i}^2\right) \tag{2-6}$$

CSI known to both Tx and Rx

When the channel varies slowly in time, it is practically possible to feed backed the estimated CSI to the transmitter. When the communication occurs in a duplex mode, the CSI is feed backed via feedback channel or the reverse link assuming a perfect CSI with no delay to the transmitter. Thus, the transmitter can achieve maximum capacity by allocating the available power in an optical manner to the antennas [33]. It is often named either as water-filling capacity or known-CSI capacity. In this case, the transmitted symbol vector x should be weighted by the matrix V_H, and the received signal vector is weighted by the matrix U_H^T. This procedure is called as an optimal beam forming solution giving the equivalent channel H_{eq} between x and y as,

$$H_{EQ} = U_H^T H V_H = \Lambda_H \tag{2-7}$$

Expressly, the MIMO channel matrix H is break downed into a few parallel independent SISO sub-channels. The amount of these sub-channels is equivalent to the rank H, with the gain defines as singular values of H. If Rx is the autocorrelation matrix of x and the $\lambda_{x,i}$ for i =1, ⋯ , M, the optimum water-filling solution that includes the distribution of the available power P_T, over the equivalent parallel sub-channels is defined as [34], [35];

$$\lambda_{X,i} = \left(\psi - \frac{\sigma_n^2}{\lambda_{H,i}^2}\right)^+, i = 1, \cdots, M \tag{2-8}$$

where $(S)^+=S$ if $S > 0$, and otherwise. ψ as a constant and is driven to answer the constrain on the total transmit power, $\sum_{I=1}^{M} \lambda_{X,I} = P_T$. The water-filling solution inflict that more power is allocated to the best sub-channels and less or perhaps no power to the worse ones. Thus, the water-filling capacity C_{WF} becomes [34], [35];

$$C_{WF} = \sum_{i=1}^{M} \log_2 \left(1 + \frac{\lambda_{X,i}\lambda_{H,i}^2}{\sigma_n^2}\right) \quad (2\text{-}9)$$

CSI unknown to both Tx and Rx

For the channel that is not known to both Tx and Rx, equation 2-4 can be considered as upper bound of the capacity and Δ is the coherence interval of the channel in units of channel-uses. In general, Δ value is approaching ∞, thus the channel capacity approaches this upper bound. This is happened because it is possible to track the channel variations if Δ is greater [36]. The difference between the capacity and the upper bound is less for higher SNR values because of the same reason. For larger transmit and receive antenna however, the difference gets more considerable [36]. In the fast varying channel, there is no way to estimate the channel at the receive end providing a far less capacity than the receive antenna perfect-knowledge upper bound. The capacity of MIMO channel for $M > \Delta$ does not increase even by increasing M [36]. For a rich-scattering propagation medium, the MIMO unknown CSI capacity increases linearly with $M^*(1 - \frac{M^*}{\Delta})$, where $M^* = \min\left\{M_T, M_R, \left\lfloor\frac{\Delta}{2}\right\rfloor\right\}$ at high SNR value as describes in [37].

2.4 MIMO Applications

This section will discusses in general various application implementing MIMO system and the benefits that MIMO provide to those systems [12].

One of the MIMO obvious applications is in 4G systems of more specifically LTE as discussed in Chapter 1 as LTE deployed MIMO technology directly into their systems. Aside from that, MIMO also is applied in Radio Frequency Identification

(RFID) systems where MIMO RFID backscattering channel displays a special type of cascaded structure as compared to cascaded channels that being studied such as double scattering fading or keyhole fading [38]. MIMO in RFID can increase reading reliability using space diversity, increase reading range and reading throughput and while providing channel information for free at the reader.

MIMO also enable Digital Home where it provides the coverage for the whole house with reliability and speed for multimedia streaming applications. MIMO system can connect many devices starting from phone lines, music and store devices, broadband connection and including broadband connections, computer networking devices and cabled video device. MIMO is designed as interoperable system which can influence the installed based 802.11 wireless that is already deployed such as computers, PDAs, handheld gaming devices, camera, VoIP phones and etc. MIMO technology also can be used in non-wireless communications systems such as home networking, which defines power line communications system that uses MIMO technique to transmit multiple signals over multiple AC wires.

2.4.1 MIMO in Wireless LAN

Higher performances can be achieved in data transmission by employing MIMO systems as shown in [11]–[13], [34], [36]. For example, the network bandwidth, reliability and range are enhanced by signaling technique implemented in MIMO systems. Among the communication systems that is taking advantages of channel capacity enhancement are WLAN and Wireless Metropolitan Area Network (WMAN). The IEEE 802.11 WLAN and IEEE 802.16 WMAN standards are based on OFDM. Bandwidth requirement is reduced because OFDM is a multi-carrier modulation system, while maintaining orthogonal modulated signals so that it will not interfere with each other. These systems have the advantage of principally deploying in indoor environments and suburban environments that has a rich multipath environment.

Other motivations in MIMO-OFDM system for improvement in performance and transmission rate are when the CSI is available at the transmitter. The distribution of the total transmit power over transmit antennas can be optimized using water-filling technique. Using this technique, the information symbols and power is allocated

optimally over frequency and space in MIMO-OFDM communication. The number of antennas employed in a router can be any number where typically MIMO router has three or four antennas. These systems induce a revolution for the next broadband system focusing on home networking that covering many products such as HDTV, Video-on-Demand, next-generation game consoles and other new products. A more sophisticated home entertainment can be created, applying high level of QoS to promote multimedia connectivity.

Antenna polarization is defined as “adaptive polarization”. The intelligence behind this process is the router has the capability to focus the polarization signals and the router gets feedback from client adapter. In multipath environment, the signals suffer multipath effect such as bounce off of walls, ceilings and any other obstacle. As the result, the original signal arrives by different paths and polarizations at the receiving ends. However, these reflections can improve the SNR instead if adaptive antenna polarization algorithms are employed because more than one original signal is sent. As a benefit, a reliable signal is provided by this adaptive transmitting feature provides at extreme ranges. Other benefit also includes dead spots elimination, which providing a reliable, high speed whole home coverage for application in the future.

MIMO networking is capable in enhancing data rate in communication system by 10 to 20 times more than current systems. The systems can increase the spectral efficiency using multipath reflections to construct parallel channels in the same frequency bandwidth.

2.4.2 MIMO in Cooperative Sensor Network

Figure 2.11 shows a sensor network that consists of self-contained circuit with its sensor and RF interface. As the recent hardware gets more advances, the signal processing function can be integrated into just a single chip. As an example, an RF transceiver, base band processors and sensor interface can be integrated into one device that is so small and operates as wireless sensor node. This device usually operates with small batteries that reduce its power capabilities where in many cases, it needs to function without battery replacement for many years. Therefore, it is

important to consider energy consumption and energy-efficient transmission schemes when designing to transfer data in sensor networks.

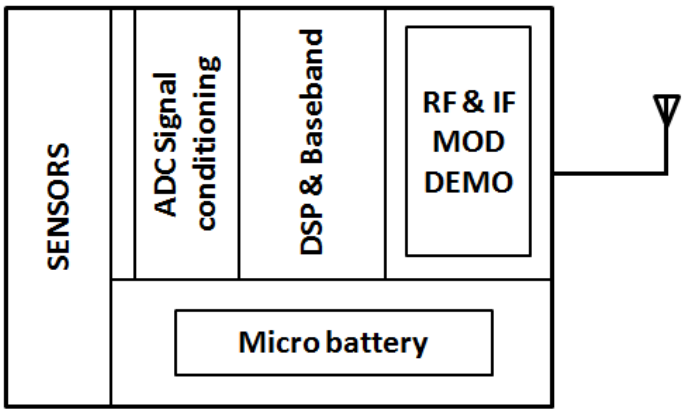

Figure 2.11: Typical wireless sensor node.

Moreover, it is unlikely to do the maintenance especially for the battery as the sensor nodes usually are deployed in remote and dangerous locations [39]. Sensor networks has draw attention to many new, promising applications such environmental monitoring, intrusion detection, surveillance, geo localization, military and industrial [39], [40].

Communication between sensor nodes needs to be robust and low power. MIMO system is designed to enhance the overall performance without increasing the bandwidth or total power radiated from transmitter as compared to conventional SISO system. MIMO system is known as a promising system that seriously considered for sensor network system. The transmission reliability has been increased by signal processing techniques utilizing multiple transmit and receive antennas such as STC.

In surveillance application, the effectiveness of the sensor network depends on the ability of sensor nodes to relay the data. The communication is constrained because most nodes are possibly out of range. In this case, MIMO with the greater range is favorable because the sensor nodes has the ability to form a completely connected network named as cohesion, which promises the favorable outcome of the final application [41].

One of the increasing demands in communication is Mobile Ad Hoc Networks (MANET) which is mobile networks with distributed transmitters and receivers. In

this technique, the transmitters and receivers do not put together their information, due to many reasons such as bandwidth and resource limitation, or geographical depressiveness or security and privacy concern. It is very interesting to study MIMO system in ad hoc networks with interference transmission because multiple antennas arrangement at the transceivers has spatial selectivity that gives inherent multiplexing capability.

Energy-efficient techniques generally minimize the transmission energy only, which is dominant in the total energy consumption. This function is very reasonable for long-range applications. The cooperation among sensors is allowed in the network to transmit and/or receive information because it can reduce energy consumption and transmission delays over some distance.

As a conclusion, it can be said that MIMO system needs less transmission energy than SISO system with the same throughput. However, it is impractical to conduct direct application of multi-antenna techniques to sensor networks because the physical size of a sensor node is limited and basically can support a single antenna only. A cooperative MIMO system can be introduced if individual single-antenna nodes supported co-operating on information transmission and/or reception, such as energy-efficient MIMO schemes [42]. In summary, MIMO produces significant improvement in network performance characteristics such as network robustness, latency and power consumption.

2.4.3 MIMO in Mesh Network

Wireless mesh networks are another way to transmit voice, data and video specializing in outdoor environments [43]. It can provide the same network capacity, reliability and security as wired network, but with the advantage of wireless flexibility. Aiding with advance technology, many organizations such as industrial organizations, port authorities, public safety agencies and municipalities depends on mesh networks to give necessary connectivity to their staffs and workers.

A mesh is defined as multi-path, multi-hope WLAN and wide area network that is suitable for outdoor environment. A reliable networking can be formed almost

everywhere with a mesh, without disrupting the running cable or fiber or the need for the cost. In the previous condition, voice, video and data network is separated but mesh system has a powerful multiservice platform which can combine all these elements onto a single network. In conclusion, it is easier to manage and operate the converged network while at the same time the organization maintains the control of services provided. Other benefit is the cost to purchase and maintain the network will be less as it needs fewer devices.

A modern mesh network works by searching the best route automatically through the network which still functions seamlessly even if a mesh link or a node fails. This process is possible because the network has the capability to self-forming and self-healing, with low maintenance costs and administration. Moreover, in a crowded environment where the line of sight (LOS) becomes a problem, a wireless mesh has come out as a solution.

MIMO antenna technology offers large potential for mesh networks because it guarantees high channel capacity over large area in order to support high bandwidth applications [44]. It is capable to exploit rich scattering environment that can increase the potential of multipath components. Thereby, MIMO is suitable for urban, dense and in-building environments which are exactly the settings for mesh networks. MIMO link is capable of different transmission strategies with different benefits. However, in order to realize the full potential of MIMO technology, higher layers must be constructed to bring out the full potential of MIMO link capability.

Mesh networks have several applications and the popular one is in municipals, public safety and industrial organization. Big cities can deliver a large-scale mesh network where a productive workers and first-responders can be achieved regardless their position in the community. Also known as Muni-Wireless, it is a single infrastructure but with several, different municipal applications and this property can make the operation simpler while reducing the networking cost. Employees can do their works effectively while in the field using extensive Wi-Fi. Other than that, Wi-Fi known as hot zones are very convenience in public that allows further development in business.

Wireless mesh networks that has high channel capacity can be delivered with ease and efficiently almost anywhere by public safety agencies especially to improve

situational awareness and support emergency communications. These networks serve as a temporary or permanent network where using these wireless mesh, safety authorities such as police, fireman and other first responders can use the video surveillance cameras to monitor and provide secure Wi-Fi access to centralized databases and applications remotely.

Another application of wireless mesh networks is connecting industrial operations and sites which due to their geography are very difficult to provide networking. These sites are construction areas, mining and oil and gas fields, for examples. Similar as discussed above, field workers can communicate easily with access to key applications because it enable functions as surveillance of IP video and access control. These functions can protect the field operations as well as the crew of the organizations. As an example, the cameras will monitor the crews to make sure that the physical security is maintained and maintenance operations are performed. Other function is tracking and locating people as well as high-value equipment to reduce theft and improves efficiency.

CHAPTER 3

ON CHANNEL CAPACITY ENHANCEMENT USING BEAM RADIATION PATTERN

3.1 Overview

There is an increasing demand in communication system today as to provide a wireless mobile data services that has the capability of empowering higher voice and data rates but at the same times managed to accommodate higher capacity users. Particularly for indoor communication system, countless research regarding channel capacity enhancement were carried out to oversee this situation [45]–[48]. As were discussed in Chapter 2, high capacity in a channel can be obtained by utilizing MIMO technology and a considerable amount of studies related to maximizing channel capacity have been reported [2]–[4]. In multi antenna environment, optimizing the radiation pattern and polarization are very effective especially in enhancing the channel capacity. A low correlation coefficient can be obtained using pattern and polarization diversity [49] and an optimized radiation pattern can be delivered by adjusting the electrical length of the parasitic elements of Yagi-Uda thus enhancing channel capacity and improving antenna performance [50].

In addition, the channel capacity of a hybrid polarization system outperformed a single polarization system due to the independence of the propagation paths of the two polarizations [51]. The capacity of the system also can be improved significantly

by using antennas radiating different polarizations compared with antennas with the same polarization [52]. Improving the channel capacity in wireless communication system however is not an easy task. The challenge presents because there is a need to transmit data at high speed, but the present circumstances especially lacking of frequency band is limiting the ability and becomes a problem. Therefore, it is important to improve the limited frequency band transmission speed. Aside from that, another challenge is the environment itself. Indoor environment is a multipath environment where the radio wave is reflected by the ceiling, walls, floors and etc. When the signal is reflected, the strength of the reflected signal is reduced and the propagation path becomes longer. Thus, the receiver side didn't receive the original signal instead the superimpose signals having travel through the multipath.

3.1.1 Channel Capacity Definition

The description in this section is mainly referred from [53]. Channel capacity is defined as the maximum amount of information that can be transferred over a communication channel per unit time. The channel capacity equation for SISO systems is represented by;

$$C = \log_2(1 + \gamma) \tag{3-1}$$

where γ is the SNR and the unit is [bits/s/Hz]. However, if the signal is sufficiently larger than the noise, the following equation is obtained;

$$C \approx \log_2 \gamma \tag{3-2}$$

And even the SNR value is doubled, the increasing in the channel capacity is only just 1 as shown in the following;

$$C \approx \log_2 \mathbf{2}\gamma = \log_2 2 + \log_2 \gamma \; = 1 + \log_2 \gamma \tag{3-3}$$

However, if two completely parallel signals are sent form two antennas, the increasing in the channel capacity is large. In this case, when the transmitting power is allocated equally to the transmitting antennas, the channel capacity for each transmission path will be as follows;

$$C \approx \log_2 \frac{\gamma}{2} = \log_2 \gamma - \log_2 2 = \log_2 \gamma - 1 \tag{3-4}$$

From equation (3-4), it is proved that although the SNR is divided into half, the decrement in channel capacity is only 1 for each transmission path. Thus, the total channel capacity will become;

$$C \approx 2\log_2 \frac{\gamma}{2} = 2\log_2 \gamma - 2\log_2 2 = 2\log_2 \gamma - 2 \tag{3-5}$$

Comparing with equation (3-2), it is clear that the channel capacity is largely increase for multi antenna system.

In multi-streams MIMO systems, when the channel matrix is unknown on the transmitting side, the channel capacity C is given by the following equation;

$$C = \log_2 det\left(I + \frac{P_t}{N_t \sigma^2} HH^H\right) \tag{3-6}$$

where P_t and σ^2 are the total transmitting power and noise level, respectively. $\{\cdot\}^H$ represents a complex conjugate transpose, and $\boldsymbol{I}$ is an identity matrix. Channel response, $\boldsymbol{H}$ is given by;

$$H = \begin{bmatrix} h_{11} & \cdots & h_{1M_T} \\ \vdots & \ddots & \vdots \\ h_{N_R 1} & \cdots & h_{N_R M_T} \end{bmatrix} \tag{3-7}$$

where h_{ji} is an impulse response between the *i* th transmitting and the *j* th receiving antennas. In (3-6), channel capacity is determined on the transmitting side since it depends on P_t. The transmit symbol vector at the *i* th transmitting antenna element and the received signal at the *j* th receiving antenna are denoted by s_i and x_j. Since transmitting power from each element is equal in SDM without CSI on the transmitting side, the received power at the *j* th element is expressed as;

$$P_{r,j} = E[|x_i|^2] = E\left[\left|\sum_{i=1}^{M_T} h_{ji} s_i\right|^2\right] = \sum_{i=1}^{M_T} \left|h_{ji}\right|^2 E[|s_i|^2] = P_{t,i} \sum_{i=1}^{M_T} \left|h_{ji}\right|^2 \tag{3-8}$$

where $P_{t,i}$ is the transmitting power at the i th transmitting antenna element. The average received power $\bar{P}_r$ is calculated by;

$$\bar{P}_r = \frac{\sum_{j=1}^{N_R} P_{r,j}}{N_R} = \frac{P_{t,i}}{N_R} \sum_{i=1}^{M_T} \sum_{j=1}^{N_R} |h_{ji}|^2 \tag{3-9}$$

Thus, the transmitting power at the j th transmitting antenna element is expressed as;

$$P_{t,i} = \frac{\bar{P}_r N_R}{\sum_{i=1}^{M_T} \sum_{j=1}^{N_R} |h_{ji}|^2} \tag{3-10}$$

Since the element has the identical transmitting power from each element is equal, the total transmitting power P_t is represented by;

$$P_t = \sum_{i=1}^{M_T} P_{t,i} = \frac{\bar{P}_r M_T N_R}{\sum_{i=1}^{M_T} \sum_{j=1}^{N_R} |h_{ji}|^2} \tag{3-11}$$

By substituting (3-11) in (3-6), the channel capacity is transformed as follows;

$$C = \log_2 det \left(I + \frac{P_r}{M_T \sigma^2} \frac{H}{\sqrt{\frac{1}{N_R M_T} \sum_{i=1}^{M_T} \sum_{j=1}^{N_R} |h_{ji}|^2}} \frac{H^H}{\sqrt{\frac{1}{N_R M_T} \sum_{i=1}^{M_T} \sum_{j=1}^{N_R} |h_{ji}|^2}} \right)$$

$$= \log_2 det \left(I + \frac{\rho}{M_T} H_n H_n^H \right) \tag{3-12}$$

where $\rho = P_r/\sigma^2$ is the average SNR at each receiving antenna, and $\boldsymbol{H_n}$ is a normalized channel response matrix denoted by;

$$H_n = \frac{H}{\sqrt{\frac{1}{N_R M_T} \sum_{i=1}^{M_T} \sum_{j=1}^{N_R} |h_{ji}|^2}} \tag{3-13}$$

In (3-12), the channel capacity is determined on the receiving side since it's depends on ρ.

Moreover, when CSI is known on the transmitting side, a channel can be divided into multiple independent Eigen paths. The channel capacity C is given by the sum of the channel capacity in each eigen path C_k as follows [54];

$$C = \sum_{k=1}^{K} C_k = \sum_{k=1}^{K} \log_2\left(1 + \frac{\lambda_k P_k}{\sigma^2}\right) \tag{3-14}$$

where $\lambda_k$is the k th eigenvalue derived by the eigenvalue decomposition;

$$HH^H = V\Lambda V^H,\ \Lambda = diag(\lambda_1, \dots, \lambda_K) \tag{3-15}$$

$K = \min(M_T, N_R)$ is the number of eigenpaths, and P_k is the transmitting power allocated for k th eigen path, which is represented by;

$$P_k = \max\left(\eta - \frac{\sigma^2}{\lambda_k}, 0\right),\ \sum_{k=1}^{K} P_k = P_t \tag{3-16}$$

where η is a constant. The SNR of the k th detected sub-stream is expressed as;

$$\rho_k = \frac{\lambda_k P_k}{\sigma^2} \tag{3-17}$$

In (3-6), the amplitude level of h_{ji} is related to the received SNR while the total transmitting power is fixed. Therefore, the effect of SNR is included in eigen values derived by the eigen value decomposition of HH^H. In contrast, in (3-12), there is no impact of the SNR on eigen values derived from the eigen value decomposition of $H_n H_n^H$ because SNR (ρ) and $H_n H_n^H$ are completely separated. In (3-14), the effect of SNR is included in eigen values because λ_k is expressed using SNR from (3-17); $\lambda_k = \rho_k \sigma^2 / P_k$. The next section focuses on the channel capacity of (3-12) defined on the receiving side and the normalized channel matrix to consider correlation and SNR separately.

3.1.2 Relationship between Channel Capacity and Spatial Correlation

The description in this section is based on [53], [55]. In a 2 x 2 MIMO system, the spatial correlation coefficient between received signals is given by;

$$\gamma_s = \frac{h_{11}h_{21}^* + h_{12}h_{22}^*}{\sqrt{(|h_{11}|^2 + |h_{12}|^2)(|h_{21}|^2 + |h_{22}|^2)}} \tag{3-18}$$

where $\{\cdot\}^*$ denotes the complex conjugates. Here, the received powers at the receiving antenna 1 and 2 are represented by;

$$P_{r,1} = |h_{11}|^2 + |h_{12}|^2,\ P_{r,2} = |h_{21}|^2 + |h_{22}|^2 \tag{3-19}$$

When the received power imbalance between antenna 1 and antenna 2 are defined as $\beta = P_{r,1}/(P_{r,1} + P_{r,2})$, $P_{r,1}$, $P_{r,2}$ and γ_s are transformed (3-13) as;

$$P_{r,1} = 4\beta, \qquad P_{r,2} = 4(1-\beta), \qquad \gamma_s = \frac{h_{11}h_{21}^* + h_{12}h_{22}^*}{4\sqrt{\beta(1-\beta)}} \tag{3-20}$$

The following equations are given by substituting (3-20) into the transformed formula of (3-12):

$$C = \log_2\left(1 + 2\rho + 4\beta\rho^2(1-\beta)(1-|\gamma_s|^2)\right) \tag{3-21}$$

In (3-21), the SNR and spatial correlation, as well as the received power imbalance, have an impact on channel capacity.

3.1.3 Modeling by Ray Tracing Method for Channel Response Matrix H

In MIMO system, a matrix containing impulse responses between transmit and receive antennas elements is referred as channel response matrix, H. In this section, the modeling of the channel response matrix, H is explained using the ray tracing method.

In the multipath propagation environment, the transmission rays of the radio wave radiated from the transmitting antenna is reflected by the obstacles before reaching the receiving antenna. Ray tracing method is a method of tracking the trajectory of their respective rays. There are two types of ray tracing method, the ray launching method and the imaging method where the amount of calculation and the estimation accuracy for each of them is different. In this research, the ray launching method is used to estimate the channel capacity. In ray launching method, a large number of rays are emitted in all directions from the transmission point, repeatedly being reflected and deflected before reaching the receiving point. The estimation accuracy for this method is low compared to the imaging method, thus it is possible to have a sufficient accuracy by increasing the number of rays emitted from the transmission. Figure 3.1 shows the conceptual diagram of the ray launching method.

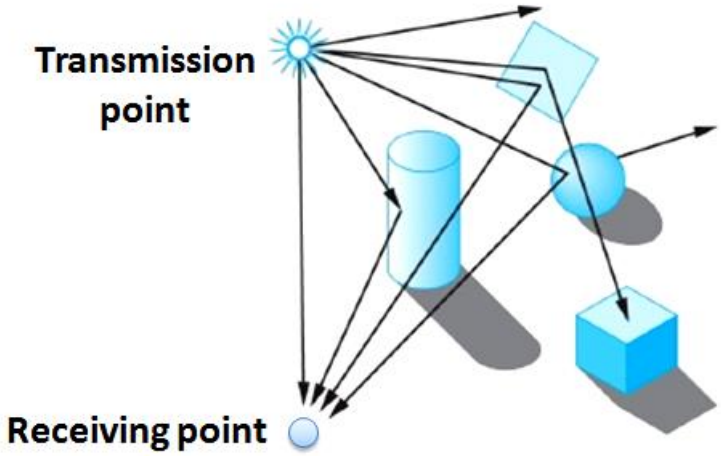

Figure 3.1: Conceptual diagram of the ray launching method.

When the transmitted signal hit the obstacle, losses due to the reflection and transmission occurs where the reflection coefficient related is according to the Fresnel equation [56]. Fresnel's equations describe the reflection and transmission of electromagnetic waves at an interface. The reflection and transmission coefficients are given for waves parallel and perpendicular to the plane of incidence. The calculation in this paper does not take into account the thickness of the wall and the reflection coefficient for vertical and horizontal polarization is given as follows;

$$\Gamma_{TE} = \frac{\cos\theta_1 - \sqrt{\varepsilon_c - sin^2\theta_1}}{\cos\theta_1 + \sqrt{\varepsilon_c - sin^2\theta_1}}, \qquad \Gamma_{TM} = -\frac{\varepsilon_c\cos\theta_1 - \sqrt{\varepsilon_c - sin^2\theta_1}}{\varepsilon_c\cos\theta_1 + \sqrt{\varepsilon_c - sin^2\theta_1}}$$

$$\varepsilon_c = \epsilon_r - \frac{j\sigma}{\omega\varepsilon_0} \tag{3-22}$$

where θ_1 is the incident angle of the signal with respect to the wall and ε_c is the complex dielectric constant of the wall. The dielectric constant of vacuum is $\varepsilon_0 = 8.854\ x\ 10^{-12}$ while the electrical properties for concrete that is used in the simulation are as follows; dielectric constant $\varepsilon_r = 6.76$, conductivity $\sigma = 0.0023$, and relative permeability $\mu_r = 1$. The simulation was conducted at frequency 3.5 GHz, thus giving $\omega = 2\pi f = 2\pi\ x\ 3.5\ x\ 10^9$. The relationship between the incident angle and the reflection coefficient is shown in Figure 3.2 where TE(H) and TM(V) is for horizontal and vertical polarization respectively [57].

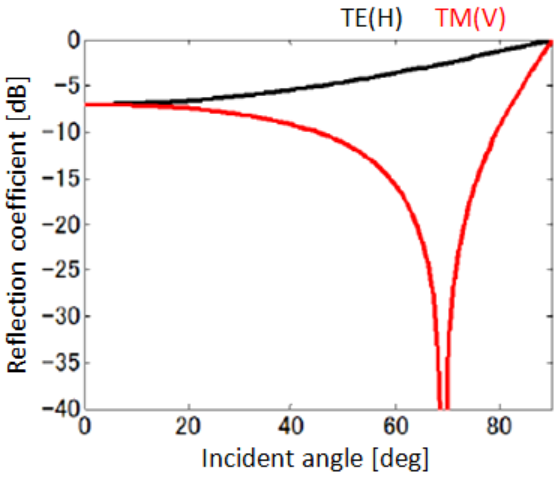

Figure 3.2: Reflection coefficient for concrete.

3.2 Channel Capacity and the Simulation Characteristics

Channel capacity can be enhanced using MIMO system as being discussed in Chapter 2. As shown in Figure 2.3, the capacity will increase as we increase the number of antenna used in the system. In this chapter, the channel capacity was calculated using EEM-RTM [57] software according to a few arrangements and the results is presented

followed by discussion of respective results. One of the objectives is of course to show the enhancement of the MIMO system but the target objective is to show improvement in channel capacity when an antenna with beam pattern is used instead of dipole antenna. Also, in the later part of this chapter, the channel capacity also is calculated when we manipulate the position of the antenna in the room as we considered the best position for each antenna considering the radiation pattern emitted from it.

In this chapter, 4 x 4 MIMO system was considered. The simulation parameter for channel capacity calculation is described first in this section. Two types of antennas were used for comparison purpose considering their radiation pattern. The dipole antenna was used for common radiation pattern while a directional antenna such as in Chapter 4 was used for beam radiation pattern. As we didn't really need the antenna but only the radiation pattern for the simulation process, the patterns were constructed first using MATLAB program and at the same time, the simulation rooms were built on EEM-RTM software. Then the constructed patterns were used for tracing the ray in EEM-RTM and the output matrix was called in MATLAB to calculate the channel capacity according to the formula discussed in section 3.1.

In this section, the simulation parameters for channel capacity calculation will be described. The radiation patterns characteristics are explained and the rooms' conditions as well as transmit and receive antenna arrangements are discussed. The antennas used are assuming 4 x4 MIMO configurations capable of both vertical and horizontal polarization.

3.2.1 Simulation Environments and Parameters

Before channel capacity can be calculated in MATLAB according to the formula previously discussed, the rooms visualizing the real condition needs to be created in EEM-RTM software. For this study, channel capacities were calculated in three different room sizes visualizing an indoor environment. The size for each room is shown in Figure 3.3, labeled as size A for the smallest room, Size B for the middle room and Size C for the biggest room. The height (Z) of all rooms was set at 3 m while the width (X) and the length (Y) of each room were as shown in the figure, accordingly. For the dimension of the room, it is set that the rooms were in rectangle shape instead

of square shape where the length Y is longer than the width X to demonstrate the influence of the different in dimension.

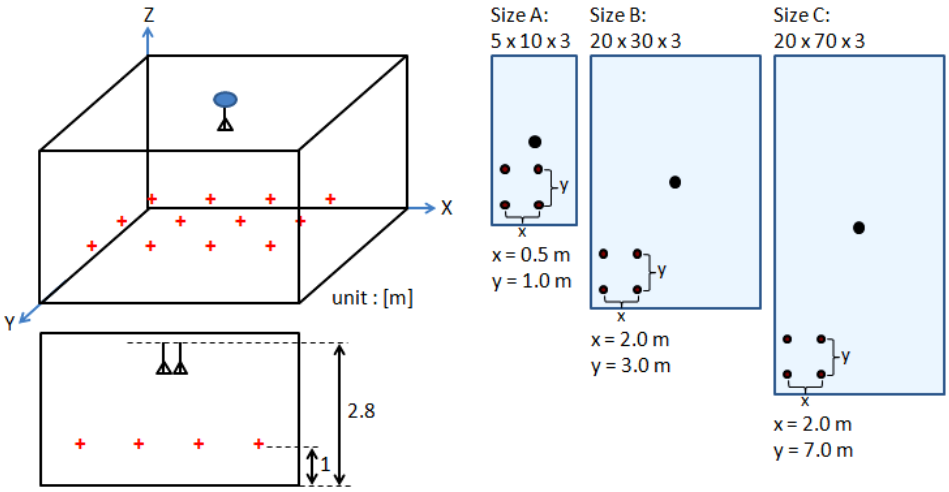

Figure 3.3: Model of the room for simulation with the size for every room and the distance for receiving points in each room described.

The rooms were assumed closed space with no door or window. All the wall, floor and ceiling were made of concrete with electrical properties as discussed in Section 3.1.3. A LOS environment was assumed where there were no other objects or obstacles aside from transmit and receive antennas inside the rooms. The transmitting point consisting of 4 dual polarizations antennas was put at the center of the rooms, 2.8 m in height from the floor while the receiving points consisting of 4 dual polarizations antennas were placed at 1 m height from the floor, where the distance were kept at the same length from each other. Since the total points for each room was 81 points regardless the size of the room, the distance for each receiving point in x- and y- direction in each room will be different and is shown in the Figure 3.3.

The transmit antenna capable of transmitting 4 radiation patterns, labeled as T_{X1}, T_{X2}, T_{X3} and T_{X4} representing 4 x 4 MIMO system is shown in Figure 3.4. The distance between each antenna in both transmit and receive antenna was $\lambda/2$, which is equal to 42.8 mm for 3.5 GHz frequency. The position for each receiving point in each room was arranged by dividing the dimension of the width and length of the room by 10 as pointed as red points in the figure, hence the total receiving points in every room. Each point consists of 4 receive antenna, labeled as R_{X1}, R_{X2}, R_{X3} and R_{X4}. Thereby, channel capacity was calculated at these 81 points providing an average

capacity in the whole room. Both transmit and receive antenna consist of dual polarization, vertical and horizontal polarization and the arrangement is as shown in Figure 3.4.

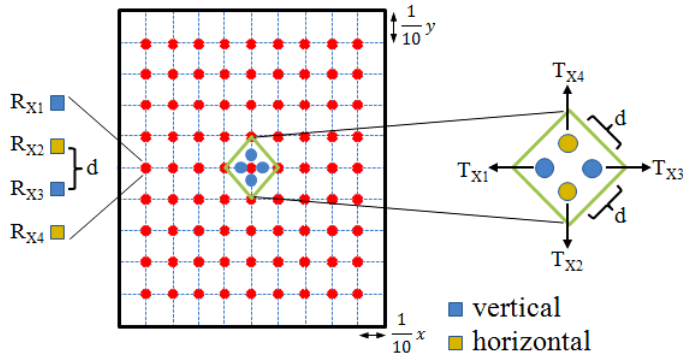

Figure 3.4: Receiving points in a room and transmitting antenna.

Channel modeling was performed using the ray tracing method, where the channel response matrix is the response matrix of time without considering the time variation of the channel. The maximum reflection time was set at 5 and neither diffraction nor scattering was taken into consideration during simulation. Table 3.1 shows the simulation parameter for channel capacity calculation. The frequency was set at 3.5 GHz for MIMO LTE environment. The electrical property for the wall was set as per discussed in the previous section. The transmission and noise power was set -5 dBm and -85 dBm respectively.

Table 3.1: Simulation parameter.

Frequency	3.5 GHz
System	4 x 4 MIMO
Channel modeling	Ray Tracing
Maximum reflection time	up to 5 times
Transmission power	-5 dBm
Noise power	-85 dBm
Wall material Relative permittivity Conductivity	Concrete 6.76 0.0023 S/m

3.2.2 Transmitting and Receiving Antenna

Two types of transmit antenna will be used in channel capacity calculation for comparison purpose with respect to their radiation pattern. The first one was a common pattern antenna and dipole antenna was used for the simplicity, where the radiation pattern in xz- and yz-plane is shown in Figure 3.5. The polarization for dipole antenna is along the length of the dipole, thus its polarization can be arranged by putting the dipole in the vertical or horizontal position accordingly. The gain for dipole antenna is 2.01 dBi.

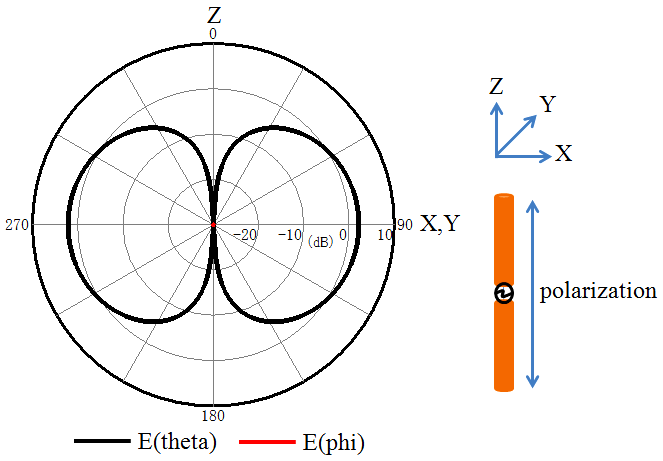

Figure 3.5: Radiation pattern for dipole antenna.

The other antenna used for transmit antenna was a beam-pattern antenna as shown in Figure 3.6. For beam-pattern antenna, both horizontal and vertical plane has the same directivity where F/B ratio is infinite. The beam-pattern directivity (D), HPBW (h) and gain (G) as well as the 3D radiation pattern can be obtained using the following equation;

$$D(\theta) = \begin{cases} cos^{h}(\theta) & \left(0 \le \theta \le \frac{\pi}{2}, \frac{3\pi}{2} \le \theta \le 2\pi\right) \\ 0 & \left(\frac{\pi}{2} \le \theta \le \frac{3\pi}{2}\right) \end{cases}$$

$$h = -\frac{\log_{10} 2}{\log_{10} \cos(\theta_{h)}}$$

$$Gain = 10\log_{10}\frac{4\pi}{\theta_{HP}\varphi_{HP}} \tag{3-23}$$

where θ_{HP} and φ_{HP} is the HPBW of E- and H-plane respectively ($\theta_{HP} = \varphi_{HP}$).

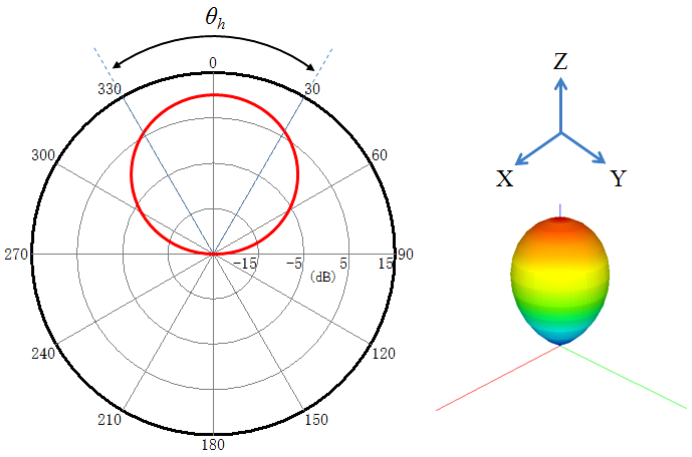

Figure 3.6: Radiation pattern for beam-pattern antenna.

All receive antennas have isotropic pattern as shown in Figure 3.7. The vertical and horizontal polarization was arranged in alternating as shown in Figure 3.4, thereby providing an equal number of vertical and horizontal polarization antenna in the room. This way, an average capacity in the room can be calculated.

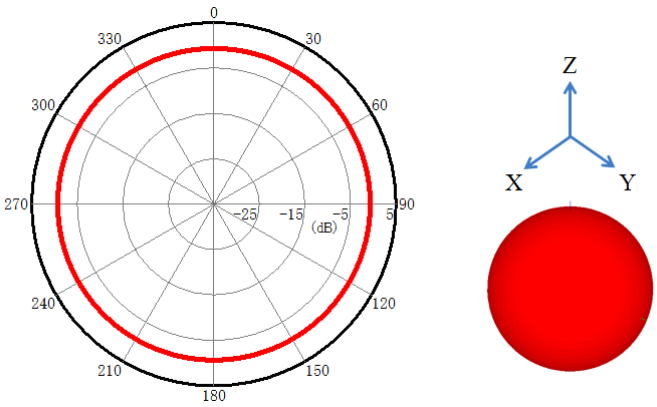

Figure 3.7: Radiation pattern for receive antenna.

3.3 Channel Capacity Simulation and Results

In this section, various simulation results that were performed are discussed. The first one was parameter analysis for both transmit and receive antenna setting. This simulation was performed to confirm the best setting or arrangement for the next simulation. The second one was channel capacity calculation with the transmit antenna set in the center of the ceiling. The results were compared between the dipole antenna and the beam-pattern antenna. The third one was channel capacity simulation when the transmit antenna was set in other places beside center of the ceiling, considering the best position in term of the radiation pattern for beam-pattern antenna. The fourth simulation was conducted at different frequencies, which were 4.5 GHz and 6.0 GHz.

3.3.1 Channel Capacity of Different Antenna System

As were discussed in previous chapter, multi antenna system as in MIMO can increase the overall capacity as compared to single antenna system. Although the theory has been prove before [12], [15], [27]–[30], a simple simulation with the arrangement according to this study was done to support and prove the theory as well. The simulation was run in the smallest room, room Size A and dipole antenna was used for transmit antenna while the receive antenna had isotropic pattern. The results are shown in Table 3.2 where 3 types of system are compared. From the table it is confirmed that as the antenna for both transmit and receive antenna increase, the channel capacity also increase.

Table 3.2: Chanel capacity comparison between antenna systems.

Antenna System	Capacity [bit/s/Hz]
SISO	11.38
2 x 2 MIMO	16.77
4 x 4 MIMO	18.60

3.3.2 Transmit and Receive Antenna Parameter Analysis

The parameter analysis was divided into two parts, one for receive antenna and one for transmit antenna. The analysis was done by changing the arrangement for antenna at each point, according to 3 patterns as shown in Figure 3.8. The receive antenna was arranged in vertical line as in Pattern A, diamond shape as in Pattern B and horizontal line as in Pattern C. On the other hand, the transmit antenna arrangement was fixed to just one pattern, the diamond shape. The comparison was done in term of channel capacity itself, capacity distribution and also average eigen value.

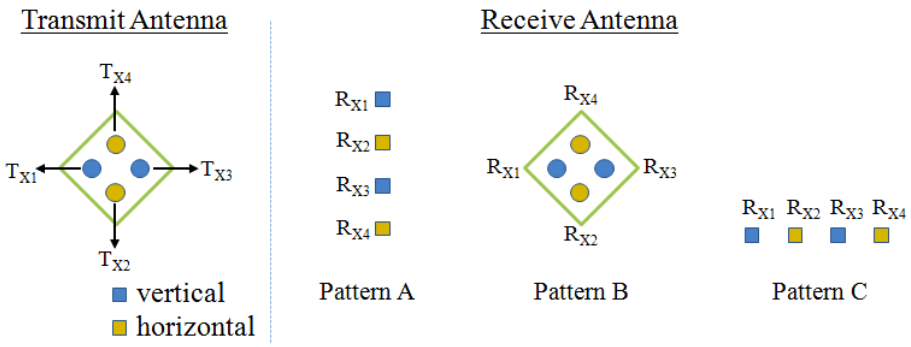

Figure 3.8: Comparison between receive antenna arrangement.

Receive Antenna Analysis

In this section, each receive point which consists of 4 antennas were arranged in 3 different arrangements named as Pattern A, Patter B and Pattern C. The vertical and polarization antenna was arranged alternately to avoid high correlation between each antenna which can reduce the channel capacity. All the receive antenna had isotropic pattern while the transmit antenna used both dipole antenna with gain of 2.01 dBi and beam-pattern antenna with HPBW of 60° and gain of 10.6 dBi.

Table 3.3 shows the channel capacity result in bit/s/Hz, for 3 different arrangements for receive antenna in the smallest room. From the table, it is revealed that the highest capacity is obtained when receive antenna was arranged in vertical line which is Pattern A, followed by Pattern C and Pattern B. These results are true for both dipole and beam antenna.

Table 3.3: Comparison of channel capacity for 3 different arrangements for receive antenna.

Rx	Dipole	Beam 60°
Pattern A	32.46	34.60
Pattern B	23.40	24.68
Pattern C	26.94	28.12

The capacity distribution for channel capacity results shown in Table 3.3 is described in Figure 3.9. From the figure it is confirmed that the capacity distribution for Pattern A is the best compared to Pattern B and C, parallel to the results shown in Table 3.3. Considering the transmit antenna was at the center of the room, Pattern A gave the most fair and equal coverage to all receive points, with the nearest to the transmit antenna get the strongest signal. In Pattern B, the coverage is quite fair and equal for dipole antenna but for beam-pattern antenna, some receiving points received a noticeable weaker signal compare to the neighboring points. For Pattern C, although the distribution might be comparable to Pattern B, there is obvious vertical line pattern in the distribution for both dipole antenna and beam-pattern antenna. Putting aside the channel capacity results, it is obvious from this results that Pattern A is the most favorable output for capacity distribution.

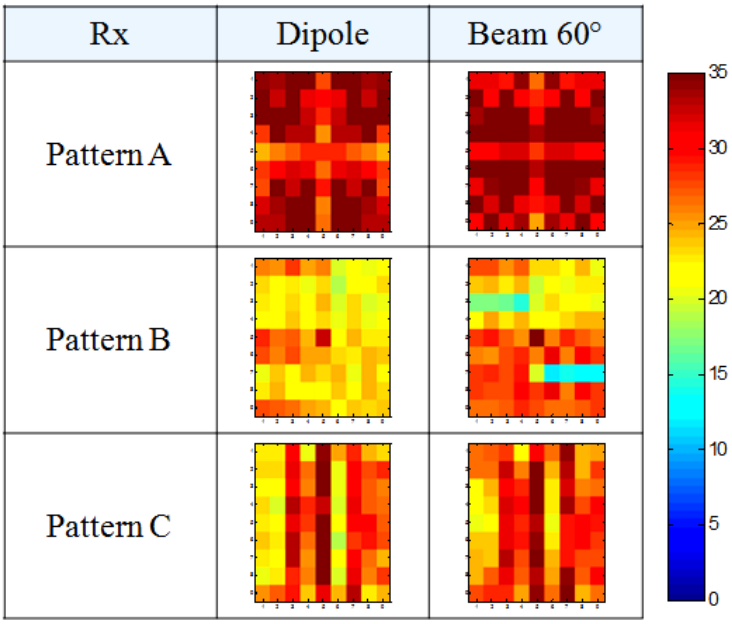

Figure 3.9: Comparison of capacity distribution for 3 different arrangements for receive antenna.

As in MIMO, spatial coefficient between the inter-elements of an antenna is important to reduce the correlation between them. Here, the eigen value of the spatial coefficient matrix was examined and compared between 3 different arrangement for receive antenna. The eigen value was calculated based on channel capacity matrix which gives the average value for each room. And as the simulations consists of 4 x 4 MIMO antenna, there are 4 eigen values for each calculation as shown in Table 3.4.

Table 3.4: Comparison of channel capacity for 3 different arrangements for receive antenna.

Rx	[dB]	Dipole	Beam 60°
Pattern A	e_1	-59.2	-57.7
	e_2	-53.2	-51.7
	e_3	-45.0	-42.3
	e_4	-38.2	-35.7
Pattern B	e_1	-80.0	-70.0
	e_2	-65.2	-63.0
	e_3	-48.9	-48.1
	e_4	-37.3	-35.3
Pattern C	e_1	-65.2	-64.0
	e_2	-55.9	-55.7
	e_3	-43.0	-45.5
	e_4	-38.3	-35.3

The highest eigen value is given by e_4 and the lowest is given by e_1. If we look at dipole antenna result for room Size A, the highest eigen value is obtained from Pattern B with -37.3 dB, while Pattern A and Pattern C gave a close results at -38.2 dB and -38.3 dB respectively. However, the highest channel capacity is obtained from Pattern A, followed by Pattern C and B, which is completely opposite from the eigen value results. However, if we look at all eigen value (e_1, e_2, e_3 and e_4) and make a comparison again, it is shown that the value for Pattern A is averagely higher, followed by Pattern C and Pattern B. Thereby, the overall analysis is parallel to the channel capacity results in Table 3.3.

In channel capacity results, Pattern A gives the highest capacity followed by Pattern C and Pattern B. The eigen value results in overall analysis also shows the same results. Looking at this pattern, it is concluded that the antenna arrangement in straight line either in vertical or horizontal gives higher capacity when is compared to

diamond shaped arrangement which is Pattern B. This results show that the correlation between the antennas is lower when arranged in straight line as the distance between each antenna is increased. Setting the polarization of the 4 antenna alternately (vertical-horizontal-vertical-horizontal) for both transmit and receive antennas also decrease the correlation between the antennas. It is also concluded that although the fourth eigen value is dominant for channel capacity, the other eigen values also an important factor in enhancing the channel capacity.

Transmit Antenna Analysis

From the receive antenna analysis in the previous section, we confirmed that Pattern A with receive antenna arranged in vertical line gives the highest channel capacity. Thereby, in this section for transmit antenna analysis, the receive antenna arrangement was fixed to that pattern only while the transmit antenna was arranged in 3 different arrangements to compare. Similar to receive antenna analysis, the transmit antennas were arranged alternately to decrease the correlation and two antenna types, dipole and beam-pattern antenna were used as comparison.

Table 3.5 shows the channel capacity comparison for different transmit antenna arrangements in the smallest room. From the table it is revealed that when receive antenna was arranged in vertical line, the channel capacity for dipole antenna and beam-pattern antenna will be different depends on the arrangement of transmit antenna. For dipole antenna, the highest channel capacity is obtained when the transmit antenna was arranged in vertical line as the receive antenna, while for beam-pattern antenna the highest capacity is obtained when the transmit antenna was arranged in horizontal line. Pattern B shows the lowest capacity for both dipole and beam-pattern antenna.

Table 3.5: Comparison of channel capacity for 3 different arrangements for transmit antenna.

Rx	Dipole	Beam 60°
Pattern A	34.38	34.98
Pattern B	32.46	34.60
Pattern C	33.82	35.63

Similar to the analysis for receive antenna, this results show that higher capacity can be achieved when both transmit and receive antenna were arranged in straight line. The highest capacity is achieved for beam-pattern antenna at 35.63 bit/s/Hz when the transmit antenna was arranged according to Pattern C. In fact, the results for beam-pattern antenna are quite close to each other regardless the transmit antenna arrangement as compared to dipole antenna.

The reason for different results between the dipole antenna and beam-pattern antenna lies on the radiation pattern. As the beam pattern is directed to certain direction, the correlation among each other is less compared to dipole radiation pattern. This can be seen from the capacity distribution in Figure 3.10. Especially for dipole, when the antenna was arranged in Pattern B, the distribution especially in antenna line in the center of the room is noticeably less than other parts of the room.

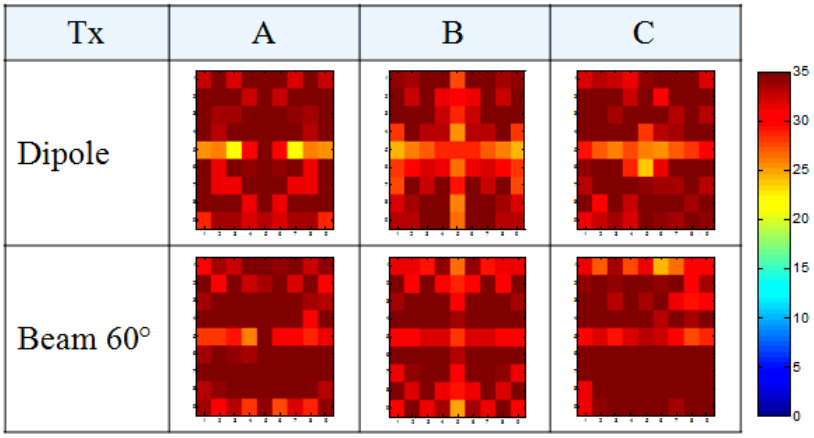

Figure 3.10: Comparison of capacity distribution for 3 different arrangements for transmit antenna.

3.3.3 Channel Capacity in Various Arrangement

In this section, various simulations on channel capacity calculation were carried out according to specific conditions to evaluate the factor that might affect the channel capacity as well as the capacity distribution of each antenna. And the channel capacity will be discussed by the comparison between the antennas with different radiation patterns, in 3 different room sizes. A common pattern antenna as in dipole antenna will be compared to beam pattern antenna to see the influence of the radiation pattern to the channel capacity. The comparison setting will use Pattern B, which is the diamond shape arrangement as in previous section for transmit antenna while receive antenna will be arranged in vertical line as shown in Figure 3.11.

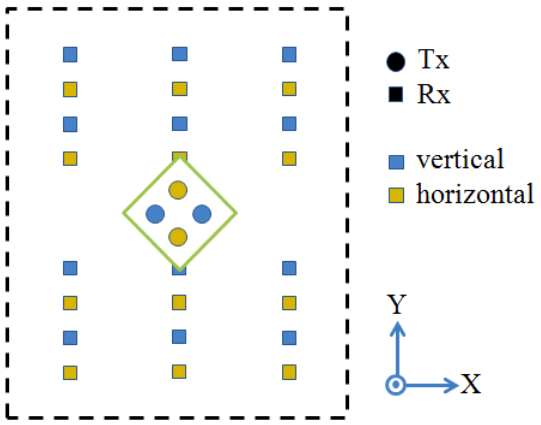

Figure 3.11: Simulation arrangement for transmit and receive antenna.

Channel Capacity of Different Room Size

In this section, simulation was done in 3 different room sizes to see the influence of the room size towards channel capacity and capacity distribution. In general, in term of channel capacity, as the room gets bigger the capacity will be lower. However, capacity distribution cannot be predicted as it was influenced by many factors such as the reflection of the signal and the correlation between the radiation patterns. Table 3.6 shows the channel capacity results was bit/s/Hz in all 3 rooms as comparison between dipole antenna and beam-pattern antenna. The gain for dipole antenna was 2.01 dB while for beam-pattern antenna was 10.6 dBi with HPBW of 60°.

Table 3.6: Channel capacity comparison in 3 different rooms.

Tx	A [5 x 10 x 3]	B [20 x 30 x 3]	C [20 x 70 x 3]
Dipole	32.46	24.19	20.64
Beam 60°	34.60	23.56	16.26

From the table above, it is shown that the highest capacity is obtained by beam-pattern antenna in the smallest room at 34.60 bit/s/Hz but at the same time the lowest capacity also by beam-pattern antenna in the biggest room at only 16.26 bit/s/Hz. However aside from Room A, the capacity for dipole antenna is higher than beam-pattern antenna in both bigger rooms. In general from these results, it is confirmed that the bigger the room the lower the capacity. Also in the overall, the channel capacity for dipole antenna is higher compared to beam-pattern antenna for this configuration.

Figure 3.12 shows the capacity distribution of the channel capacity in each room for both dipole and beam-pattern antenna. Parallel to channel capacity results in Table 3.6, the strongest signal is received in the smallest room, and gets weaker as the room gets bigger. Due to the different in radiation pattern shape and gain, there is distinctive distribution between dipole antenna and beam-pattern antenna. For dipole antenna, as 4 radiation patterns radiated at the same time, the interference towards each other decrease the signal strength at the center of the room as shown in the figure. However, as the distance from the transmit antenna increase, the signal received gets stronger even at the end corner of the room as shown in room Size A. The similar distribution can be seen in other rooms but as the room gets bigger, the signal strength gets weaker as shown in room Size C.

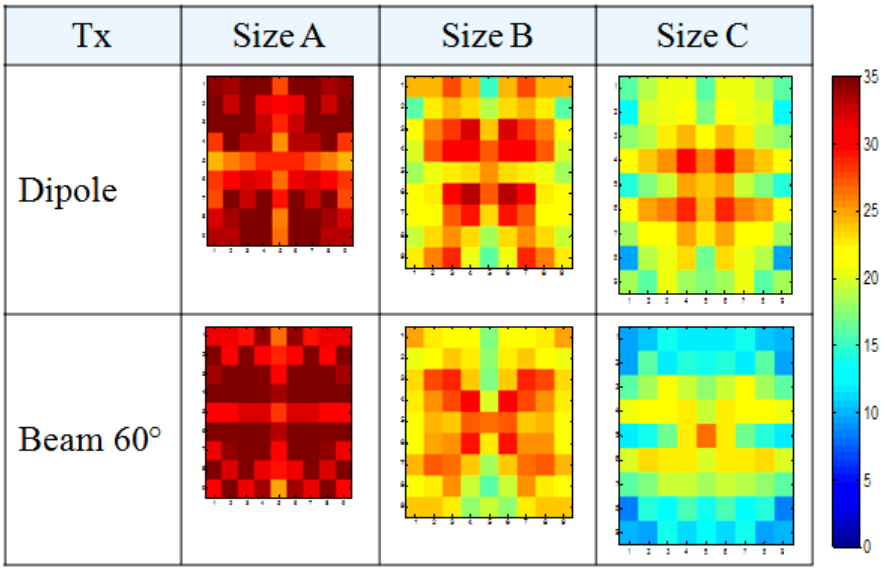

Figure 3.12: Capacity distribution for different room sizes.

On the other hand, the distribution for beam-pattern antenna is slightly different as the immediate receiving point received the strongest signal and the signal gets weaker as the receiving points are further from transmit antenna position. This result shows that the influence of the radiation in beam pattern antenna towards each other is lower compare to radiation pattern in dipole antenna. However, due to the beam shape of the radiation pattern, there are a lot more unreachable or shadowed region in beam-pattern antenna distribution as compared to dipole antenna distribution as clearly shown in room Size C. However, this drawback is reduced by the radiation pattern itself as beam pattern deliver higher gain as compared to dipole antenna pattern, which means covering further area if not wider as higher gain radiates further.

Channel Capacity of Different Beamwidth

In the previous section, the channel capacity and the capacity distribution for different rooms was discussed. On the whole, it is confirmed that the bigger the room the smaller the channel capacity will be. In this section, the channel capacity was calculated for beam-pattern antenna only but the comparison was done with different beamwidth instead; 60°, 90° and 120°. Respectively, as the beamwidth gets bigger the

gain will becomes smaller, where the gain for each beamwidth used is 10.6 dBi, 7.07 dBi and 4.57 dBi. The simulation was done in all 3 room sizes.

Table 3.7 shows the results for channel capacity between 3 beam widths for transmit antenna in all 3 room sizes. The highest capacity is obtained by beamwidth 90° in the smallest room at 34.83 bit/s/Hz and the lowest capacity is attained by beamwidth 60° in the biggest room at 16.26 bit/s/Hz. In general, as the room gets bigger the capacity gets lower as similarly found in previous section. However, the results in the table below demonstrates that in each room, there are only slight different in capacity value even if we increase the beamwidth, with 34.60, 34.83 and 34.46 bit/s/Hz in the smallest room. Similar pattern is also obtained in Room B and Room C. Another interesting discovery also can be seen in capacity results for biggest room where the capacity increases as we increase the beamwidth, approaching the capacity for dipole antenna capacity. This result is impressive considering the HPBW is only 1/3 of radiation pattern for dipole antenna.

Table 3.7: Channel capacity between different beamwidth for transmit antenna.

HPBW	A [5 x 10 x 3]	B [20 x 30 x 3]	C [20 x 70 x 3]
60°	34.60	23.56	16.26
90°	34.83	24.44	17.84
120°	34.46	24.39	18.38

The reason for similar results obtained for each room is because as the beamwidth gets bigger, the gain for respective beam will be smaller. In other words, although the coverage area will be wider, the distant in which the beam radiates will be shortened. Thereby the simulation results produced such a similar capacity value for all beam widths especially in the smallest rooms as the distribution covers all the room. The increasing capacity as the beamwidth gets bigger can be seen in capacity distribution shown in Figure 3.13, where similar distribution pattern can be seen in each beamwidth but with increasing in signal strength. However, although higher capacity is obtained for beamwidth of 120°, its distribution covers until the same distance as for beamwidth 60°, but only with stronger signal. This shows the plus minus condition between beamwidth and gain with respect to channel capacity.

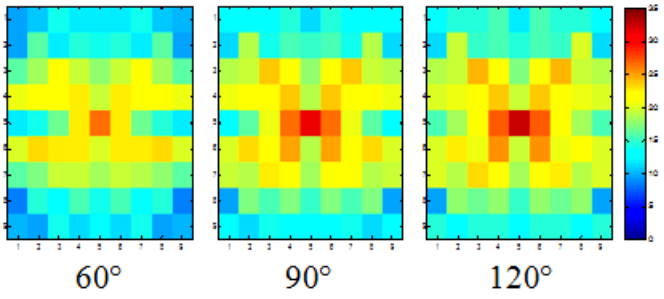

Figure 3.13: Capacity distribution in different beamwidth for transmit antenna.

Figure 3.14 shows the comparison of channel capacity for different radiation pattern for transmit antenna in all room sizes. In the overall, room Size A which is the smallest room gives the highest capacity followed by Size B which is the middle room and Room C which is the biggest room. Thus it is confirmed from this result that the bigger the room the lower the capacity. In the smallest room, beam-pattern antenna obtained higher capacity as compared to dipole antenna proving that the channel capacity can be enhanced using directional beam antenna pattern. In room Size B, the highest capacity is also achieved by beam-pattern antenna with beamwidth 90°. However, there is not much different in capacity results between each antenna which averaging around 24 bit/s/Hz. In the biggest room however, the capacity for dipole antenna exceeds all other antenna at 20.64 bit/s/Hz with the capacity increases as the beamwidth gets bigger.

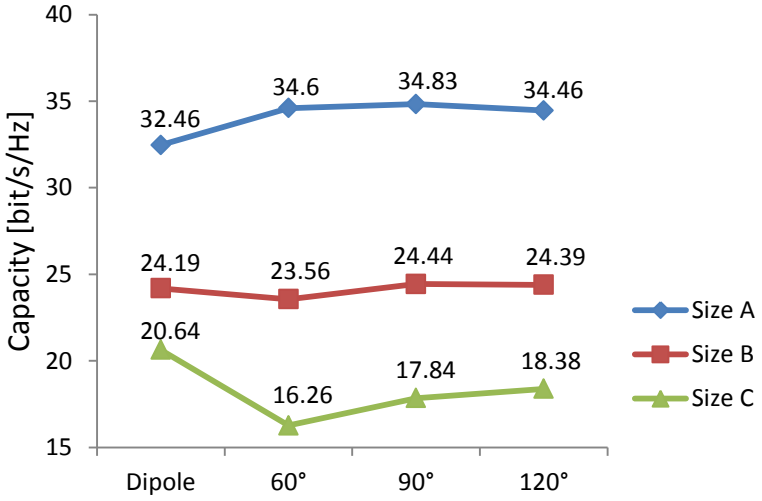

Figure 3.14: Channel capacity comparison for different transmit antenna in all 3 rooms.

Channel Capacity of Different Frequency

In the previous simulation, all the simulations for channel capacity calculation were done at frequency of 3.5 GHz which correspond to LTE environment. However as discussed in Chapter 1, there are other operating frequencies for LTE system and it will be considered here as well. In this section, the channel capacity calculation were done for another 2 LTE frequencies; 4.5 GHz and 6.0 GHz which gives the distance between antenna of $\lambda/2$ of 33.33 mm and 25 mm respectively. The simulation were done in comparison between different transmit antenna, in all 3 room sizes. All the parameters characteristic are the same as the previous section.

Table 3.8 shows the channel capacity results for different radiation pattern used for transmit antenna where again the simulation were done in all 3 room sizes. The highest capacity is obtained in the smallest room by beam-pattern antenna with HPBW of 90° at 25.07 bit/s/Hz while the lowest capacity is obtained in the biggest room by beam-pattern antenna with HPBW of 60°. From the table also we can see that the capacities in each room are comparable with each other with only just a slight different. In fact for middle room, the capacity for dipole antenna and beam-pattern antenna with HPBW of 60° is almost the same.

Table 3.8: Channel capacity for 4.5 GHz.

Tx	A [5 x 10 x 3]	B [20 x 30 x 3]	C [20 x 70 x 3]
Dipole	23.67	16.98	14.72
Beam 60°	24.91	16.68	12.04
Beam 90°	25.07	17.14	13.05
Beam 120°	24.93	17.10	13.09

Table 3.9 shows the channel capacity results simulated at another operating frequency of LTE which is 6.0 GHz. The highest capacity is obtained in the smallest room by beam-pattern antenna with HPBW OF 60° at 23.12 bit/s/Hz but at the same time the lowest capacity is also obtained by the same transmit antenna but in the biggest room at 10.17 bit/s/Hz. Again as for 4.5 GHz, the capacities results in each room are comparable to each other with the smallest room averaging around 22 bit/s/Hz, the middle room averaging around 15 bit/s/Hz and the biggest room averaging around 11 bit/s/Hz.

Table 3.9: Channel capacity for 6.0 GHz.

Tx	A [5 x 10 x 3]	B [20 x 30 x 3]	C [20 x 70 x 3]
Dipole	21.87	15.25	12.01
Beam 60°	23.12	14.33	10.17
Beam 90°	23.03	14.89	10.93
Beam 120°	22.91	14.87	11.02

The comparison of channel capacity for different operating frequencies is summarized in Figure 3.15 where the blue line shows capacities for Room A the smallest room, red line is for Room B the middle room and green line is for Room C the biggest room. A similar pattern can be seen in general where at all 3 operating frequencies, the smallest room gives the highest capacity followed by middle room and biggest room complementing the finding before that the bigger the room the lower the capacity.

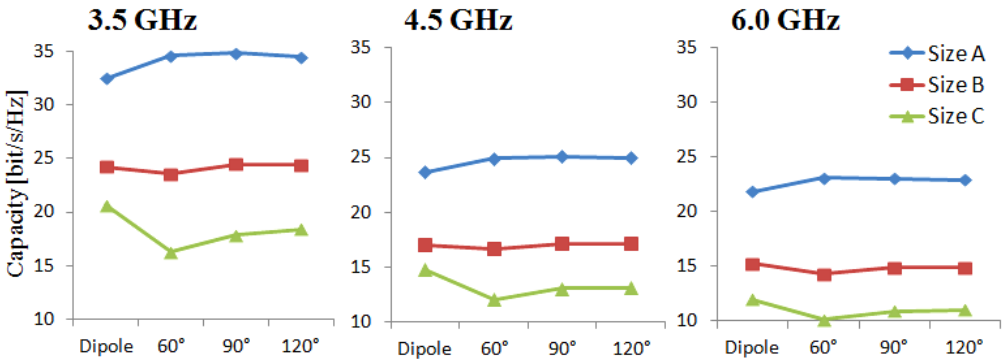

Figure 3.15: Channel capacity for different operating frequencies.

Another observation also shows that the highest frequency in each room is obtained at frequency 3.5 GHz followed by at frequency 4.5 GHz and 6.0 GHz, although the later 2 frequencies shows just a slight different in capacity. Thus, it is concluded that the higher the frequency the lower the capacity of the channel will be. This condition is caused by the distance, d between each antenna in a point, for both transmit and receive antenna. As the frequency gets higher, the distance will be smaller thus the correlation between antennas in each point will be higher. As the arrangement for transmit antenna in this simulation was in diamond shape, the

influence of the radiated pattern towards each other is higher thereby lowering the overall capacity in the room.

3.4 Channel Capacity and the Radiation Pattern

In the preceding section, simulations on channel capacity were done and discussed in consideration of the room, the beamwidth and the operating frequency. All the simulations were executed the same room condition where the transmit antenna was in diamond shape and was fixed at the center of the room. However as revealed by results in previous section, the beam-pattern antenna is capable of enhancing the capacity in the room in a few situations, higher than the capacity of dipole antenna. Considering these findings, in this section the configuration for channel capacity simulation was arranged with the benefit to the shape of the radiation pattern instead, which is beam pattern. The transmit antenna was fixed in a few different position other than the center of the room.

If we consider the radiation pattern for dipole antenna which has donut shaped pattern, it is obvious that the antenna should be place at the center of the room where the antenna radiates in all direction and covers wider area. However, if we consider the radiation pattern and the property of beam-pattern antenna in which the beam is focused to an angle and the coverage is depended on HPBW, it is evident that the beam-pattern antenna should be placed either at the wall or the corner of the room instead of at the center. This approach will utilized the beam characteristic to the fullest and therefore further increase the capacity especially in bigger area.

The simulation was done at frequency 3.5 GHz, for 4 x4 MIMO systems in all 3 room sizes. The receive antenna was fixed into one arrangement which was in vertical line. The transmit antenna was considered for 4 different positions with respect to benefit for beam-pattern antenna and the arrangement is shown in Figure 3.16. In Position A, the transmit antenna was fixed as the same arrangement as the previous arrangement as a standard for comparison in channel capacity improvement while in

Position B the transmit antenna was fixed at the x-axis of the wall creating the longest distance coverage in Y direction. In Position C contrary to Position B, the transmit antenna was set at the Y-axis of the wall creating widest coverage in X direction instead. Finally in Position D, the transmit antenna was fixed at one corner of the room generating equal coverage in both X and Y direction. The transmit antenna used dipole antenna and beam-pattern antenna for all 60°, 90° and 120° HPBW.

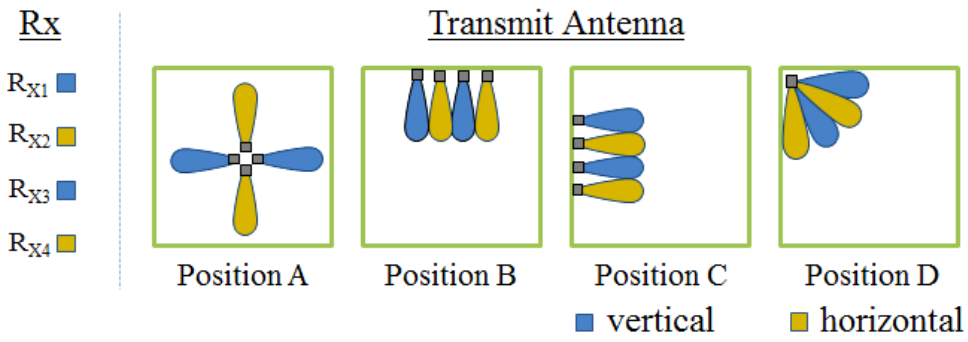

Figure 3.16: Different arrangements for transmit antenna position.

Table 3.10 shows the channel capacity results in comparison of transmit antenna position for different radiation pattern in all room sizes.

Table 3.10: Channel capacity results for different transmits antennas position.

Tx		Size A	Size B	Size C
Position A	Dipole	32.46	24.19	20.64
	Beam 60°	34.60	23.55	16.26
	Beam 90°	34.83	24.44	17.84
	Beam 120°	34.46	24.39	18.38
Position B	Dipole	31.34	22.16	16.72
	Beam 60°	37.23	26.56	19.60
	Beam 90°	35.98	26.56	19.56
	Beam 120°	35.28	26.06	19.14
Position C	Dipole	31.53	21.83	16.57
	Beam 60°	36.04	25.03	18.28
	Beam 90°	36.48	25.71	19.86
	Beam 120°	36.24	25.56	20.33
Position D	Dipole	32.00	22.37	16.13
	Beam 60°	37.01	25.66	18.62
	Beam 90°	36.02	25.34	18.96
	Beam 120°	35.26	24.70	18.55

In general, all the capacity for beam-pattern antenna for new transmit antenna position exceeds the capacity in Position A and according to this finding alone already proves that the channel capacity can be enhance using beam-pattern antenna. The highest capacity is obtained in Position B for 60° beam-pattern antenna at 37.23 bit/s/Hz, providing 7.6% increment as compared to previous capacity as shown in Position A. And although in overall the lowest capacity is still given by the biggest room by beam-pattern antenna in Position A for 60° beam-pattern antenna at 16.26 bit/s/Hz, the capacity results for biggest room becomes noticeably increases for all beam-pattern antenna approaching the results for dipole antenna in Position A. This is the biggest achievement as we managed to address the problem in previous section and increases the capacity for beam-pattern antenna in the biggest room.

Figure 3.17 shows the capacity distribution for every position of the transmit antenna in the smallest room, for all type of radiation patterns. In one look, aside from dipole antenna all the beam-pattern antenna give better distribution with stronger signal coverage. What more interesting is almost half of the room receives strongest signal for all beam-pattern antenna for all Pattern B, C and D, where this condition didn't occurred at all in Position A regardless the type of the antenna. This figure also confirmed that channel capacity for beam-pattern antenna is higher as compared to dipole antenna when the position was manipulated with benefit to radiation pattern.

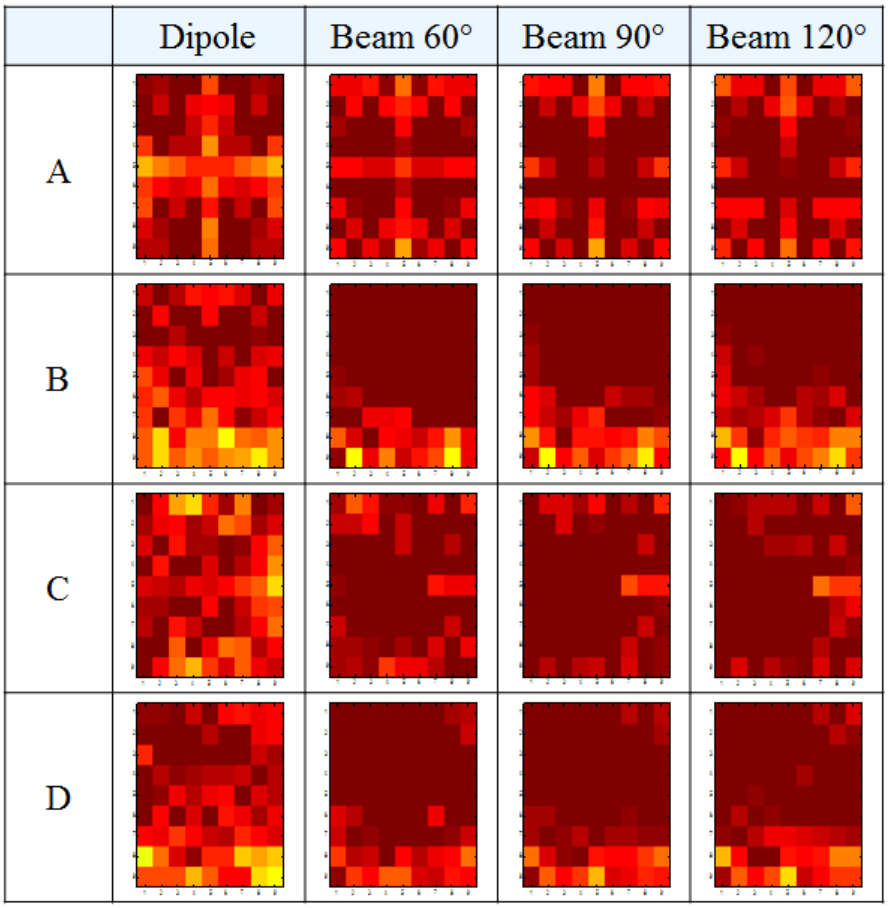

Figure 3.17: Capacity distribution for the room Size A in comparison of transmit antenna position.

Figure 3.18 shows the capacity distribution for different position of transmit antenna in the middle room. The capacity distribution shows similar pattern as the distribution on the smallest room but with gradually less strength in signal as compare to smallest room. Even so, the capacity distribution as well as the strength is better and improved for beam-pattern antenna as compared to previous arrangement in Position A. The results also show that the beam-pattern antenna has better capacity distribution than dipole antenna when the transmit antenna was arranged in position beneficial according to its radiation pattern.

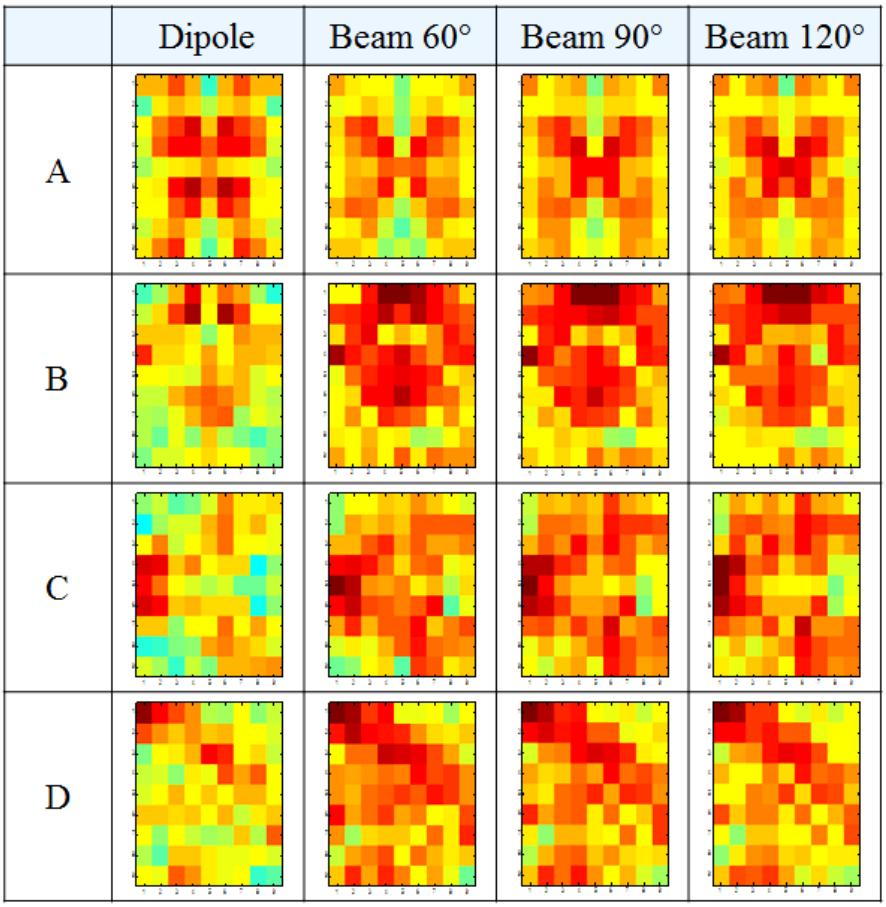

Figure 3.18: Capacity distributions for the room Size B in comparison of transmit antennas position.

Subsequently, Figure 3.19 shows the capacity distribution for different transmit antenna positions in the biggest room. The channel capacity results shown in Table 3.10 reveals that the capacity for beam-pattern antenna improved as we changed the transmit antenna position to the wall or the corner of the room. This improvement can be seen in the figure as well as the strength of the signal gets stronger especially for Position B as compared to Position A. Unfortunately, this stronger signal is still incapable to reach the end of the room as we can see many shadowed regions in Position B and D especially. Thus, it is concluded that although Position B gives higher capacity with stronger signal, Position C covers wider area with comparable channel capacity as Position B. From the figure also it is confirmed that dipole antenna in Position A gives equal capacity distribution in bigger area.

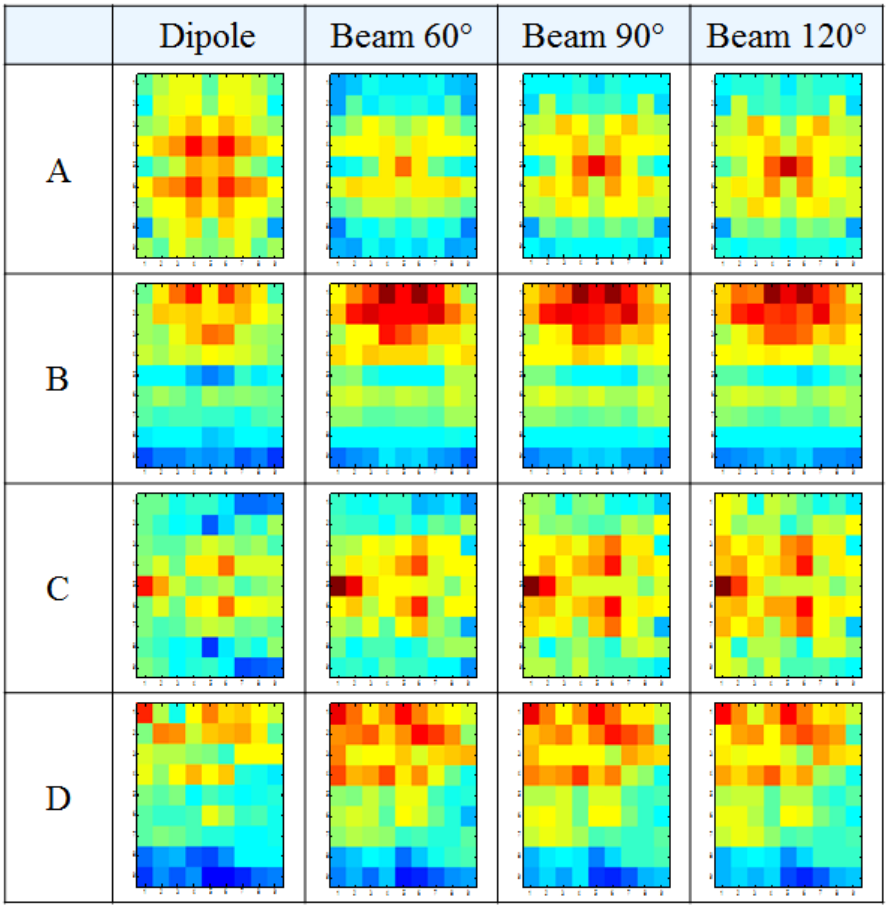

Figure 3.19: Capacity distributions for the room Size C in comparison of transmit antenna position.

Figure 3.20 shows the channel capacity comparison for different position of transmit antenna in all 3 rooms. The blue line represents the smallest room, the red line represents the middle room and the green line represents the biggest rooms. From the figure we can summarize that the channel capacity for beam-pattern antenna is improved and higher than dipole antenna even as the room gets bigger for Position B, C and D, unlike the previous results as in Position A. By manipulating the radiation pattern of the beam-pattern antenna according to optimum position, the capacity of the channel can be enhanced, higher than the capacity in Position A even for a bigger area.

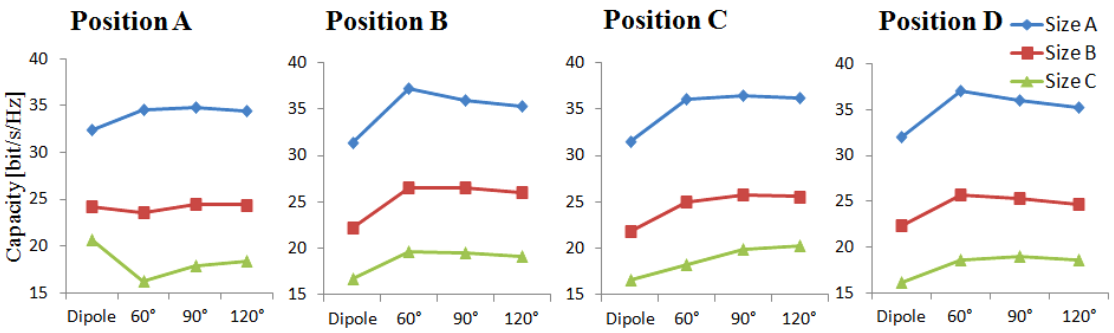

Figure 3.20: Channel capacity comparison for different transmit antenna position.

3.5 Summary

In this chapter, the channel capacity corresponds to MIMO system was discussed and simulated according to various conditions and arrangements. The theory for channel capacity calculation was discussed first before the simulation results are discussed in the later section. Among the results, it was proven that multi-antenna system gives higher capacity than single antenna system. The correlation between each antenna in one point for both transmit and receive antenna presents an important factor in channel capacity as lower correlation provides higher channel capacity. From the results, it was concluded that as the room gets bigger, the capacity gets lower especially when the transmit antenna was placed in the center of the room. Although the channel capacity for dipole antenna especially in the biggest room outperforms the channel capacity for beam-pattern antenna, it was still showed that the beam-pattern antenna can increase the channel capacity even with smaller HPBW. Furthermore, when the transmit antenna was placed with benefit to the radiation shape of beam-pattern antenna, a huge improvement was achieved especially in the biggest room as well as overall increment in all the rooms as compared to dipole antenna. Moreover, in the smallest room half was covered by the strongest signal equally as described in capacity distribution results. As a summary, the channel capacity can be enhanced using multi-antenna system employing beam-pattern antenna with higher capacity than dipole antenna.

CHAPTER 4

A LOW PROFILE DIRECTIONAL ANTENNA WITH DUAL POLARIZATION

4.1 Overview

In the previous chapter, we already demonstrated that high channel capacity can be developed by employing MIMO technology. In this study, we particularly focused on optimizing the radiation pattern and polarization as a method to enhance the channel capacity. Thus, it is important to encompass these factors into antenna design so that we can produce an antenna with good radiation pattern and polarization that will help improving channel capacity as a whole. One of an important design consideration is of course high performance characteristics but miniaturization is as well. A low profile structure is most desirable because it will be easy to install and the overall costing will be economical. However, a notable problem regarding miniaturization of an antenna is mutual coupling of the inter-element. As the size of the antenna becomes smaller, the arrangement of the antenna elements especially the spacing between the elements will be small and narrow and this condition will increase the mutual coupling between the elements instead. This issue can be addressed separately and one of the methods is by using a matching network as reported in [58]. However, this method will be unnecessary when we can design an antenna that is small enough in size without reducing the channel capacity and effectively utilizing it polarization [5], [6], [59]–[61].

At the moment however, only few studies have examined miniaturization with consideration of radiation patterns, particularly the design of low profile antenna with directive patterns.

In this chapter, a low profile directional antenna intended for small base station is presented, as an antenna that can produced directional, dual polarization antenna that will enhanced the capacity in a channel as was discussed in Chapter 3. Although there are similar researches regarding this topic as reported in [5], [6], [60], [61], this antenna is designed with an emphasis on radiation pattern instead. An unlike the MIMO antenna that is previously designed considering radiation pattern in [59], our priority is to produce a more directive pattern in both vertical and horizontal polarization plane. In the previous research, a BS MIMO antenna mounted on the ceiling for downlink transmission had being evaluated and it is demonstrated that the directive radiation patterns with a tilted angle in downward direction are effective for enhancing SNR and channel capacity compared with a sleeve antenna configuration [62]. The MIMO antenna used in [62], which is 30 mm in height was constructed using cavity-backed slot antenna as vertical element and dipole antenna as horizontal element was proposed in [63]. Although dual polarization was achieved in [63], partitions needed to be used inside the cavity in 4 elements adaptation to suppress mutual coupling.

In this study however, we utilized a dipole as the horizontal element and a loop antenna as the vertical element with much lower height at 18 mm. And by using a loop, the need for cavity and partition is eliminated and the design became much simple and with low mutual coupling too. The antenna configuration also was fed independently, which eradicated the need for complex feeding circuit such as phase shifter for example. The design also provides a space in the center of the structure which can be utilized according to desirable applications. Previously, a similar antenna with resonance frequency of 2.4 GHz was discussed in [64] but in this chapter we discuss instead an antenna that is operating at 3.5 GHz, with lower structure in height and also at much lower mutual coupling.

The design for dual polarization directional antenna is carried out according to these conditions with the target output of the radiation pattern is summarized as in Figure 4.1;

- Operating frequency 3.5 GHz spectrum band
- Two orthogonal polarization for 4 x 4 MIMO system
- Vertical and horizontal polarization, where it can be switched independently and simultaneously
- The tilt angle relative to the horizontal plane which is downward elevation angle is equals to 30°
- The HPBW of the antenna characteristic is less than 80° in both vertical and horizontal polarization.

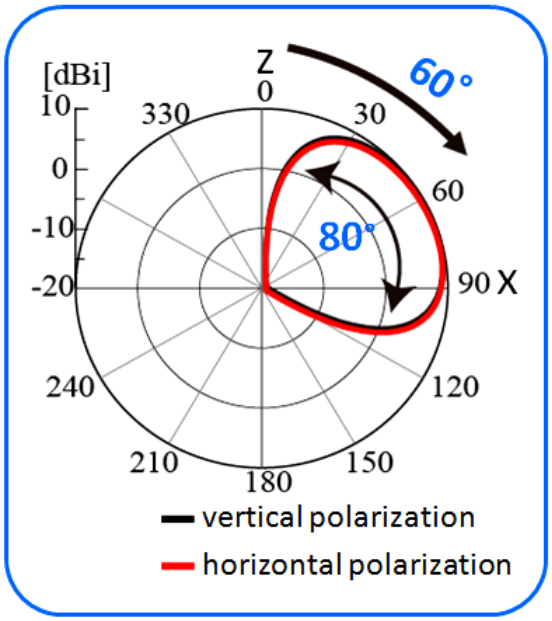

Figure 4.1: Target output for radiation pattern.

4.2 Low Profile Vertical and Horizontal Elements

The most common antenna that can provide a vertical polarization element is a monopole antenna mounted on a ground plane. The characteristics for monopole are actually quite similar to dipole, if not because of the existence of the ground plane. And although the radiation above the ground plane is similar to dipole, the fields below the ground plane are zero with the impedance of one half of that of a full dipole antenna.

The absence of radiation or field below the ground plane makes the antenna effectively twice as directive as dipole antenna instead. The presence of ground plane also effecting the radiation patterns in which it radiates in a slanted direction, away from the horizontal plane. Although the resulting radiation pattern is still omni directional, the direction of peak-radiation has changed from the xy-plane to an angle elevated from that plane [65].

Initially from monopole antenna, there are many antenna with similar but adjusted characteristics that has been introduced such as quarter-wave monopole antenna, horizontally folded monopole antenna, inverse-L antenna and inverted F antenna. However, in this study we elected a loop antenna as a suitable presentation of the vertical polarization element in the antenna structure.

4.2.1 Loop Antenna as Vertical Polarization Element

In the initial stage of the study, we need to confirm the vertical element of the antenna structure. Loop antenna was chosen because it is vertically polarized with tilted radiation pattern without having to feed using phase shifter. However, a single loop antenna on a ground plane has a bi-directional pattern in x-plane axis as shown in Figure 4.2(a). Therefore, we need to concentrate the radiation emitted from above the ground plane to a specific direction and this can be done by a simple method of placing the reflector parallel to the loop antenna. When the reflection plane is sufficiently large, it is possible to narrow the directivity into a single direction as shown in Figure 4.2(b).

A single loop with a reflector was designed first to confirm its antenna characteristics as shown in Figure 4.3. The loop was mounted on a square ground plane that had the dimension of 220 x 200 mm (2.57λ). It was fixed at one of the 4 corners of the ground plane to make room for other arrays, with the distance of 55 mm (0.64λ) from the edge of the plane. The height and the length of the loop antenna were 10 mm (0.12λ) and 15.5 mm (0.18λ) respectively. A reflector was added to the structure, 35 mm from the loop antenna towards the center to suppress and shape the radiation pattern into beam-like pattern and tilted into an angle. The addition of the reflector had shifted the resonance frequency of the antenna to a lower frequency,

thus it was necessary to adjust the length of the reflector accordingly while at the same time, the length of the reflector also controls the tilted angle of the radiation of the array. The height of the reflector was fixed to 10 mm as the loop antenna and the length of the reflector was 16 mm (0.19λ).

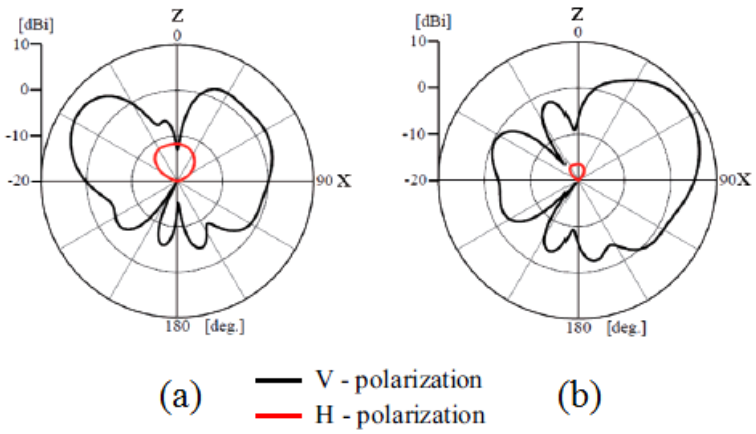

Figure 4.2: Radiation pattern in xz-plane for (a) loop antenna and (b) loop antenna with reflector.

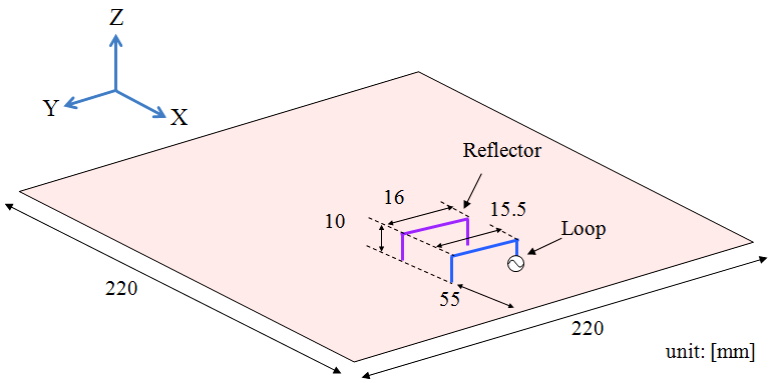

Figure 4.3: Layout of a single loop antenna with a reflector.

The reflection characteristic of the single loop array is shown in Figure 4.4 where it is confirmed that the resonance frequency is at 3.5 GHz with S_{11} reading at -18.79 dB and the bandwidth is more than 200 MHz at -10 dB which shows a broadband characteristic. A good vertically polarized radiation also is obtained at 3.5 GHz where the horizontal polarized wave is sufficiently suppressed as describes in red line in the figure. The radiation characteristic of the vertical polarization wave is

confirmed as in the figure with the tilted angel at 46°, HPBW of 53° and the gain of 7.2 dBi. From these results we confirmed that the loop array gives the vertical polarization element to the antenna structure.

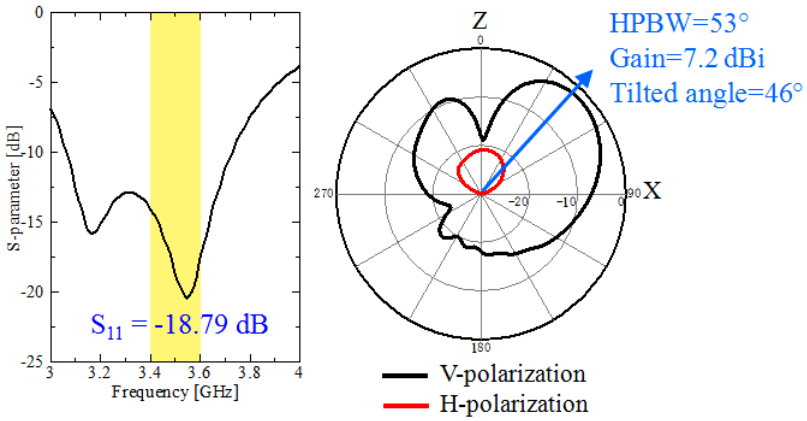

Figure 4.4: Antenna characteristics for loop array.

Another three pairs of loop array were added and arranged symmetrically opposite to each other to produce another 3 additional arrays, thereby radiation patterns, realizing 4 beams in vertical polarization in 4 different directions. When all the radiating elements were fed independently but simultaneously, we found that the additional arrays give similar patterns as the first one where there is only slight difference in performance. These output performances are able to be maintained simply by adjusting the length of the loop antenna and the distance between this feeding element and the edge of the ground plane, without altering the height of the element. This new structure realized an antenna with 4 vertically polarized beams in 4 different directions.

4.2.2 Dipole Antenna as Horizontal Polarization Element

Upon successfully confirming the characteristics of vertically polarized element with desired results, the next step was to add the horizontal polarization element into the structure to form dual polarization elements as targeted. At first, only one element of dipole array was mounted on the ground plane, added with a dipole antenna and a director defined by black and red element in Figure 4.5. The dipole array was added

parallel to the loop array with the height of the array at 15 mm (0.18λ) and the length of the dipole antenna and the director was 18.5 mm (0.22λ) and 19 mm (0.22λ) respectively. The dipole antenna was positioned at 35 mm (0.41λ) from the edge of the ground plane and the distance between each of the element in the arrays, loop and reflector and dipole antenna and director was 25 mm (0.29λ). A director, similar to a reflector concentrate the wave emitting from dipole antenna that originally has omni directional radiation pattern to a specific direction and forms a beam pattern instead.

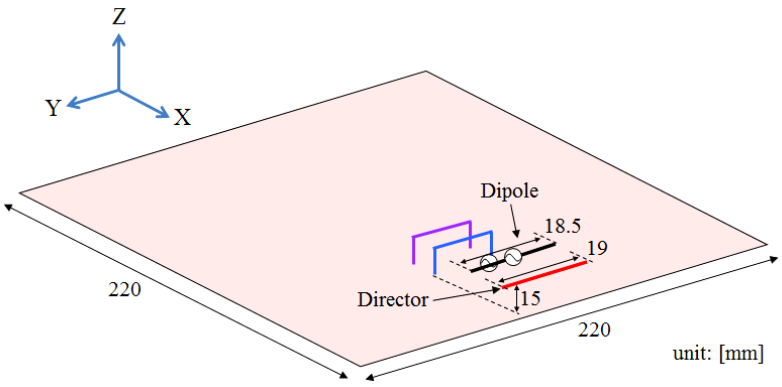

Figure 4.5: Layout of a loop array and a dipole array mounted on ground plane.

Figure 4.6 shows the antenna characteristics for the antenna structure after the dipole array was added. The reflection characteristic shows that both loop array and dipole array resonance at 3.5 GHz with S_{11} for loop antenna is -18.8 dB while the dipole matched at much lower value at -13.9 dB. The bandwidth however shows a significant different between the loop and dipole antenna at -10 dB but it is still wide enough to be considered broadband. The mutual coupling between these two elements also is very low at -30.6 dB.

When only the feeding element of the dipole was mounted, the emitting wave forms a half circle shape pointing to z-direction due to the reflection from the ground plane. The director was mounted to tilt the obliquely upward beam as obtained and showed in the Figure 4.6. The radiation pattern characteristic shows that the dipole antenna tilted at 45° with the HPBW of 81.6° and the gain of 7.54 dBi while the characteristic for loop array is the same at previous results. Comparing with Figure 4.4, we noticed that although the beam is tilted at around the same angle the HPBW and the gain of the dipole antenna has bigger values. Reviewing the target of the study

which is to obtain similar and comparable results especially in term of radiation pattern characteristics, marginally bigger result for dipole array raised an issue which will be address later as we progress towards the study.

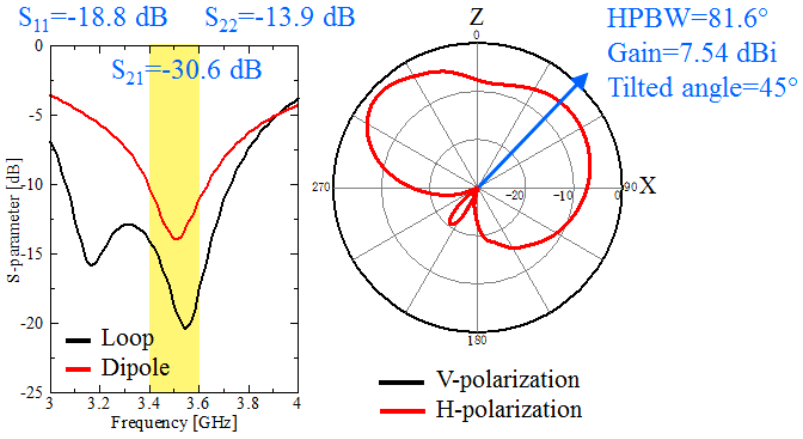

Figure 4.6: Antenna characteristics for dipole array.

The combination of dipole antenna and another antenna such as slot antenna or even loop antenna is not exactly a new approach in designing dually polarized antenna principally because dipole antenna easily delivers good characteristic together with simplicity in configuration as horizontal element. Nonetheless, in this design the loop and dipole antenna is fed independently using just simple feeding circuit and efficiently produced dual polarized element for the antenna design. The lengths of the arrays were adjusted accordingly respective to its reflector or director while looking at the radiation pattern as it controls the tilted angle of the radiation. The impedance for dipole was matched by adjusting the height of the dipole array as the resonance frequency increases and shifted to higher value as the height gets smaller, making it difficult to match the impedance properly.

The reflection characteristics in Figure 4.4 and Figure 4.6 show the same value for $S_{11,loop}$ even after the dipole array was added. This result confirmed that the added dipole array has a very small influence on the loop array and this exhibits as one of the important benefits of using dipoles as horizontal polarization element aside from simple and easy configuration. This analysis is important to confirm the influence of both vertical and horizontal elements against each other.

4.2.3 Four Arrays of Loop and Dipole Antennas

Upon confirming the antenna characteristics for both vertically and horizontally polarized elements, the other 3 pairs of loop and dipole arrays were added into the structure to complete the dually polarized 4 radiation patterns in 4 directions. Vertically polarized element consists of a loop antenna and a reflector while horizontally polarized element was composed by a dipole antenna and a director. Figure 4.7 shows the complete antenna structure in two dimensional, from xy- and xz-axis. The loop antennas which are the blue line in the structure were denoted as Port 1 to Port 4 while the dipole antennas which are the black line were denoted as Port 5 to Port 8. The reflector and director were described in purple line and red line respectively. The height and the length of the arrays were kept as the preceding measurement as from the previous analysis we already confirmed that the results is acceptable. The distance from the center to the reflector was 25 mm, while from reflector to loop antenna, loop antenna to dipole antenna and dipole antenna to director was 30 mm, 20 mm and 25 mm respectively. The dimensions of the elements were optimized accordingly to produce the best antenna characteristics out of this structure.

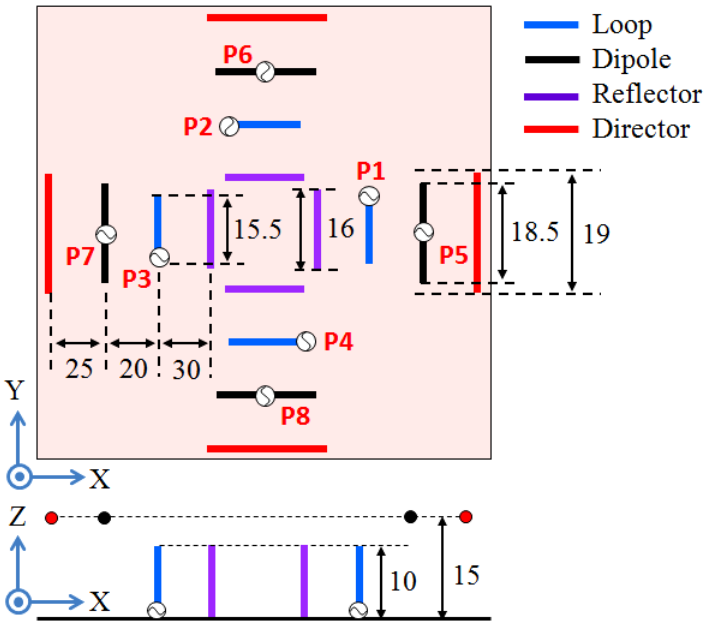

Figure 4.7: Layout of four arrays of loop and dipole structure.

The simulation process was done for all the ports, Port 1 to Port 8 to evaluate the antenna performance as well as to verify that all the vertical and horizontal elements give the similar results to each other. Encouragingly we found that all the antenna arrays provide identical output performance in both the reflection characteristic and radiation patterns. Figure 4.8 and Figure 4.9 shows the antenna characteristics for Port 1 and Port 3 representing vertically polarized element and Port 5 and Port 7 representing horizontally polarized element. From the figure we confirmed that all the S_{11} parameters, $S_{11,loop}$, $S_{33,loop}$, $S_{55,dipole}$ and $S_{77,dipole}$ is below -10 dB at 3.5 GHz. The bandwidth for loop array is wider than the dipole array approaching 200 MHz and 100MHz respectively. Although the impedance is just about -11.6 dB, the mutual coupling results show a good performance where the mutual coupling between vertical and horizontal (S_{51}), horizontal and vertical (S_{15}), vertical and horizontal element in the opposite side (S_{71}) and horizontal and vertical in the opposite side (S_{71}) is very low at below -40 dB. These readings show that the mutual coupling between the adjacent antenna and the opposing antenna is very good which is desirable for MIMO configuration.

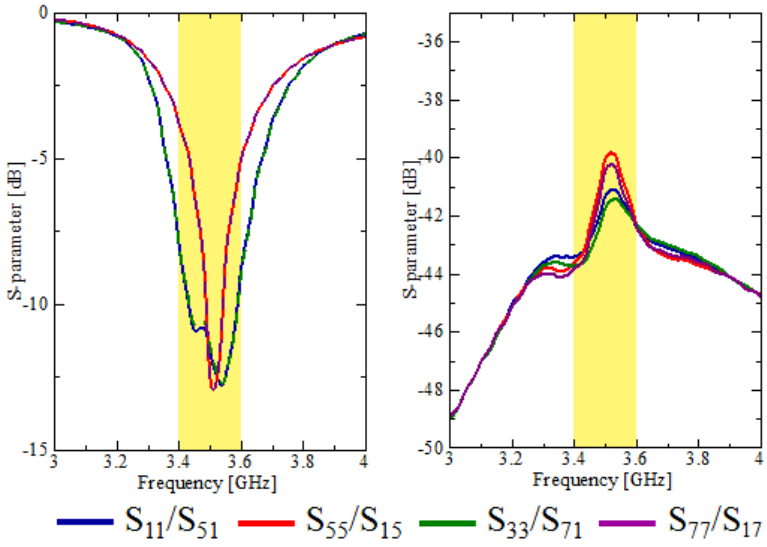

Figure 4.8: Reflection characteristics of the four array of loop antennas structure.

In term of radiation patterns in Figure 4.9, we confirmed that all the vertical elements as well as the horizontal elements emitting identical radiation patterns to each other. The vertically polarized patterns are showed in black line for Port 1 and Port 3 while the horizontally polarized patterns in red line representing Port 5 and

Port 7. The direction of the patterns are opposite from each other showing the opposite location of the antenna. Although the tilted angle for loop antenna and dipole antenna is similar which is around 55°, the gain for loop antenna is slightly smaller with 6.93 dBi as opposed with 7.54 dBi. Unfortunately, the HPBW for dipole antenna is way much bigger passing over 80° while the loop antenna reading at 56°. Looking at the figure at a glance also confirmed that the target to obtain similar pattern for both vertical and horizontal element could not be achieve using this configuration. Although the HPBW of dipole antenna need to be improved, it is confirmed from these favorable results that with just simple structure, we can produce a dual polarization antenna with good performance characteristics.

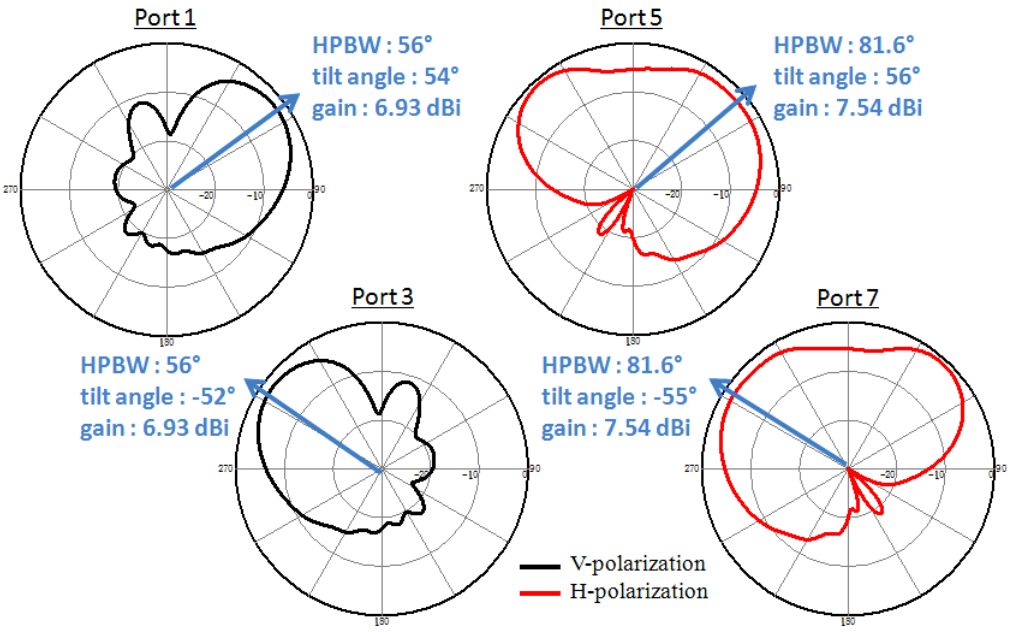

Figure 4.9: Radiation patterns for loop arrays and dipole arrays of the antenna structure in xz-plane.

4.3 Design Improvement

In the preceding section, we have discussed the initial configuration for antenna structure with reflector and director as a waveguide, guiding and shaping the antenna pattern into beam-like pattern while tilting it into a direction. We have also confirmed that the symmetrical structure gives the similar characteristic for each array of loop

and dipole antenna and as a result 4 orthogonal directional patterns are obtained with similar characteristic performance. Using these knowledge, in the next section we will discuss the improvement of the antenna design to address the arisen problem in both reflection characteristic and radiation characteristic.

4.3.1 Design Improvement with Added Reflector

In the first stage of the design, all the basic requirements are fulfilled but without satisfying results. There is a different in value for gain and much worse for HPBW value between vertical and horizontal element that yield a problem as the loop array will be underperformed by the dipole array. In fact, the radiation pattern for dipole antenna still shows a pattern similar to a single dipole antenna with omni directional pattern rather than beam-like pattern. Considering that the problem lies on radiation pattern rather than matching the impedance, we considered adding another reflector to the radiating element especially dipole antenna to improve the radiation pattern.

A reflector was first added to the antenna structure composing a loop antenna and a reflector for loop array and a dipole antenna, a director on the outside and a reflector on the inside of the ground plane for dipole array. This combination represents one corner array in the whole antenna structure. As the length of the elements control the pattern of the emitted wave, the length was adjusted accordingly while at the same time matching the impedance at 3.5 GHz. However, we found that the additional reflector not only conform the pattern for dipole array but loop array as well. The reflection characteristics also get affected by the extra element where it was hard to match the impedance for both loop and dipole array.

Thereby, the height of the dipole array was adjusted to 18 mm (0.2λ) while for loop array was maintained at 10 mm (0.12λ). Another reflector also was added to loop array to recompense the affected pattern and amend it to an acceptable pattern according to the predetermined target. As we need to set the distance between the radiation elements as large as possible so that the mutual coupling will be as low as possible, the loop antenna was placed at 50 mm (0.58λ) from the center while the dipole antenna at 75 mm (0.88λ), with the distance at 0.29λ from each other. Figure 4.10 shows the complete layout of the antenna structure in both 2 and 3 dimensional.

The 2 dimensional layouts in xy-axis shows only 2 complete arrays of loop and dipole for easier explanation. The dimension for each element was optimized with the priority on the radiation characteristics performance. The distance between the loop arrays was adjusted to be closer at 6 mm (0.07λ) with loop antenna in blue line, reflector in purple and the added reflector in green line. The length of the array was fixed at 25 mm (0.29λ) for loop and 24.5 mm (0.29λ) for reflectors. On the other hands, the distance between the dipole arrays was set at 19 mm (0.22λ) with dipole antenna in black, director in red and reflector in green line. The length of dipole antenna was optimized at 41.5 mm (0.48λ) with both director and reflector at 43 mm (0.5λ).

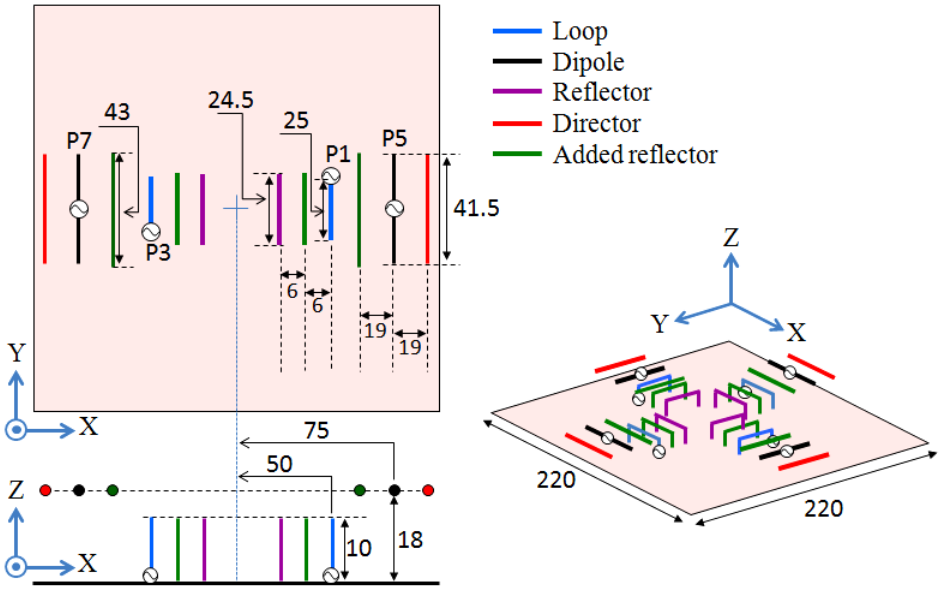

Figure 4.10: Layout of improved antenna structure.

The antenna characteristic performance is shown in Figure 4.11 with describe the characteristic for Port 1_{loop} and Port 5_{dipole} only as representation of vertical and horizontal element respectively as the other ports also shows same characteristics due to the symmetrical property of the structure as confirmed in previous analysis. Interestingly, the added reflector gave benefit to dipole antenna and influenced the characteristic of dipole array only without really affecting the characteristic of loop array considering the small distance between the two radiating elements as shown in the figure. This was achieved because for loop array, the null pointed towards z-direction is small enough and un-affected by the existence of the reflector. The HPBW for Port 1_{loop} decrease from 56° to 53.3° from previous configuration while for Port

5_{dipole} also decreases from 81.6° to 69°. This result shows a huge improvement for dipole array which is the main target for this design improvement. The tilted angle however increase from 54° to 57.9° and 56° to 59.6° respectively, which a little bit disappointing although it is still below 60°. The gain however, has been increases from 6.9 dBi to 8.52 dBi and 7.54 dBi to 9.96 dBi respectively. Although this shows a favorable result, there is about 1.44 dBi different between Port 1_{loop} and 5_{dipole} which should be aware of. However, the cross polarization are sufficiently low, and directional patterns with suppressed backward radiation are obtained. From these results we can see the improvement in the performance of each array as we confirmed the similar radiation pattern characteristics for both vertical and horizontal element.

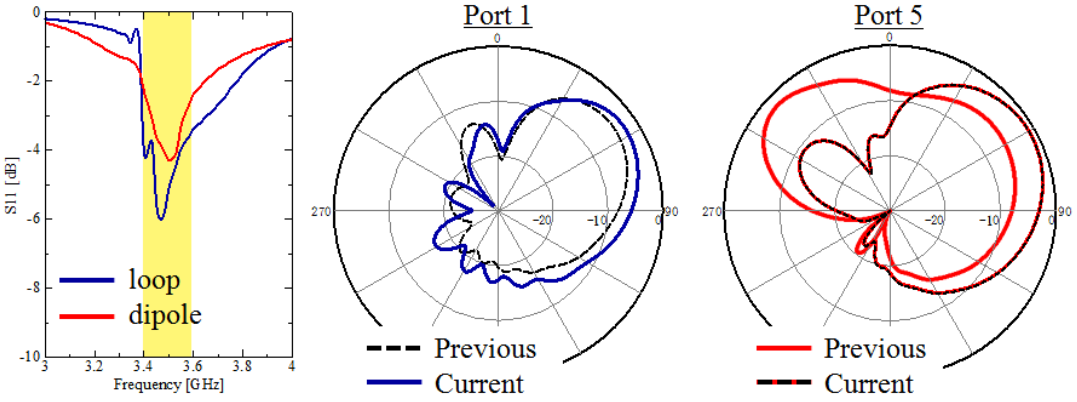

Figure 4.11: Reflection and radiation characteristics for improved antenna configuration.

Unfortunately however, the reflection characteristic obtained from this structure is not as good as the previous structure as the S_{11} result for Port 1_{loop} and Port 5_{dipole} read at -6 dB and -4 dB respectively. This result is highly influenced by the length of the elements as it controls the matching of the impedance for the radiating elements. At the same time however, the length also affect the shape of the tilted beam that we opted to produce better results for the radiation pattern instead of the reflection characteristics. However, this issue will be addressed later in the final stage of the design as we need to match the impedance below -10 dB.

In this configuration, another reflector was added for both loop array and dipole array making each array consists of three elements. Although the element itself was really simple to produce with a line of wire or a folded wire, it was still favorable if we can reduce the number of element in each array and make the structure simpler.

However, as the target is to reduce the HPBW for dipole array and turn the radiation pattern into a beam-like pattern, this configuration is acceptable if not because of the high reflection characteristic value. As a result, we managed to improve the radiation pattern for dipole array without altering the previous pattern for loop and with higher gain. However, the reflection characteristic is not very good and need to be improved instead.

4.3.2 Design Improvement with Printed Dipole

In the previous two antennas structure that has been discussed before, we have confirmed the favorable results in radiation pattern where we are able to produce orthogonal directional pattern with quite similar characteristic performance. However, there is a problem in the reflection characteristic where S_{11} for both arrays is less than -10 dB which is not good enough. One of the methods to improve the reflection characteristic is by using a printed dipole instead of just as simple wire dipole. Also, if we want to make a prototype out of the design, a printed dipole is favorable as the feeding line structure of the dipole antenna is not considered for simplicity. Therefore, in the final stage of the design we replaced the dipole antenna with a printed dipole antenna instead.

A printed dipole was constructed using an FR-4 substrate where a dipole shape was printed on both sides. The substrate had a dielectric of $\mathcal{E}_r$ = 4.5, the thickness of 1.6 mm with the microstrip line as feeding line. The configuration of the printed dipole is shown in Figure 4.12. Towards the ground plane, the microstrip conductor increases in width from 1 mm to 4 mm forming a tapered shape where it functions as a balun. The height of the printed dipole antenna was fixed at 18 mm (0.2λ) as for dipole antenna. The width is fixed at 6 mm (0.07λ) while the length from the center is optimized at 17.75 mm (0.21λ). The whole length of the substrate itself was 37.5 mm (0.44λ) and the printed part had 1 mm space from the edge of the substrate. The dimension of the printed dipole was optimized accordingly to produce good reflection characteristic as this is the main target of replacing dipole antenna with printed dipole antenna. Figure 4.12 also shows the reflection characteristic of as compared with dipole antenna when we load the printed dipole antenna alone which reads at -37 dB.

This shows a huge improvement from the previous results which is at -4 dB and completely addressed the issue regarding high S_{11} results in the previous structure.

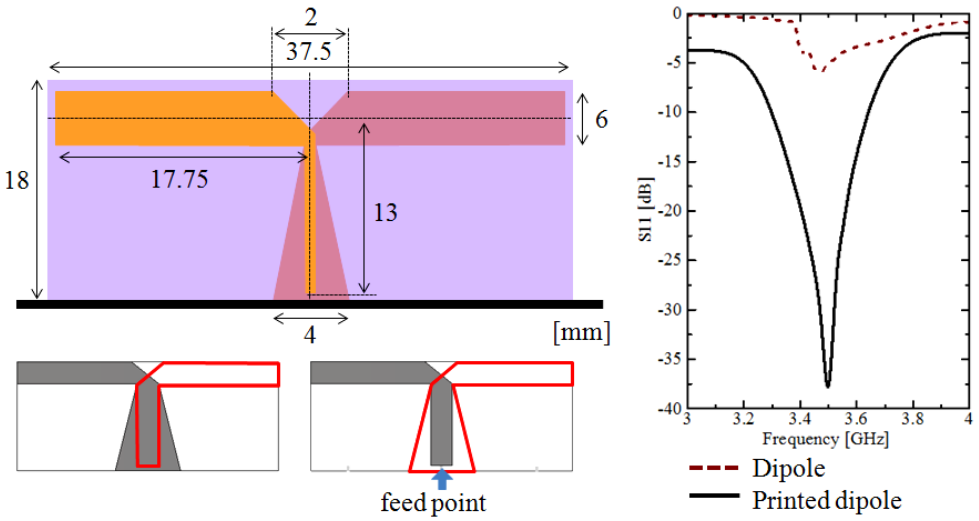

Figure 4.12: Layout of the printed dipole antenna and the reflection characteristic comparison.

Figure 4.13 shows the proposed antenna configuration with printed dipole antenna replacing dipole antenna as horizontally polarized element. As we replaced the dipole with the optimized printed dipole antenna, the other elements also need to be optimized as well as the antenna characteristic changes with the new configuration. Most important, there is a huge improvement in configuration as we managed to reduce the number of element needed in the design. As the printed dipole antenna emitted similar radiation as dipole, it will need both director and reflector to produce directional beam with tilted angle as analyzed before. On the contrary for loop array, only one reflector is needed instead of 2 as compared in previous configuration while at the same time still keep a good characteristic for radiation pattern. This is possible by increasing the distance between the loop and its reflector.

The final configuration for antenna design incorporate dual orthogonal polarization with a loop antenna and a reflector for vertically polarized array and a printed dipole, a director and a reflector as horizontally polarized array. Each element in an array was fixed at the same height which is 10 mm (0.12λ) for loop array and 18 mm (0.2λ) for printed dipole array. The position of the loop antenna was maintained at 50 mm (0.58λ) from the center of the ground plane while the position of the printed dipole antenna was moved to 85 mm (λ) from the center making the director position

exactly at the edge of the ground plane. The reflector was fixed at 30 mm (0.35λ) from the loop antenna while both the director and the reflector were positioned at 14 mm (0.16λ) from each side of the printed dipole antenna. The length of each element was optimized at 29.5 mm (0.34λ) and 30 mm (0.35λ) for loop antenna and reflector and on the other side is 37.5 mm (0.44λ), 36 mm (0.42λ) and 42 mm (0.49λ) for printed dipole antenna, director and reflector, respectively. In the figure also we illustrates the symmetrical arrangement of the array where loop arrays are denote as Port 1 to Port 4 in blue line while printed dipole arrays are denote as Port 5 to Port 8 in purple line. The reflectors are described in green line and the directors in red line. This symmetrical arrangement is capable of producing dually orthogonal beams in 4 direction producing 8 beams in total.

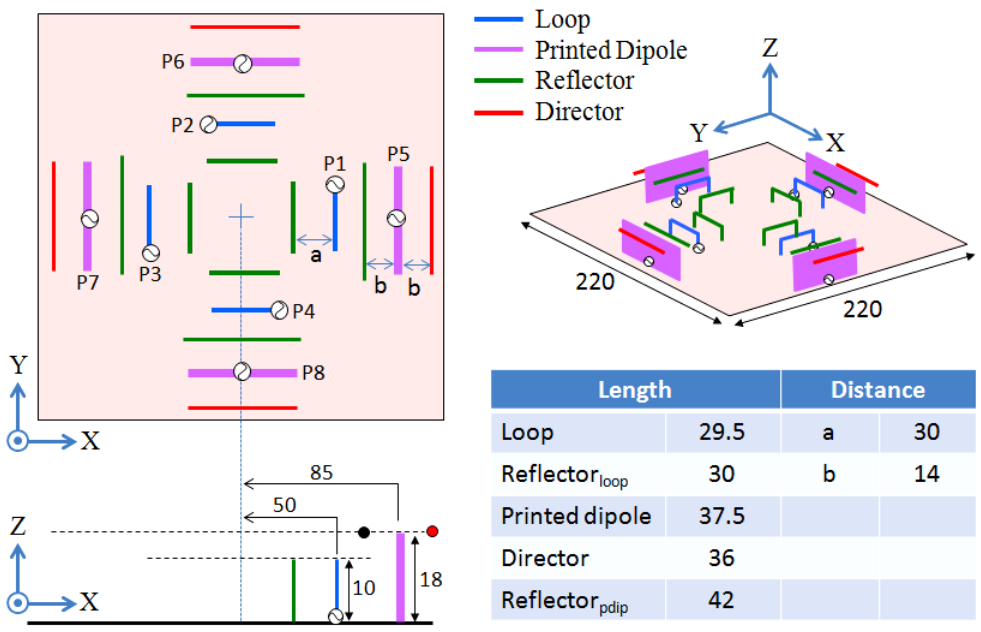

Length		Distance	
Loop	29.5	a	30
$Reflector_{loop}$	30	b	14
Printed dipole	37.5		
Director	36		
$Reflector_{pdip}$	42		

Figure 4.13: Layout of the final structure of the antenna design.

Figure 4.14 shows the radiation patterns for Port 1_{loop} and Port $5_{printed\ dipole}$ in xz-plane with both the radiation pattern tilted at similar angle. The cross polarization for both arrays are sufficiently low, and directional patterns with suppressed backward radiation are obtained. The HPBW for loop array is 55.1° while for printed dipole array is 79.2° which is much bigger if compared between the two. However, it is still within our target which is below 80°. The tilted angle is pointing at 41.8° and 57.9° respectively while the gain reads at 7.02 dBi and 8.02 dBi with just 1 dBi in

different. Although in the figure we only illustrates one pattern for each polarized radiating element, the radiation patterns for other ports also show the same patterns due to the symmetrical property of the structure.

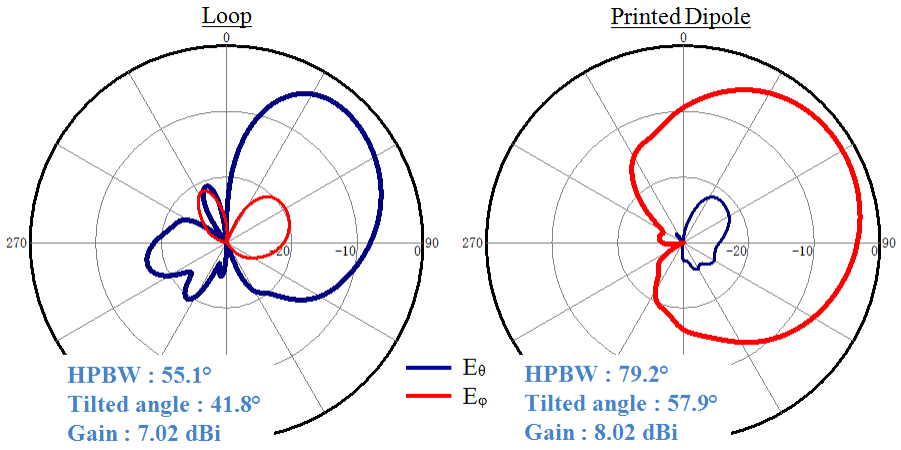

Figure 4.14: Radiation characteristic for the antenna structure.

On the other hand, the reflection characteristic as illustrated in Figure 4.15 shows that the $S_{11,loop}$ and $S_{55,printed\ dipole}$ are at -15.79 dB and -14.2 dB which is sufficiently below -10 dB and a huge improvement from -6 dB and -4 dB from the previous result. The mutual coupling between vertical and vertical elements (S_{21} and S_{31}) are less than -25 dB, while between horizontal and horizontal elements (S_{65} and S_{75}) are very low which is less than -55 dB with. The mutual couplings between vertical and horizontal elements (S51, S61, S71, S25 and S35) are less than -20 dB. Almost all the mutual couplings between the polarization elements are less than -25 dB which is adequately low due to orthogonal polarization. The correlation coefficient result for all the ports is shown in Figure 4.16 which read below 0.001 indicating a very low level of coupling between the ports. These results show that the performance and efficiency of the antenna is very good and addressed all the problems regarding the antenna design.

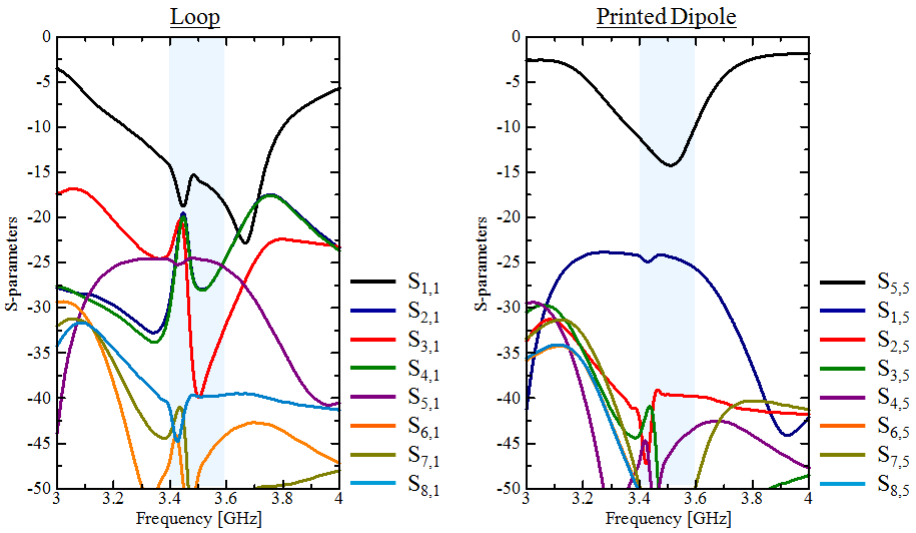

Figure 4.15: Reflection characteristic for the antenna configuration.

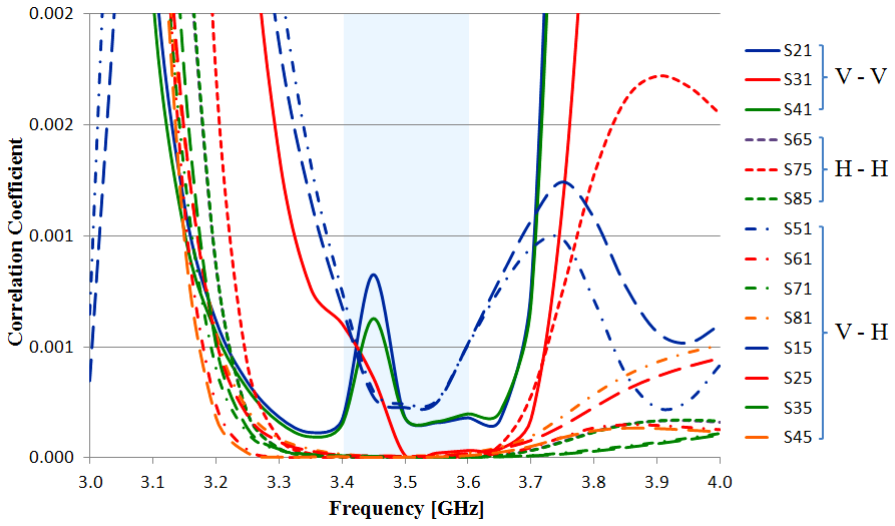

Figure 4.16: Correlation coefficient for the antenna structure.

4.4 Channel Capacity for Dually Polarized Directional Antenna.

As a continuation from Chapter 3, in this section we will discuss the channel capacity calculation using the real radiation pattern obtained from the antenna designed in this chapter. Following the example from previous arrangement where all the simulation were done assuming 4 x 4 MIMO system, this section also will assume a 4 x 4 MIMO arrangement. Therefore 2 vertically radiating element which is loop antenna and 2 horizontally radiating element which is printed dipole antenna were used, represented as Port 1 and Port 3 and Port 6 and Port 8 respectively. Although the simulation arrangement was the same as before in term of the size of the room and the arrangement for receive antenna, the arrangement for transmit antenna will be completely the same as the proposed antenna arrangement with the actually distance between each elements as shown in Figure 4.17. The antenna radiation characteristics for transmit antenna also are according to the proposed antenna results as was shown in Figure 4.14 with the HPBW of 55.1° and 79.2° and the gain of 7.02 dBi and 8.02 dBi for vertical and horizontal element respectively. All the simulations were done at operating frequency of 3.5 GHz.

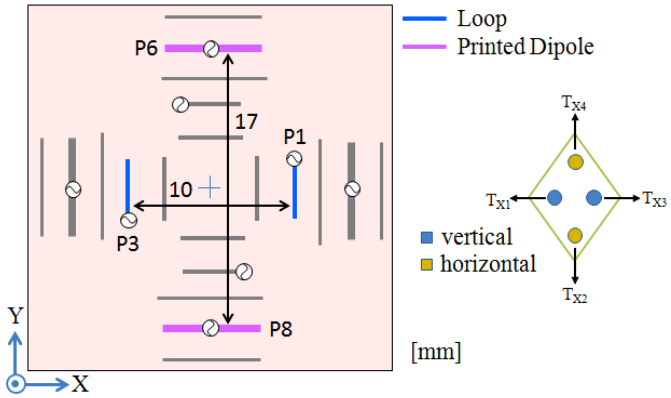

Figure 4.17: Transmit antenna configuration for channel capacity calculation.

As we already confirmed in Section 3.4, higher capacity can be achieved for beam-pattern antenna if the transmit antenna position is manipulated with benefit to the radiation pattern. Thus, in this section the channel capacity for proposed antenna

also was calculated in 3 different positions which is Position A at the center of the room, Position B at the wall in x-axis and Position C at the wall in the y-axis which is illustrated in Figure 4.18. The simulations were done in all 3 room sizes and the discussion covered both channel capacity and capacity distribution with comparison to the dipole antenna.

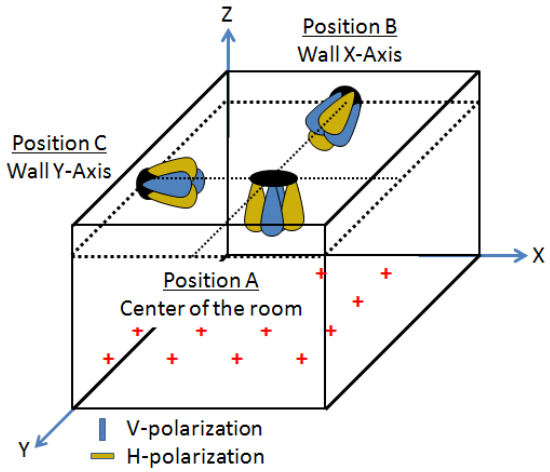

Figure 4.18: Transmit antenna position for channel capacity calculation.

Figure 4.19 shows the channel capacity results for proposed antenna configuration in 3 different room sizes. For the smallest room which is Room A, the channel capacity for beam-pattern antenna is higher than dipole antenna with 36.1 bits/s/Hz as compared to 31.5 bits/s/Hz when transmit antenna was fixed in Position C while higher capacity again is obtained by beam-pattern antenna in Room B when the transmit antenna was arranged in Position B with 25.3 bits/s/Hz as compared to 22.2 bit/s/Hz. Unfortunately however for Position A, the capacity for dipole antenna is higher instead of beam-pattern antenna with 20.6 bits/s/Hz as compared to 18.9 bits/s/Hz.

In term of capacity distribution, in a glance the capacity distribution for beam-pattern antenna gives stronger coverage in the area closer to transmit antenna position including in Position A which the channel capacity for dipole antenna is higher than beam-pattern antenna. The capacity distribution for dipole antenna on the other hand is rather scattered and only gives strong signal in certain receiving points only. The capacity distribution for middle room and biggest room also give similar distributions as Room A although we didn't included the results here.

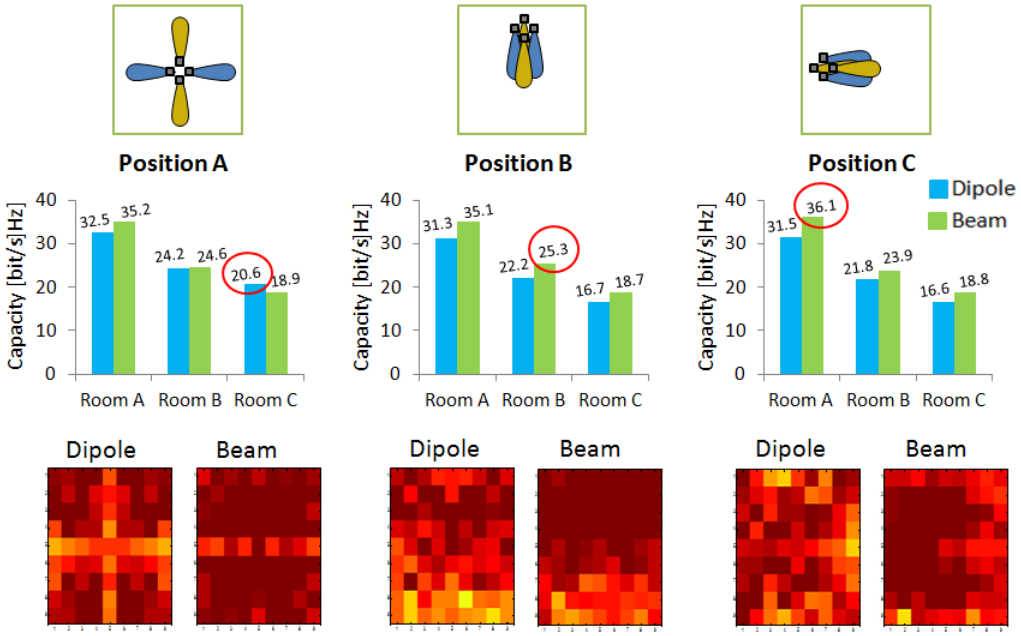

Figure 4.19: Channel capacity results and capacity distribution for proposed antenna configuration.

A low profile directional antenna with dual polarization is capable of producing up to 8 beams, 4 beams in vertical polarization and 4 beams in horizontal polarization. Thus the channel capacity was also calculated using all the 8 beams as transmit antenna but the receive antenna was still kept as the previous arrangement which was 4 antennas arranged in straight line, delivering 8 x 4 MIMO system. The transmit antenna was fixed at the center of the room and the simulation was done in all 3 room sizes, at operating frequency of 3.5 GHz. The results however are compared between the 4 x 4 MIMO modes instead for both channel capacity and capacity distribution.

Figure 4.20 shows the simulation results for channel capacity calculation. As expected, channel capacity for 8 x 4 MIMO give higher results than 4 x4 MIMO in all rooms with 43.37, 32.08 and 25.78 bits/s/Hz for Room A, B and C respectively. We confirmed that although the transmit beam increased twice in number, the increment in channel capacity are not twice as the MIMO mode however. This finding concludes that in normal application, we might not need to use all the beams but it is more practical to use the beams according to application instead. The capacity distribution however shows a strong, even and complete coverage in Room A when all 8 beams were used and distribution also stronger for Room B and C compared to 4 x 4 MIMO although the distribution in the biggest room still shows some shadowed region.

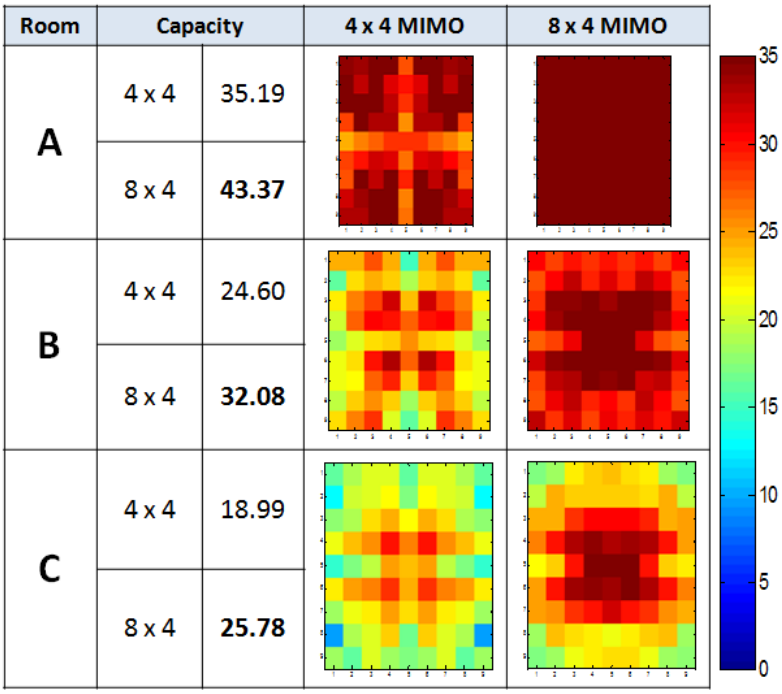

Figure 4.20: Channel capacity and capacity distribution results for 8 x 4 MIMO.

4.5 Summary

In the previous chapter, we have analyzed channel capacity improvement when a beam radiation pattern was used instead of omni direction pattern as in dipole antenna. Thus in this chapter, we proceeded with the discussion on low profile directional with dual polarization antenna as an antenna that is capable of producing dually polarized beam radiation patterns. The proposed antenna was constructed using loop antenna and reflector as vertically polarized element and printed dipole antenna, director and reflector as horizontally polarized element. The combination of these two arrays was arranged in 4 corners of a ground plane in symmetrical arrangement which gives 4 orthogonal directional radiation patterns in 4 different directions. The reflection characteristic and radiation characteristic in each array shows a similar results to each other due to this symmetrical arrangement which in return making it easier for designing process. By designing just a corner of the array, we managed to produce up to 8 beams, with up to 4 beams in both vertical and horizontal polarization. The reflection characteristic was sufficiently low with less than -10 dB and the mutual couplings between all the elements are less than -25 dB.

The reflection coefficients also show a very good characteristic with 0.001 at 3.5 GHz. The HPBW was less than 80° and the tilted angle was within 40° to 60° which was within our original target. As the antenna was fed individually, we can produce the beam according to the state of the mobile station and the desired requirement. As the design presented was originally from [64] but at 2.4 GHz instead, we concluded that the low profile structure of the antenna was flexible as it can be adjusted according to favorable resonance frequency by simply adjusting a few parameter of the element in the array. This discovery is very beneficial as it offers possibilities of not just operating at two but more frequencies.

CHAPTER 5

THREE LAYERS SWITCHED MULTI BEAMS ANTENNA WITH DUAL POLARIZATION

5.1 Overview

In the previous chapter, we have discussed one type of antenna that is capable of producing beam shape radiation pattern which is a low profile directional antenna with dual polarization. This type of antenna is chosen because we particularly focused on optimizing the radiation pattern and polarization as a method to enhance the channel capacity. And high channel capacity can be developed by employing MIMO technology by maximizing channel capacity using radiation pattern and polarization as demonstrated in Chapter 3. Thus one of the specifications for designing an antenna in my research is an antenna with good radiation pattern and polarization that will help improving the channel capacity as a whole. In this chapter, these antenna characteristics are achieved through switched beam system.

Smart antenna system combines multiple antenna elements with signal processing capability to optimize its radiation pattern automatically in response to signal environment. Smart antenna systems are customarily categorized as either switched beam or adaptive array systems. Switched beam antenna system forms multiple fixed beams with heightened sensitivity in particular directions. These antenna systems detect signal strength, choose from one of the several predetermined,

fixed beams, and switched from one beam to another as demanded by channels throughout sector. Instead of shaping the directional antenna pattern with the metallic properties and physical design of a single element, for example as sectorized antenna, switched beam system combines the outputs of multiple antennas in such a way as to form finely sectorized or directional beams with more spatial selectivity than it can be achieved with conventional, single element approaches. On the other hand, adaptive array system represents the most advanced smart antenna approach to date. Using a variety of new signal-processing algorithms, the adaptive system takes advantages of its ability to effectively locate and track various types of signals to dynamically minimize interference and maximize intended signal reception [66], [67].

Switched beam system is one of the smart antenna technologies that can improved the antenna functionality and efficiency by reducing the performance problems such as multipath fading and co-channel interference, thereby increasing the channel capacity. Switched beam allows signal gain that provides better coverage, rejects interference that decreases capacity, allows spatial diversity that produces multipath rejection and enables power efficiency that reduces energy and expenses.

In this chapter, we describes a dual-polarized and switched multi-beams antenna that is used to optimized the propagation characteristics which can increases the channel capacity. This antenna also is intended for small base station operation, with a bandwidth that is wide enough for LTE environment. The conditions for the antenna design are as follows:

- Use for small base station operation in LTE environment
- The operating frequency is realized at 2.6 GHz with bandwidth of 100 MHz which is from 2.55 GHz and 2.65 GHz
- The antenna array provides three-beams switching in both E- and H-plane with polarization switching, with tilted angle of ±15°
- The antenna is fed through two ports simultaneously
- Dual and orthogonal polarization

5.2 Microstrip Patch Antenna

Research regarding microstrip patch antenna has been studied by many since 1950s [68]. The idea however remains as an idea without any real development until 20 years later when the printed circuit board (PCB) technology emerged in 1970s. Along with this development, microstrip antenna has been researched and studied to the point it became the most common antenna in the industry. Microstrip patch antenna in it basic form consists of a dielectric substrate with a radiating patch on one side and a ground plane on the other side. The patch, which can take any shape, acts as a resonant cavity where the top and bottom becomes short circuits wall and the side becomes open circuit. When the antenna is excited at their frequency resonance, a strong field is set up inside the cavity and a strong current conducting on the bottom surface of the patch. A few desired characteristics of this antenna aside from low profile and low fabrication cost are; it supports both linear and circular polarization while capable of operating in dual and triple frequencies. Microstrip patch antenna produces a wide beam radiation pattern but unfortunately it gives a very narrow bandwidth which makes it excluded from modern communication system. Thus, the evolution of microstrip patch antenna is directed towards bandwidth enhancement where researchers studied and developed different designs to achieve this.

In this section, a simple design and development of double layer with slot microstrip patch antenna is presented. The proposed antenna is developed as the extension study of the basic microstrip patch antenna itself. This research started from the very basic form of microstrip patch antenna and engineered towards developing a wide bandwidth with narrow beams antenna. The aim for this study is to provide an in-depth research and analysis on its characteristic so that the knowledge learned can be applied to improve the performance of final design in the research.

5.2.1 Microstrip Patch Antenna with Microstrip Feed

The basic form of a simple microstrip patch antenna consists of a dielectric substrate mounted on the ground plane and a radiating patch of any shape on the other side as shown in Figure 5.1. The antenna is usually fed by a microstrip transmission line. The

patch, microstrip transmission line and ground plane are made of high conductivity metal which is typically copper.

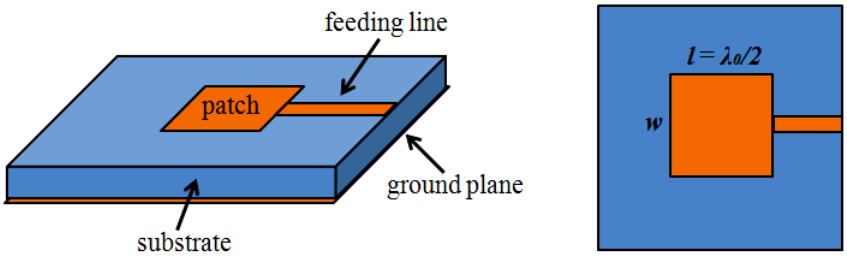

Figure 5.1: Basic form of microstrip patch antenna.

The patch sitting on top of the substrate can be of any shape but we consider a square shape as shown in the figure for easier explanation. The length of the patch is labeled as $\boldsymbol{l}$ and width $\boldsymbol{w}$ and has a thickness of $\boldsymbol{h}$ with dielectric permittivity of $\boldsymbol{\varepsilon_r}$. Although the thickness of the ground plane as well as the microstrip patch is not critically important as other parameters, the height however typically much smaller than the wavelength of the operation frequency that should not be much smaller than 0.025 λ for an efficient antenna. Further explanations are mainly referred from [69].

The patch acts as resonant cavity where it is short-circuit walls on top and bottom and it is open-circuit walls on the sides. In cavity, only certain modes are allowed to exist, at different resonance frequency. If the antenna is excited at a frequency *f*, a strong field is set up inside the cavity and a strong current is set on the bottom surface of the patch. The radiation of the microstrip antenna can be explained by the fringing fields around the antenna.

Figure 5.2 describes how microstrip patch antenna radiates. The current at the end of the patch is zero because it is an open circuit end while the current level is maximum at the center of the patch for the half-wave patch. This low current value at the feed explains why the impedance is high when we fed the antenna at the end. Since the patch antenna can be considered as an open circuited transmission line, the voltage reflection coefficient will be 1. In this condition, the voltage and current will be out of phase where the voltage is minimum at the start of the patch and maximum at the end of the patch. Therefore the fields underneath of the patch will create fringing of the fields around the edges.

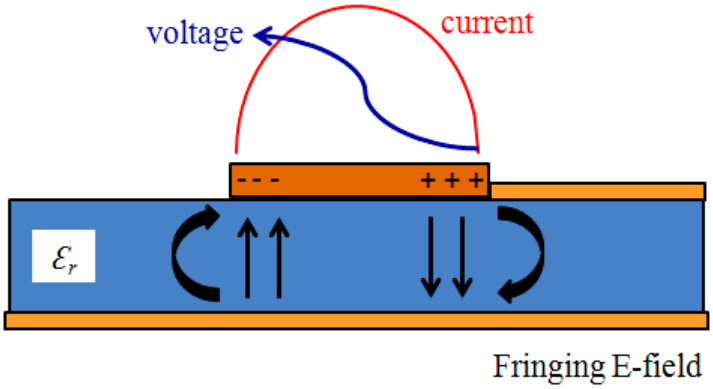

Figure 5.2: Side view of microstrip patch antenna with e-field shown underneath.

This fringing fields are responsible for the radiation where the fringing fields near the surface of the patch antenna are both in the +y direction. Thus, the fringing E-fields on the edge of the microstrip patch antenna add up in phase and produce the radiation for microstrip antenna. The current adds up in phase on the patch antenna as well although an equal current with opposite direction is on the ground plane which cancels the radiation. This condition explains why the microstrip antenna radiates but the microstrip transmission line does not. The radiation arises from the fringing fields, which are due to the voltage distribution instead of current describes the patch antenna as voltage radiator as opposed to the wire antenna which is current radiator.

A better radiation can be achieved if the fringing fields become more "bowed" as they extend farther away from the patch where this can be produced by using smaller permittivity, $\mathcal{E}_r$ for the substrate. In contrast, a high value of $\mathcal{E}_r$ is desired when making a microstrip transmission line as the fields will be more tightly contained due to less fringing resulting in less radiation. Theoretically, the parameters of the microstrip patch antenna can be calculated using equations where the dimension from the calculation can be used as a guide during simulation. For the resonance frequency of 2.6 GHz and dielectric constant, $\mathcal{E}_r$ of 2.6, the wavelength will be;

$$\lambda = \frac{c}{f} = \frac{3\ x\ 10^8}{2.6\ x\ 10^9} = 115.38\ mm$$

Thus λ_0 will be;

$$\lambda_0 = \frac{\lambda}{\sqrt{\varepsilon_r}} = \frac{115.38}{\sqrt{2.6}} = 71.56\ mm$$

From these 2 equations, we can write the f_0 as;

$$f_0 = \frac{c}{\sqrt[2]{\varepsilon_{reff}}}\left[\left(\frac{m}{L}\right)^2 + \left(\frac{n}{W}\right)^2\right]^{\frac{1}{2}}$$

The width of the patch can be calculate as,

$$W = \frac{c}{2f_0\sqrt{\frac{(\varepsilon_r + 1)}{2}}} = 43\ mm$$

And the length can be calculated as;

$$\varepsilon_{reff} = \frac{\varepsilon_r + 1}{2} + \frac{\varepsilon_r - 1}{2}\left[1 + 12\frac{h}{W}\right]^{-\frac{1}{2}}$$

$$\Delta L = 0.412h\frac{\left(\varepsilon_{reff} + 0.3\right)\left(\frac{W}{h} + 0.264\right)}{\left(\varepsilon_{reff} - 0.258\right)\left(\frac{W}{h} + 0.8\right)}$$

$$L_{eff} = \frac{c}{2f_0\sqrt{\varepsilon_{reff}}}$$

$$L = L_{eff} - 2\Delta L = 35.51\ mm$$

Figure 5.3 shows the simple form of microstrip patch antenna used for simulation purpose. A substrate with dielectric constant, $\mathcal{E}_r$ of 2.6 was placed on a ground plane with the width, w of 70 x 70 mm. A square patch of 0.45 λ_0 which is equal to 32.2 mm was set at the center of the substrate while the height of the substrate was set at 3 mm. The antenna was fed with a 2.4 mm x 19 mm microstrip feed line instead of coaxial feed to provide a planar structure and because it is easier to fabricate as it can be etched on the same substrate. This antenna geometry serves as the basis of parametric studies of antenna characteristic.

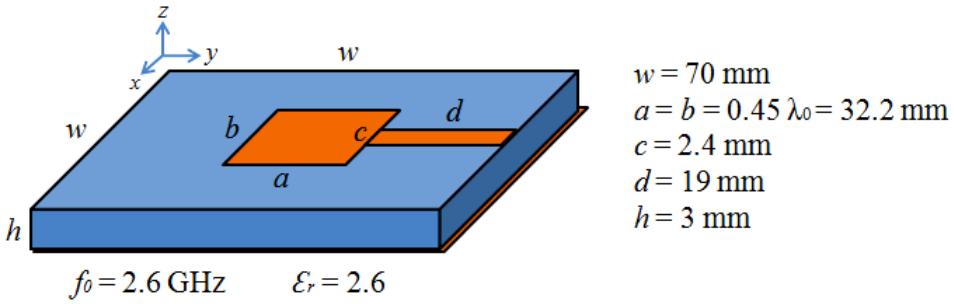

Figure 5.3: Simple microstrip patch antenna with measurement.

Figure 5.4 shows the antenna characteristic for microstrip patch antenna shown in Figure 5.3. The S_{11} is optimized at 2.6 GHz with the -10 dB impedance bandwidth of 24 MHz, which is just 0.9 % that shows a narrow bandwidth as describes in the theory. The radiation pattern shows a wide beam pattern where both xz- and yz-plane gives the same pattern.

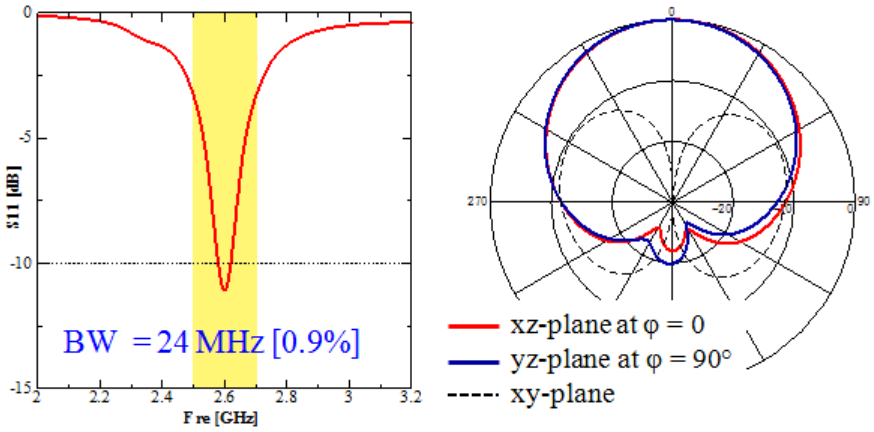

Figure 5.4: Antenna characteristic for simple microstrip patch antenna.

5.2.2 Microstrip Patch Antenna and Parameter Analysis

This section presents the analysis of the basic parameters for microstrip patch antenna. As the patch is the element that influenced the output of the antenna characteristic the most, the analysis is concentrated on the patch only. The parameters that are studied regarding the patch are the size, width, length and shape of the patch.

Different Patch Size Effect

The first parameter studied was the patch size. The optimum size calculated for 2.6 GHz operating frequency was 0.45 λ_0. In this experiment, a square patch was used which meant that the length and the width of the patch is on same size, giving a equals to b. Three patch sizes were measured, 0.4 λ_0 for the green line, 0.45 λ_0 for the red line and 0.5 λ_0 for the blue line in Figure 5.5. The antenna geometry for the experiment as well as the S-parameter result is shown in Figure 5.5. The S parameter result shows that larger patch matches bigger resonance frequency although there is a limit on how big the patch can be as we need to match the impedance at below -10 dB (blue line). Smaller patch also shows a better impedance matching as shown by green line in the figure and at the same time gives a bigger bandwidth at 103 MHz compare with 24 MHz for red line.

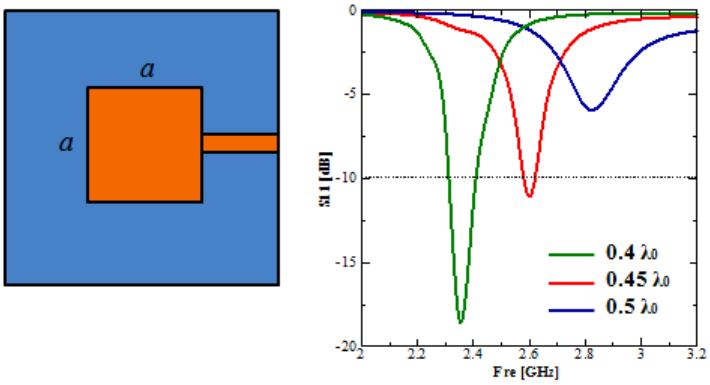

Figure 5.5: Antenna characteristic for different patch size analysis.

Different Patch Length Effect

The second parameter studied was the length, ***a*** of the patch. In this experiment, the width, ***b*** of the patch was fixed at 0.45 λ_0 while ***a*** was measured at 3 different sizes, 0.4 λ_0 for green line, 0.45 λ_0 for red line and 0.5 λ_0 for blue line. As the length, ***a*** was changing while the position of the patch remains, the feeding line gets shorter as the length gets bigger. Figure 5.6 shows the antenna geometry for experiment and the S-parameter result. Contrary to size patch analysis, as we increase the length of the patch the operating frequency gets smaller as shown by the blue line. At the same time,

the bandwidth also the biggest for longer patch length. From this analysis we confirmed that the length of the patch largely affects the resonance frequency as well as the bandwidth of the microstrip patch antenna.

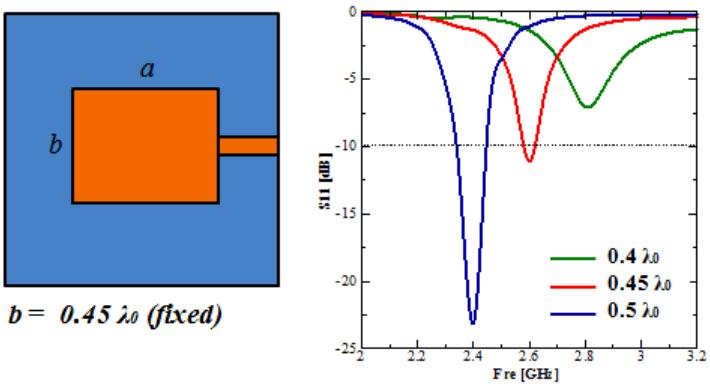

Figure 5.6: Antenna characteristic for different patch length analysis.

Different Patch Width Effect

For the third parameter study, instead of the length, ***a*** of the patch, the width, ***b*** was measured instead while the length was fixed at 0.45 λ_0 and the feeding length remains unchanged. As there wasn't much different in the result as compared to previous 2 experiments, we measured the width at 0.45 λ_0, 0.55 λ_0 and 0.65 λ_0 instead for green line, red line and blue line respectively. The geometry of the experiment and the S-parameter result is shown in Figure 5.7 where we confirmed that each width matched the impedance at similar frequency which is around 2.6 GHz. However as the width gets bigger than the length of the patch, while the red line matched at higher frequency, the blue line matched at lower frequency instead. Thus we concluded that the width does not have much effect on the resonance frequency but there is certain dimension on how big the width should be to optimize the antenna performance.

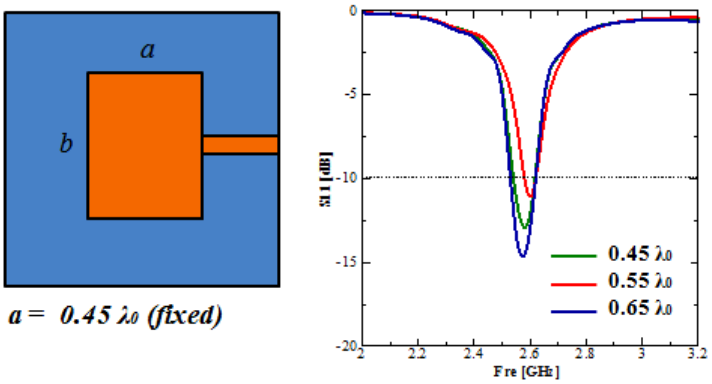

Figure 5.7: Antenna characteristic for different patch width analysis.

Different Patch Shape Effect

The last parameter studied was the shape of the patch itself. In the initial experiment, a square shape was used for its simplicity and easier explanation but in this experiment we describe the effect of the shape to the antenna characteristic. 4 types of shape were measured; circular, elliptical, square and rectangular represented by green line, red line, blue line and purple line respectively. The size for each patch was adjusted around 0.45 λ_0 and optimized to the best S-parameter result. The result as shown in Figure 5.8 describes 2 patterns for S-parameter, where square patch and rectangular patch shows similar result while circular patch and elliptical patch show another similar result. From this result we confirmed that for this size and configuration, rectangle patch gives the best results, follows by square, elliptical and circular. However, as we can see that although elliptical and circular didn't really produce a good result, which is just because the size is not suitable. If we change the size, we might be able to match good impedance at 2.6 GHz.

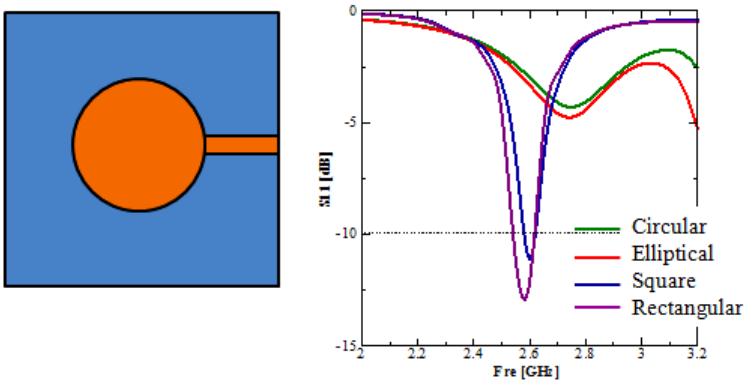

Figure 5.8: Antenna characteristic for different patch shape analysis.

5.2.3 Microstrip Patch Two Layers

Although microstrip patch antenna is very popular as it is easy to fabricate where it can be printed directly onto a circuit board, with low cost and low profile design, unfortunately however the basic form of microstrip patch antenna gives a very narrow bandwidth which makes it excluded from modern communication system. However, it produces wide-beam radiation pattern that still maintain as popular choice if we need to produce a beam pattern antenna. Thus in this section we proposed a configuration that can increase the bandwidth of the antenna. There are a few ways to achieved that and among them are by using thicker substrate with a small dielectric constant or by stacking the patch [70]–[72]. Figure 5.9 shows the antenna configuration for two layer microstrip patch antenna.

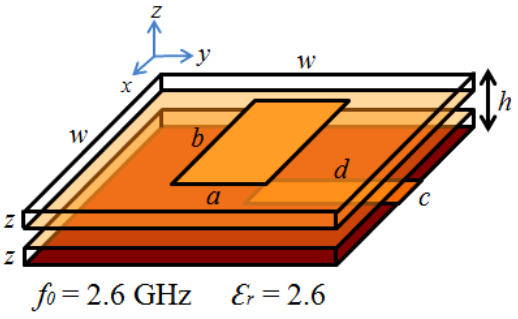

$w = 100$ mm
$a = 0.5\lambda_0 = 35.78$ mm
$b = 0.7\lambda_0 = 50$ mm
$c = 4$ mm
$d = 44$ mm
$z = 0.8$ mm
$h = 4$ mm

Figure 5.9: Geometry of microstrip patch two layers antenna.

The antenna configuration has 2 layer, with the top layer consists of a rectangular patch on the top and the feeding line was at the bottom of the second layer. Each layer was realized using substrate of 100 mm x 100 mm in size, with thickness equals to 0.8 mm and dielectric constant of $\mathcal{E}_r$ equals to 2.6. The total height of the layer from bottom to top was optimized at 4 mm. The size of the patch was 35.78 mm x 50 mm with the position was at the very center of the substrate while the size of the feeding line was 44 mm x 4 mm starting from the edge of the substrate.

Figure 5.10 shows the antenna characteristic results for the antenna configuration. The blue line represents the basic microstrip patch antenna and the red line represents the microstrip patch two layers. The S-parameter result shows that both antennas matched at 2.6 GHz but the -10 dB impedance bandwidth achieved for two layers antenna is just 0.4%, which is far narrower than the previous result. Unfortunately from this result we didn't manage to achieve the target which is to broaden the bandwidth. On the other hand the radiation pattern also is changing towards omni directional pattern instead of beam pattern.

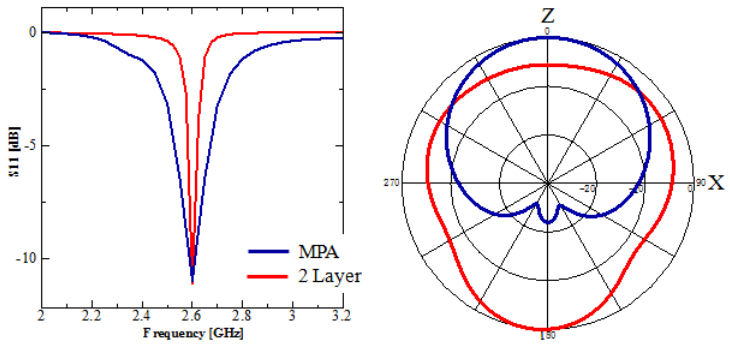

Figure 5.10: S-parameter result and radiation pattern in xz-plane for microstrip patch two layers antenna.

5.2.4 Microstrip Patch Two Layers with Slot

In the previous section we improved the antenna geometry by stacking two substrates with the target to broaden the bandwidth of the antenna. However the S-parameter shows a disappointing result where the bandwidth became smaller instead. Therefore the geometry of the antenna was further improved by adding a simple line slot on the

top of the second layer as shown in Figure 5.11. The measurements for the new configuration were kept as before with the exception of length, ***a*** that was shorten to 32.2 mm. The dimension for the slot was optimized at 2 mm x 18 mm and was positioned at 10 mm from the center of the patch or substrate. The adjustments were optimized to acquire the best antenna characteristic especially in term of S-parameter result.

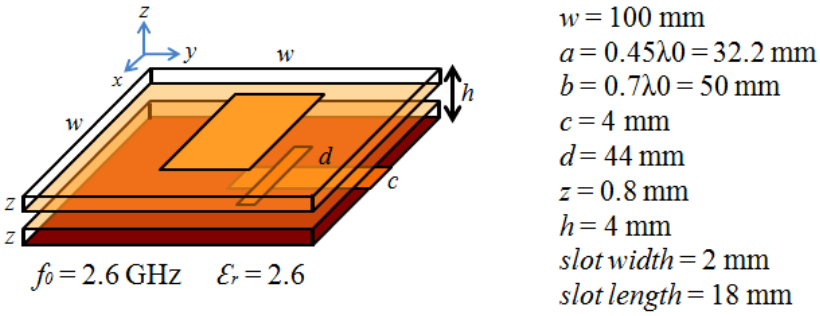

Figure 5.11: Geometry of microstrip patch antenna two layers with slot.

Figure 5.12 shows the antenna characteristic results for all 3 antenna configurations which shows the comparison in term of both S-parameter and radiation pattern in xz-plane. The green line, red line and blue line represent the microstrip patch antenna, microstrip patch 2 layers and microstrip patch 2 layers with slot, respectively. The blue line shown in the S-parameter result shows a significant improvement in the antenna performance for microstrip patch antenna 2 layers with slot. The bandwidth comparison is shown in Table 5.1 where by adding the slot to the microstrip 2 layers antenna configuration, the bandwidth is improved to 12.6 % while all the impedance are matched antenna 2.6 GHz. In term of radiation pattern however, the final antenna configuration still shows omni directional pattern instead of beam pattern but with a better shape than the antenna configuration without the slot.

Table 5.1: Comparison of bandwidth for all 3 antenna configuration.

Antenna	f_0 [GHz]	Bandwidth [MHz]
MPA	2.6	24 [0.6%]
2 Layers	2.6	10 [0.4%]
Slot	2.6	324 [12.6%]

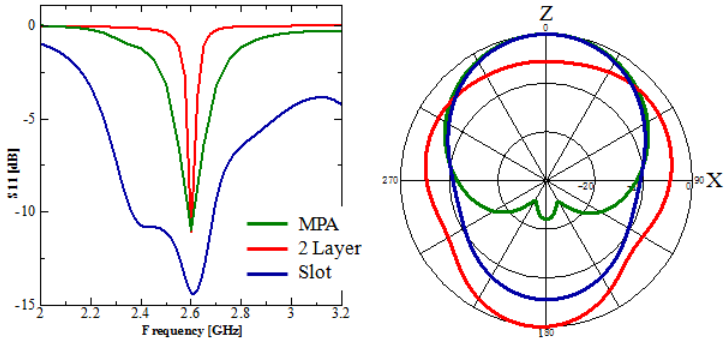

Figure 5.12: Comparison of antenna characteristic result for all 3 microstrip patch antenna configuration.

In this section, a parametric study of basic microstrip patch antenna was conducted as the first part of the research. This study was done to observed how the parameter affect the antenna in term of frequency, impedance bandwidth and radiation pattern. From there, a 2 layers antenna design was proposed with the goal of improving the bandwidth of the antenna. The obtained results show that the traditional narrowband microstrip patch antenna can be improved to wider bandwidth by stacking the patch and adding a slot.

5.3 Three Layers Switched Multi-beam Antenna

If more than one radio wave presents in a room or base station, interference among the radio waves will occur. There is also the fact that in this multi path phenomenon, it is very difficult to predict the propagation environment, thus the cause of the interference. One of the solutions to overcome this problem is by using directional switching antenna. Directional antenna has fix radiation pattern in certain direction which is pre-determined. However, if it is possible to freely control the radiation pattern, even in the multi path propagation environment which interference is surely occurred, it is likely to avoid interference. Hence, directional switching antenna having a plurality of radiation patterns and by varying the sequential pattern, optimal transmission can be selected.

In this section we assumed the room as indoor small base station and we proposed dual-polarized switched multi beams antenna. There are several methods of switching the directivity where among them is by utilizing the parasitic elements where we can excites the elements of the same shape to configure the switching antenna. As a result a directional switching antenna with low profile and miniature design with two-port 6 directional switching is realized, including polarization reconfigurable. The outcome, an antenna array of 3 beams switching in the LTE environment having the bandwidth wide enough from broadband transmission. The overall thickness is kept at 10 mm and the beams are steered using one input-two-output phase shifter in ±15° angle.

Although there is phased array antenna using phase difference between the power supplies, their application for indoor base station is small and the objective is normally to widen the bandwidth instead of switched tilted beam. In this section however we propose a dual-polarized switched beam antenna which is fed by phase difference in power supply for indoor base station. The antenna is intended for LTE, broadband environment at 2.6 GHz (2.5-2.7 GHz) and capable for polarization switching. It is important to provide reconfigurable polarization antenna because as discussed before this element is considered effective for channel capacity improvement. As low profile design is favorable especially for easy mounting at the base station, the overall height of the antenna structure is optimized at 10 mm.

5.3.1 Dual-Polarized Orthogonal Square Patch Array

As we considered the proposed antenna targeting a low profile design for small indoor base station, the planar patch antenna is a suitable choice. In general, the patch antenna formed on a dielectric substrate gives a narrow bandwidth as already confirmed in the preceding section. Improving the bandwidth can be done by using an optimally designed impedance-matching network as was found in [73], [74] for example. However as we want the simplicity in the design, the wider bandwidth can be achieved by stacking the dielectric substrate.

Figure 5.13 shows the antenna structure consists of three layers of substrate; a patch plane on the top layer, a feeding plane in the middle layer and the ground

plane at the bottom layer. Each layer was realized using substrate with the thickness equals to 0.8 mm and the dielectric constant, ε_r equals to 2.6. The height of the antenna was optimized at 10 mm to match the impedance at the desired frequency which was 2.6 GHz. The patch plane consists of three square patches in L-shape array on the top surface of the substrate to give the orthogonal array. The square shape was chosen instead of circular shape for much simpler configuration purpose. Beneath each patch on the top surface of the middle layer, there were two C-shaped slots where each slot was fed by a curve feeding line realized at the bottom surface.

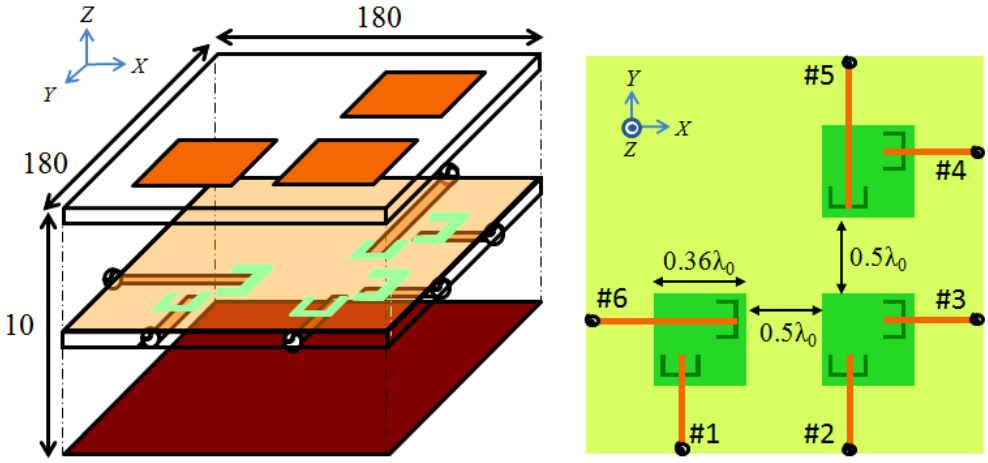

Figure 5.13: Geometry of three layers orthogonal square patch array.

The geometry of the antenna was organized to give the symmetry arrangement and the measurement was optimized to produce the best results of the antenna characteristic. The C-shaped slots with feeding line were used to extend the frequency bandwidth of the antenna elements. The slots also were adapted to excite dual and orthogonal polarization for each patch elements. The ground plane was used to suppress the backward radiation from the slots. The antenna was fed using two ports simultaneously with 4 input port combinations as shown in Table 5.2. For example if we fed the antenna through Port 1 and 2, with 3 different phase combinations of [0,0], [0,90°] and [0,-90°], 3 beams tilting at 0 and ±15° were achieved.

Table 5.2: Input port combinations and the respective input phases.

Port Combination	Beam		
	1	**2**	**3**
[1,2]	0,0	0,90°	0,-90°
[3,4]	0,0	0,90°	0,-90°
[2,5]	0,0	0,-120°	0,120°
[3,6]	0,0	0,-120°	0,120°

The input impedance of the antenna was highly dependent on the slot and layer configuration. The alignment of the slot was performed by adjusting the slot width, slot length and the arrangement of slot position. Microstrip line also can control the impedance by changing the length of the feed line. Moreover, the spacing of the layer must also be taken into account as these parameters will affect the electromagnetic coupling then control the output radiation pattern. This antenna has resistance to impact from outside as the physical antenna elements do not need to connect to feeding line. It is also really easy to manufacture as we do not need to pierce the substrate by drilling.

The antenna structure from the top had a radiating substrate with printed patch, an air gap, another substrate forming C slots on the top and microstrip line feeding at the bottom, another air gap and the ground plane at the bottom. The total height for the whole structure was optimized at 10 mm. The bandwidth of the antenna can be further widen if we increase the thickness of the air gap but as we wanted to keep the total height at 10 mm, the impedance was matched by the shape and arrangement of the slot instead. In addition, the slots were also arranged in two orthogonal arrangements to achieve the dual polarization element.

The S-parameter for this antenna structure is shown in Figure 5.14 with 4 input port combinations of P[1,2], P[3,4], P[2,5] and P[3,6] with blue line, red line, green line and purple line respectively. The blue line and the green line match nicely at 2.6 GHz and although the red line and the purple line shifted at higher frequency, their S_{11} at 2.6 GHz is still below -10 dB which is acceptable. The -10 dB bandwidth also measured at around 200 MHz for all input port combinations.

The radiation pattern for all input combination also is shown in Figure 5.14 where the colors of the beam line represent the respective input phase combinations. For P[1,2] and P[3,4], blue beam represents input phase [0,0], green beam represents [0,90°] and green beam represents [0,-90°] while for P[2,5] and P[3,6], the red beam and green beam represents the combination of [0,-120°] and [0,120°] respectively instead. From the result also we confirmed that although P[1,2] and P[3,4] produce a nice 3 beams tilted at 0 and ±15°, the radiation pattern for P[2,5] and P[3,6] has big back lobe for all 3 tilted beams because of the backwards radiation from the slots. This results show a variation in radiation pattern that we very much like to avoid thus will be fixed as we move along the research.

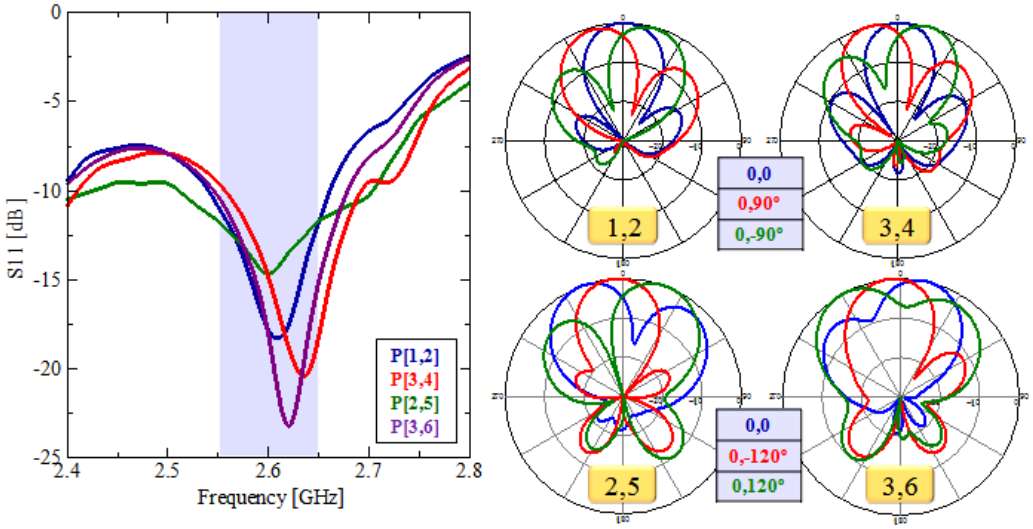

Figure 5.14: S-parameter results for every input port combination and their respective radiation patterns.

5.3.2 The Improvement of the Antenna Design

In the previous section, we defined two problems regarding the antenna characteristic for the antenna structure. The first one is that the S-parameter for 2 inputs didn't exactly matched at 2.6 GHz instead but shifted to higher frequency. The second one is that the radiation pattern for 2 input also gave big back lobes and didn't really produce a nice beam as we originally wanted. Thus, the antenna structure is further

improved to achieve a better antenna characteristic in both S-parameter and radiation pattern.

The antenna structure was kept as 3 layers of substrate as before with the patch layer on the top, the feeding layer in the middle and the ground layer at the bottom. Only the feeding layer was adjusted where the microstrip feeding line at the bottom was changed from straight feeding line to curve feeding line as shown in Figure 5.15. As the patch position was kept at the exact same position as before, the position of the C-slots was adjusted slightly to optimize the antenna characteristic.

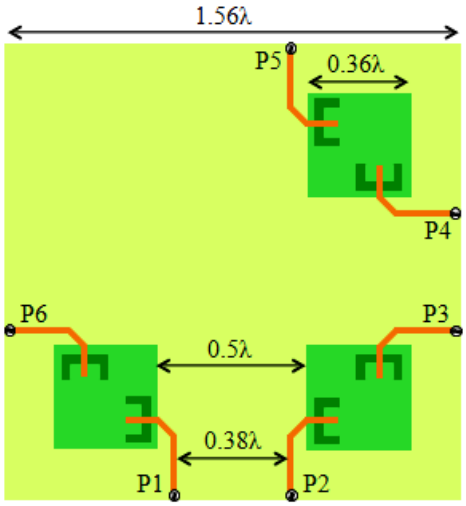

Figure 5.15: New antenna configuration with curve feeding line in xy-dimension.

The input port combination also was kept as before where we have input port combination of P[1,2], P[3,4], P[2,5] and P[3,6]. The input phase for the respective ports in shown in Figure 5.15 where the 3 beams are represented with blue, red and green color. From the we noticed that the phase difference need is 90°and 180° only and this is easily achieve compared to 120° as many common input phase circuit are concentrating around this degree.

Table 5.3: Input port combinations and the respective input phases.

Port Combination	Beam		
	1	**2**	**3**
[1,2]	0,180°	0,90°	0,-90°
[3,4]	0,180°	0,90°	0,-90°
[2,5]	0,0	0,90°	0,-90°
[3,6]	0,0	0,90°	0,-90°

The new antenna structure with curve feeding has managed to eliminate the shifted resonance frequency and back lobe problem existed in the previous design. Figure 5.16 shows the reflection characteristic for the antenna structure where the S11 results show that all the input ports match at exactly 2.6 GHz with the -10 dB bandwidth wider than 100 MHz. The first input which is represented by blue line has S11 at -18 dB, the second input in red line reads at -20 dB, the third input reads at -14 dB in green line while the fourth input in purple line reads at -21 dB. The S21 reading also show a very good results where all the input ports reads around -25 dB at 2.6 GHz.

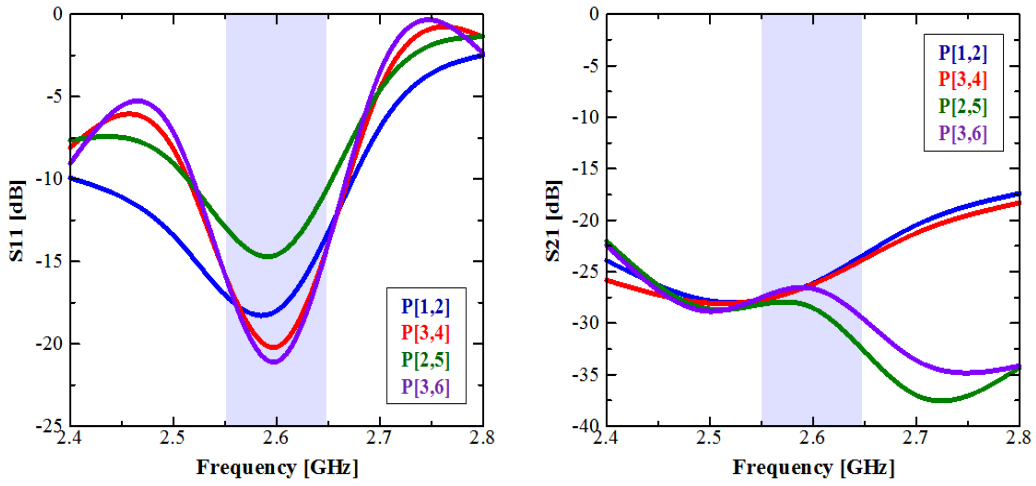

Figure 5.16: Antenna characteristic for the final design of the antenna structure.

On the other hands, the radiation pattern also has improved for all input ports where the big back lobes problem is addressed in this new design. Figure 5.17 shows that the radiation pattern for all input port excitation where each port has 3 beams tilted in 0 and ±15°. P[1,2] and P[3,6] show the pattern in xz-plane while P[3,4] and

P[2,5] in yx-plane in theta and phi respectively. Not only the back lobe problem has been eliminated, the beams also show a similar pattern with similar tilted angle as well as beamwidth which very favorable in our study.

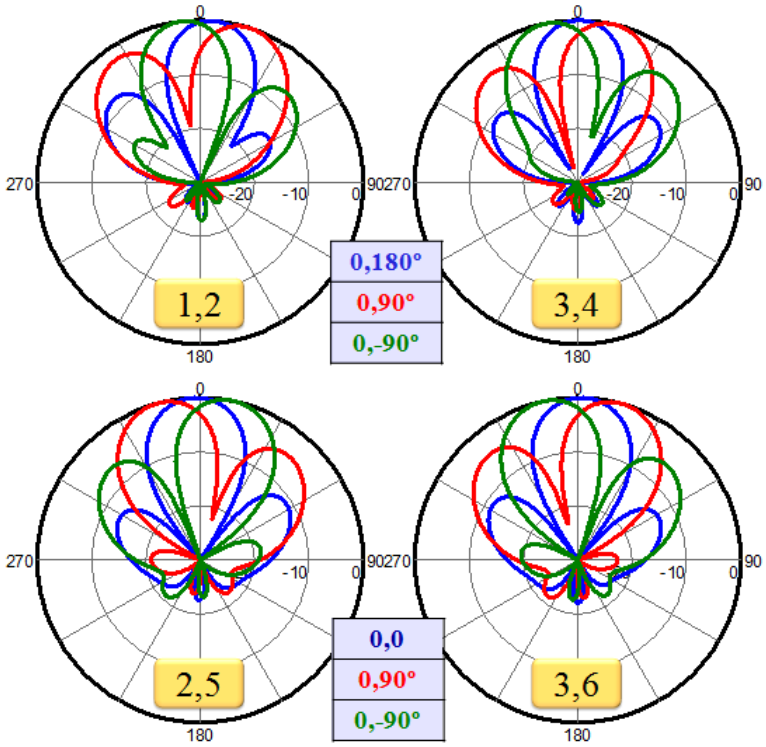

Figure 5.17: Radiation characteristic for the new design of the antenna structure.

5.3.3 Microstrip Switched-Line Phase Shifter

In this section we will discuss the feeding circuit for the antenna configuration described in the preceding section. As the phase differences needed are only 90° and 180°, we have a wider choice of Wilkinson Power Divider, a hybrid coupler or by using varactor diode. We proposed a one-input-two-output phase shifter circuit to feed the proposed antenna configuration. The concept of the feeding circuit is shown in Figure 5.18 where it has 2 parts, Wilkinson power divider and phase shifter circuit. The first parts consist of Wilkinson power divider that divides the input power equally and the second part consists of switch line phase shifter that gives the difference in output phase. The output phase difference can simply be achieved just by adjusting the length of the arm line.

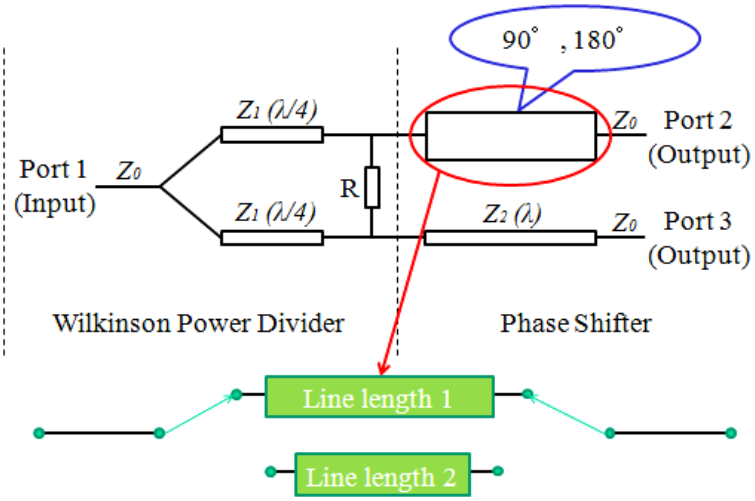

Figure 5.18: The concept for the input phase feeding circuit.

Figure 5.19 show the proposed feeding circuits applied from the concept as discussed before. The power will be supplied from Port 1 and will be divided equally before entering the phase shifter. Entering the phase shifter, there are 2 switches in each part than can be turn on or off that will give a difference length for the phase shifter, thus providing the difference in the phase as targeted. The switch can be turn on and off simply by using pin diodes. Two arms will be needed to feed the antenna as we will be using 2 ports to get 1 beam, line 1 and line 2.

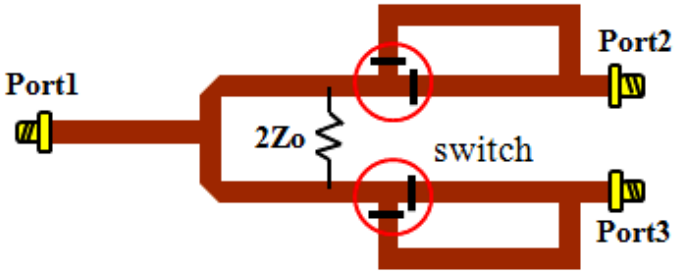

Figure 5.19: Microstrip switched line phase shifter as feeding circuit.

Figure 5.18 shows the 3 different configuration for the arm length to get the desired phase difference which is 0, ±90° and ±180°, and their respective input characteristic that shows each arrangement matched at 2.6 GHz. For the in-phase configuration which is no difference in input phase, the length for both Line 1 and Line 2 is 34.3 mm which is the longer arm and we confirmed that the phase difference is 0.

For input phase difference of ±90°, Line 1 uses the shorter arm which was 15 mm while Line 2 uses the longer arm which was 34.5 mm. The input characteristic shows that this configuration give 90° difference in input phase. For input phase ±180°, the Line 2 was measured at 54 mm instead and the input characteristic shows that we get 180° difference in phase. This one input two output feeding circuit named switched line phase shifter was fed to the antenna structure to obtained 3 beams with tilted angle at 0 and ±15°.

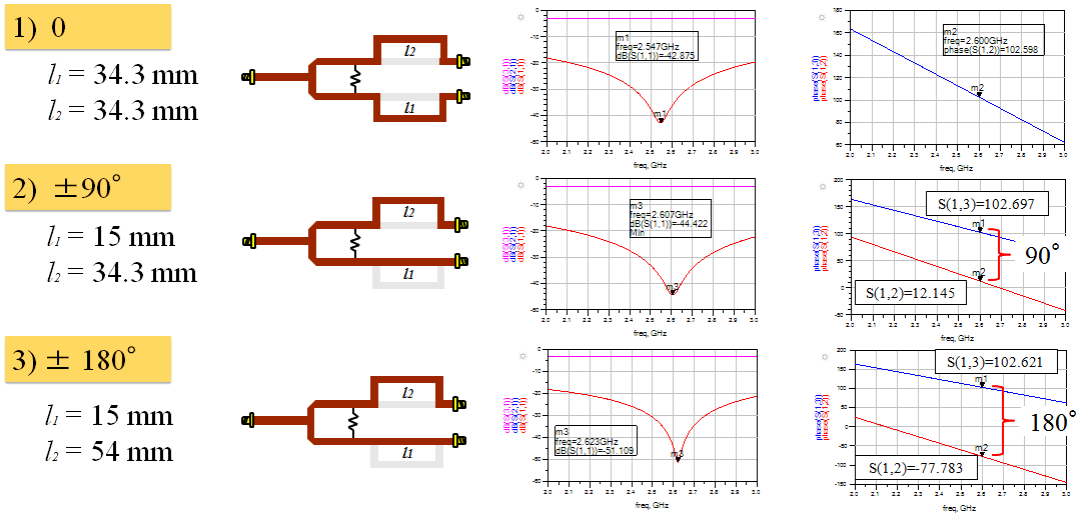

Figure 5.20: Arm line configuration for each phase difference and their respective input characteristic results.

5.4 Channel Capacity for Three Layers Switched Multibeam Antenna

As in Chapter 4, this section will present the channel capacity calculation using the real radiation pattern obtained from the antenna designed from this chapter, which is switched multibeam antenna. The arrangement for the channel capacity calculation was done assuming 4 x 4 MIMO systems as the previous chapter. Therefore 2 vertically polarized beams from port [1,2] and 2 horizontally polarized beams radiation patterns from port [3,4] were used in the simulation is shown in Figure 5.21. In each port combination excitation, 3 beams were obtained at 0° (blue line), +15°

(red line) and -15° (green line). However, for simulation purpose, only 2 beams (red and blue line) at ±15° were used in each port combination. The antenna characteristics for transmit antenna are according the proposed antenna results with HPBW of ~29.3° for all beams while the gain around ~10.8 dBi and ~9.9 dBi for vertical and horizontal polarized beams respectively. For this channel capacity calculation, the simulations were done at operating frequency of 2.6 GHz matching the proposed antenna.

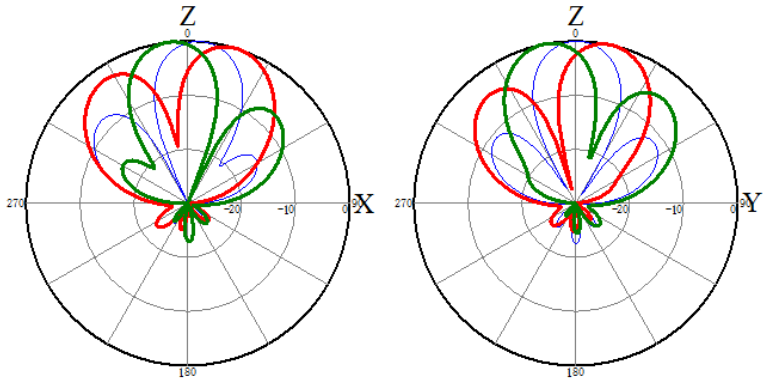

Figure 5.21: Radiation patterns for both vertical and horizontal beams used in simulation.

As in Section 4.4, the channel capacity were calculated in 3 different positions which is Position A at the center of the room, Position B at the wall in x-axis and Position C at the wall in y-axis as shown in Figure 4.18. The simulations were done in all 3 room sizes and the discussion covered both channel capacity and capacity distribution with comparison to the dipole antenna.

Figure 5.22 shows the channel capacity results for switched multi-beams antenna in 3 different room sizes. For the smallest room which is Room A, the channel capacity for beam-pattern antenna is higher than dipole antenna with 38.1 bits/s/Hz as compared to 35.8 bits/s/Hz when transmit antenna was fixed in Position B while higher capacity also is obtained by beam-pattern antenna in Room B when in Position C with 29.7 bits/s/Hz as compared to 24.9 bits/s/Hz. Unfortunately however, in the smallest room the capacity for dipole antenna is higher instead of beam-pattern antenna with 23.3 bits/s/Hz as compared to 13.9 bits/s/Hz when the transmit antenna was fixed in position A. However, looking at the overall results, the capacity for beam-pattern antenna is confirmed higher than dipole antenna in all room sizes

when the transmit antenna was fixed at the wall of the room, either in x-axis or y-axis, which is Position B and C relatively.

In term of capacity distribution, the distribution for beam-pattern antenna gives stronger and even coverage in the area closer to transmit antenna position. On the other hands, even though the capacity distribution for dipole antenna is comparable for the smallest room, we confirmed that the distribution in an area in line with dipole antenna is weaker compare to other area. This condition occurs because of the influence among the radiation patterns. The capacity distribution for beam-patterns antenna did not show the same condition as dipole due to low correlation between the elements.

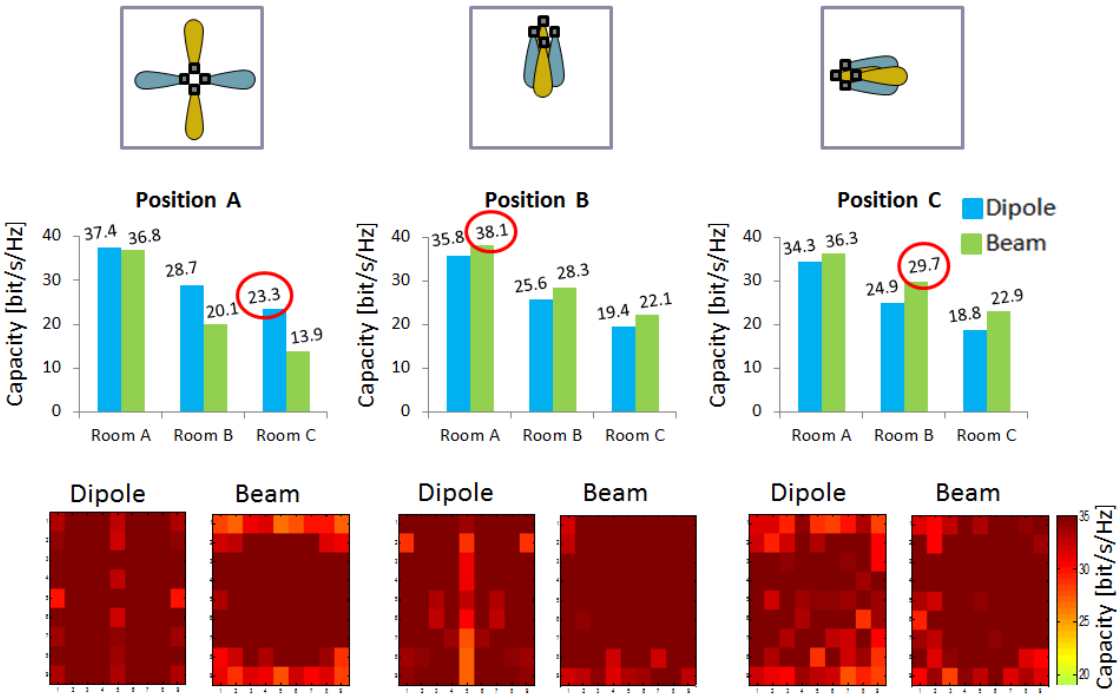

Figure 5.22: Channel capacity results and capacity distribution for proposed antenna configuration.

5.4 Summary

In this chapter we discussed microstrip antenna in common that has been attracting attention as a means to solve the interference problem in 4G mobile communication as in LTE. Both correspond to the polarization diversity and it is very practical for small

indoor base station as it has a low profile configuration. In the first section we discussed first the basic concept of microstrip patch antenna and we showed the antenna characteristic that has a narrow bandwidth as predicted by many previous research. We also then showed that the bandwidth problem can be solved just by stacking the substrate and adding the slot to widen the bandwidth of the antenna.

The next level of the research we discussed a three layer switched beam antenna that consist of patch layer, feeding layer and ground layer. The L-shape square patch gave the orthogonal array for the antenna while the slot coupled with feeding line was used to extend the frequency bandwidth of the antenna. The C-shaped slot at the feeding layer also was adopted to excite dual and orthogonal polarization for a single patch elements and this automatically give the dual-polarization element to the antenna structure. Although the height of the air gap between the layer will extend the bandwidth of the antenna, the total height was optimized at 10 mm for a low profile design that easy application especially for small indoor base station. The ground plane was used to suppress the backward radiation from the slot thus eliminating the big back lobe problem that we faced in the earlier design. The final design also adopted a curve feeding line because it provide a better radiation patterns with small backward radiation for all input port and at the same time this new geometry also provide a symmetrical arrangement for the antenna configuration. The antenna was fed using two ports simultaneously with the phase excitation of 0, ±90° and ±180° to provide phase difference in the phase excitation thus producing the 3 tilted beams at 0 and ±15°.

The antenna then was fed using microstrip switched line phase shifter that consists of Wilkinson power divider in the first part of the circuit that divides the input power equally. The second part of the circuit consists of phase shifter that has two arms with different length that was controlled by a pin diode acting as a switch that can be turn on or off. The different in the arm length produce the difference in phase excitation as we wanted and this simple configuration for the phase shifter circuit was favorable as it will be very easy to make thus applied.

For the future work, there is a need for measurement of the actually antenna in the actual indoor propagation environment to collect and analyzed the experimental data. We also need to prove that the channel capacity can be improve using beam pattern with dual polarization as this is the main target for this research. Also for

commercialization purpose, it is required to measure both the antenna structure and the feed system together as in this study, the antenna structure and the feeding circuit is studied separately. It is necessary to consider the effect on the antenna elements during the re-adjustment of the impedance matching and switching characteristic.

CHAPTER 6

CONCLUSION

As time passes, the revolution of mobile communication generation becomes more faster because of a surge of increase of user in wireless mobile. The era of mobile communication started from first generation (1G), second generation (2G), third generation (3G) and now is the era of fourth generation (4G). Each generation defines their own technologies with their own threshold speed, composing of many technologies, services as well as applications. For the 4G, the technology has becomes closely entwined with the generation itself where LTE as the technology is considered as 4G which integrated with one core network and several radio access networks.

Chapter 1 discussing the LTE technology including LTE requirements, architecture, operation protocol and the most important is the MIMO system implemented in LTE technology. The discussion is further revolved around LTE-Advance (LTE-A) and the 5G technology and beyond. Chapter 2 presents the overview of MIMO systems that focusing on channel model for multiple antenna system and the discussion of channel capacity for MIMO system is carried out. The chapter is concluded with discussion of a few application of MIMO system.

Chapter 3 discusses the channel capacity corresponds to MIMO system and various simulation is carried out according to various conditions and arrangements. Among the results, it is proven that multi-antenna system gives higher capacity that single antenna system. The correlation between each antenna for both transmit and receive antenna presents an important factor in channel capacity as lower correlation

provides higher channel capacity. From the results, it is concluded that as the room gets bigger, the capacity gets lower especially when the transmit antenna is placed in the center of the room. Although the channel capacity for dipole antenna especially in the biggest room outperforms the channel capacity for beam-pattern antenna, it is still showed that the beam-pattern antenna can increase the channel capacity even with smaller HPBW. Furthermore, when the transmit antenna is placed with benefit to the radiation shape of beam-pattern antenna, a huge improvement is achieved especially in the biggest room as well as overall increment in all the rooms as compared to dipole antenna. Moreover, in the smallest room half is covered by the strongest signal equally as described in capacity distribution results. As a summary, the channel capacity can be enhanced using multi-antenna system employing beam-pattern antenna with higher capacity than dipole antenna.

Chapter 4 discusses a low profile directional with dual polarization antenna as an antenna that is capable of producing dually polarized beam radiation patterns. The proposed antenna is constructed using loop antenna and reflector as vertically polarized element and printed dipole antenna, director and reflector as horizontally polarized element. The reflection characteristic and radiation characteristic in each array shows a similar results to each other due to this symmetrical arrangement which in return making it easier in designing process. By designing just a corner of the array, we managed to produce up to 8 beams, with up to 4 beams in both vertical and horizontal polarization. The reflection characteristic is sufficiently low with less than -10 dB and the mutual coupling between all the element is less than -25 dB. The reflection coefficient also shows a very good characteristic with 0.001 at 3.5 GHz. The HPBW is less than 80° and the tilted angle is within 40° to 60° which is within our original target. As the antenna is fed individually, we can produce the beam according to the state of the mobile station and the desired requirement. The low profile structure of the antenna is flexible as it can be adjusted according to favorable resonance frequency by simply adjusting a few parameter of the element in the array. This discovery is very beneficial as it offer possibilities of not just operating at two but more frequencies.

Chapter 5 discussed the basic concept of microstrip patch antenna with narrow bandwidth characteristic as predicted. The limited bandwidth problem is solved by stacking the substrate and adding the slot into antenna configuration. The

three layer switched beam antenna that consist of patch layer, feeding layer and ground layer is proposed as antenna that is capable of producing tilted beam with dual polarization. The L-shape square patch gave the orthogonal array for the antenna while the slot coupled with feeding line is used to extend the frequency bandwidth of the antenna. The C-shaped slot at the feeding layer also is adopted to excite dual and orthogonal polarization for a single patch elements and this automatically give the dual-polarization element to the antenna structure. Although the height of the air gap between the layer will extend the bandwidth of the antenna, the total height is optimized at 10 mm for a low profile design that easy application especially for small indoor base station. The ground plane is used to suppress the backward radiation from the slot thus eliminating the big back lobe problem that we faced in the earlier design. The final design also adopted a curve feeding line because it provide a better radiation patterns with small backward radiation for all input port and at the same time this new geometry also provide a symmetrical arrangement for the antenna configuration. The antenna is fed using two ports simultaneously with the phase excitation of 0, ±90° and ±180° to provide phase difference in the phase excitation thus producing the 3 tilted beams at 0 and ±15°.

The antenna then is fed using microstrip switched line phase shifter that consists of Wilkinson power divider in the first part of the circuit that divides the input power equally. The second part of the circuit consists of phase shifter that has two arms with different length that is controlled by a pin diode acting as a switch that can be turn on or off. The different in the arm length produce the difference in phase excitation as we wanted and this simple configuration for the phase shifter circuit is favorable as it will be very easy to make thus applied.

ACKNOWLEDMENT

In the name of God, Most Beneficent, Most Merciful. All the praises and thanks to Him, the Lord of the universe. Peace upon His messenger Muhammad, the last of the prophets and the righteous followers.

I still remember the very first morning I arrived at Arai Laboratory on 22nd October 2012 full of anxious, anticipation and a little bit excited to start my PhD journey and more than three years has passed since then. I am now at the end of the long road and I am very gratitude to the Almighty God for all the strengths, wisdom, patience, perseverance and ability bestowed upon me to complete this final life as a student.

First and foremost, I would like to express my extreme gratitude, appreciation and thousand thanks to my supervisor, Professor Hiroyuki Arai, for his guidance and advice during the period of completing this study. Every time I was in doubt or questioned myself, I found that he was always there to listen and giving me advises. His knowledge, support and understanding throughout these years have made this work possible.

I wish to thank my family, my parents for giving me support and permission to come here fulfilling my dream and my sister Chee especially for always be there for me, replacing me as a big sister in the family. Their unlimited encouragement and moral support during the progress of this research really helps me make it through to the end.

I would also like to express my appreciation to the committee members, Professor Takehiko Adachi, Professor Toshihiko Baba, Associate Professor Nobuhiro Kuga and Associate Professor Koichi Ichige. I feel unfortunate that I didn't have much

opportunity to directly study under them except Ichige Sensei, but I always value all the comments and advices given to me during the course.

I would also like to express my sincere gratitude to the people that helped me starting my journey, my former lecturers and supervisors Professor Mahamod Ismail (UKM) and Ir. Muhammad@Yusoff Ibrahim (UiTM), former lecturer Professor Azah Mohamed (UKM) and former manager from Hitachi Mr. Norzalahuddin Ibrahim. These excellent 'teacher' have always giving me valuable advices and supports every time in need.

I must also thank Mr. Shumpei Fuse, Mr. Yuki Inoue, Mr. Keizo Cho, Mr. Daisuke Uchida and Mr. Kenta Abe. Although I didn't really know them in personal, I learn a lot from their invaluable papers and researches that really help me in understand and deepen my knowledge in this field especially when everything was twice harder since I am not very good in Japanese.

A very special thanks and gratitude to my one and always tutor, Mr. Takuya Okura for all the helps, in study and in life while I was here in Arai Laboratory. Not to forget to all the secretaries in Arai Laboratory, Mrs. Terashima, Mrs. Harada and Mrs. Takahashi for their kindly support. I would also like to thank all the member of Arai Laboratory, past or present, for all the lovely memories while I was here. I wish I can list down all your names and much more all your quirky moments that always makes me felt alive but there's not going to be enough papers for all that. So from the bottom of my heart, I sincerely thank all of you.

My special Spicy Club members, Mr. Shen Wang and Mr. Thomas Basikolo, I did it guys. Thank you for your encouragements, comments, advices and even jokes but most of all for always be there for me. I don't think I could do it without you guys and I am very glad that I have you guys with me throughout this journey. Let's always keep in touch and never forget this special time that we shared together.

Although I was surrounded by handsome boyfriends, I am very grateful that I have my girlfriends to take my stress off. To my bff Hsu, I will miss our session in the café as much as I already missed Ana Morice. I pray we will have the opportunity in the future to meet again, the three of us. To GengMenawan, Ria, Kirin and Wani, I always waited every Friday for our 'joushikai' because that was the most awesome time of the week. Thanks for all the gossips and foods. To Chah and Beep, thank you

for all the helps much more for being my sisters. I know I can always count on you even now. To Lan, I am sad we couldn't spend much time together. I was so happy when you come to Arai Laboratory because I always wanted a girlfriend in the lab. I will miss you so let's keep in touch. And good luck in your study. Not to forget my special thanks to Linda for our chat on almost on anything. Knowing that I can always talk to you really keeps me sane during my lonely time.

And last but not least, to my forever bff, Yam, Wawa and Cikmah, I am happy that although we are so far away now, we never lost in touch. With all the changes in our lives, you are always, always there for me. I am blessed to have you all as my friends whom I already consider as my own family. And not to forget another family member, Ika mummy Amni, you know how much I love you for being who you are.

Have faith in what you do and you'll make it through.

Roha
9th Dec 2015
Yokohama, Japan

REFERENCES

[1] T. Cisco, "Cisco Visual Networking Index : Global Mobile Data Traffic Forecast Update , 2014 – 2019," *Growth Lakeland*, 2015. [Online]. Available: http://www.cisco.com/en/US/solutions/collateral/ns341/ns525/ns537/ns705/ns827/white_paper_c11-520862.html.

[2] M. Matthaiou, A. M. Sayeed, and J. A. Nossek, "Maximizing LoS MIMO capacity using reconfigurable antenna arrays," in *International ITG Workshop on Smart Antennas (WSA2010)*, 2010, pp. 14–19.

[3] B. T. Quist and M. A. Jensen, "Optimal Antenna Radiation Characteristics for Diversity and MIMO Systems," *IEEE Trans. Antennas Propag.*, vol. 57, no. 11, pp. 3474–3481, Nov. 2009.

[4] A. M. Sayeed and V. Raghavan, "Maximizing MIMO Capacity in Sparse Multipath With Reconfigurable Antenna Arrays," *IEEE J. Sel. Top. Signal Process.*, vol. 1, no. 1, pp. 156–166, Jun. 2007.

[5] N. K. Das, T. Inoue, T. Taniguchi, and Y. Karasawa, "An experiment on MIMO system having three orthogonal polarization diversity branches in multipath-rich environment," *IEEE 60th Veh. Technol. Conf.*, vol. 2, no. 1, pp. 1528–1532, 2004.

[6] C. Y. Chiu, J. B. Yan, and R. D. Murch, "Compact Three-Port Orthogonally Polarized MIMO Antennas," *IEEE Antennas Wirel. Propag. Lett.*, vol. 6, pp. 619–622, Dec. 2007.

[7] Freescale, "Long Term Evolution Protocol Overview," *White Pap.*, pp. 1–21, Oct. 2008.

[8] M. Kottkamp, A. Roessler, and J. Schlienz, "LTE-Advanced Technology Introduction," *White Pap.*, pp. 1–41, Aug. 2012.

[9] S. S. Sahoo, M. K. Hota, and K. K. Barik, "5G Network a New Look into the Future : Beyond all Generation Networks," *Am. J. Syst. Softw.*, vol. 2, no. 4, pp. 108–112, 2014.

[10] Qualcomm Technologies, "5G - Vision for the next generation of connectivity," *White Pap.*, pp. 1–16, Mar. 2015.

[11] S. Schindler, "Introduction to MIMO: Application Note," *Rohde Schwarz White Pap.*, pp. 1–23, Jul. 2009.

[12] K. Raoof, M.-A. Khalighi, and N. Prayongpun, "MIMO Systems: Principles, Iterative Techniques, and advanced Polarization," 2007.

[13] Huawei Technologies, "WLAN MIMO: Technical Whitepaper," *Whitepaper*, no. 1, pp. 1–13, Sep. 2012.

[14] N. Chiurtu, B. Rimoldi, and E. Telatar, "On Capacity of Multi-antenna Gaussian Channels," in *IEEE International Symposium on Information Theory (ISIT2001)*,

2001, p. 53.

[15] G. J. Foschini, “Layered space-time architecture for wireless communication in a fading environment when using multi-element antennas,” *Bell Labs Tech. J.*, vol. 1, no. 2, pp. 41–59, 1996.

[16] V. Tarokh, N. Seshadri, and A. R. Calderbank, “Space-time codes for high data rate wireless communication: performance criterion and code construction,” *IEEE Trans. Inf. Theory*, vol. 44, no. 2, pp. 744–765, Mar. 1998.

[17] P. W. Wolniansky, G. J. Foschini, G. D. Golden, and R. A. Valenzuela, “V-BLAST: an architecture for realizing very high data rates over the rich-scattering wireless channel,” in *International Symposium on Signals, Systems, and Electronics (URSI1998)*, 1998, pp. 295 – 300.

[18] Mathuranathan Viswanathan, “Simulation of Digital Communication Systems Using Matlab.” [Online]. Available: http://www.gaussianwaves.com/2008/04/channel-capacity/.

[19] S. Schwarz, R. W. H. Jr, and M. Rupp, “Single-user MIMO versus multi-user MIMO in distributed antenna systems with limited feedback,” *EURASIP J. Adv. Signal Process.*, vol. 54, no. 1, pp. 1–20, Mar. 2013.

[20] A. Bayesteh and A. K. Khandani, “On the User Selection for MIMO Broadcast Channels,” *IEEE Trans. Inf. Theory*, vol. 54, no. 3, Mar. 2008.

[21] F. Boccardi and H. Huang, “A Near-Optimum Technique using Linear Precoding for the MIMO Broadcast Channel,” *IEEE Int. Conf. Acoust. Speech Signal Process.*, vol. 3, no. 3, pp. III–17–III–20, Apr. 2007.

[22] GaussianWaves, “MIMO – Diversity and Spatial Multiplexing.” [Online]. Available: http://www.gaussianwaves.com/2014/08/mimo-diversity-and-spatial-multiplexing/.

[23] S.M. Alamouti, “A Simple Transmit Diversity Technique for Wireless Communications,” *IEEE J. Sel. Areas Commun.*, vol. 16, no. 8, pp. 1451–1458, Oct. 1998.

[24] GaussianWaves, “Characterizing a MIMO channel – Channel State Information (CSI) and Condition number.” [Online]. Available: http://www.gaussianwaves.com/2014/08/characterizing-a-mimo-channel/.

[25] Wikipedia, “Channel State Information.” [Online]. Available: https://en.wikipedia.org/wiki/Channel_state_information.

[26] Ian Poole, “Antenna Beamforming.” [Online]. Available: http://www.radio-electronics.com/info/antennas/mimo/antenna-beamforming.php.

[27] E. Telatar, “Capacity of multi-antenna Gaussian channels,” *Eur. Trans. Telecommun.*, vol. 10, no. 6, pp. 585–595, Nov. 1999.

[28] G. J. Foschini and M. J. Gans, “On Limits of Wireless Communications in a Fading Environment when Using Multiple Antennas,” *Wirel. Pers. Commun.*, vol. 6, no. 3, pp. 311–335, Mar. 1998.

[29] G. D. Golden, G. J. Foschini, R. A. Valenzuela, and P. W. Wolniansky, “Detection algorithm and initial laboratory results using V-BLAST space-time communication architecture,” *Electron. Lett.*, vol. 35, no. 1, pp. 14–16, Jan. 1999.

[30] G. G. Raleigh and V. K. Jones, “Multivariate modulation and coding for wireless communication,” *IEEE J. Sel. Areas Commun.*, vol. 17, no. 5, pp. 851–866, May 1999.

[31] W. C. Jakes, *Microwave Mobile Communications*. Wiley-IEEE Press, 1998.

[32] H. Hashemi, "The indoor radio propagation channel," *Proceeding IEEE*, vol. 81, no. 7, pp. 943–968, Jul. 1993.

[33] M.-A. Khalighi, J. M. Brossier, G. Jourdain, and K. Raoof, "Water filling capacity of Rayleigh MIMO channels," in *IEEE 12th International Symposium on Personal, Indoor and Mobile Radio Communications (PIMRC2001)*, 2001, vol. 1, p. A–155 – A–158.

[34] M.-A. Khalighi, K. Raoof, and G. Jourdain, "Capacity of Wireless Communication Systems Employing Antenna Arrays , a Tutorial Study," *Wirel. Pers. Commun.*, vol. 23, no. 3, pp. 321–352, 2002.

[35] G. G. Raleigh and J. M. Cioffi, "Spatio-temporal coding for wireless communication," *IEEE Trans. Commun.*, vol. 46, no. 3, pp. 357–366, Mar. 1998.

[36] T. L. Marzetta and B. M. Hochwald, "Capacity of a mobile multiple-antenna communication link in Rayleigh flat fading," *IEEE Trans. Inf. Theory*, vol. 45, no. 1, pp. 139–157, Jan. 1999.

[37] L. Zheng and D. N. C. Tse, "Communication on the Grassmann Manifold: a geometric approach to the noncoherent multiple-antenna channel," *IEEE Trans. Inf. Theory*, vol. 48, no. 2, pp. 359–383, Feb. 2002.

[38] C. He, X. Chen, Z. Wang, and W. Su, "On the performance of MIMO RFID backscattering channels," *EURASIP J. Wirel. Commun. Netw.*, pp. 1–15, Nov. 2012.

[39] I. F. Akyildiz, Weilian Su, Y. Sankarasubramaniam, and E. Cayirci, "A Survey on Sensor Networks," *IEEE Commun. Mag.*, vol. 40, no. 8, pp. 102 – 114, 2002.

[40] C. Chong and S. Kumar, "Sensor networks: Evolution, opportunities, and challenges," *Proceeding IEEE*, vol. 91, no. 8, pp. 1247–1256, Aug. 2003.

[41] J. Burdin and J. Dunyak, "Cohesion of wireless sensor networks with MIMO communications," in *IEEE Proceedings of SoutheastCon*, 2005, pp. 547 – 551.

[42] Shuguang Cui, A. J. Goldsmith, and A. Bahai, "Energy-efficiency of MIMO and cooperative MIMO techniques in sensor networks," *IEEE J. Sel. Areas Commun.*, vol. 22, no. 6, pp. 1089 – 1098, Aug. 2004.

[43] Aruba Networks, "Next-Generation Wireless Mesh Networks," *White Pap.*, pp. 1–14, Mar. 2001.

[44] R. Bhatia and L. Li, "Throughput Optimization of Wireless Mesh Networks with MIMO Links," in *IEEE 26th International Conference on Computer Communications (INFOCOM 2007)*, 2007, pp. 2326–2330.

[45] K. Cho and Y. Inoue, "Influence of cross-polarization characteristics on indoor MIMO performance using a dual-polarized base station antenna," in *IEEE International Symposium on Antennas and Propagation (APSURSI2010)*, 2010, pp. 1–4.

[46] D. Sugimura, M. Arai, K. Sakaguchi, K. Araki, and T. Sotoyama, "A study on beam tilt angle of base station antennas for Base Station Cooperation systems," in *IEEE International Symposium on Personal, Indoor and Mobile Radio Communications (PIMRC2011)*, 2011, pp. 2374–2378.

[47] P. Wang, H. Wang, L. Ping, and X. Lin, "On the Capacity of MIMO Cellular Systems with Base Station Cooperation," *IEEE Trans. Wirel. Commun.*, vol. 10, no. 11, pp. 3720–3731, Nov. 2011.

[48] H. Arai, K. Abe, N. Takemura, and T. Mitsui, "Dual-polarized switched beam antenna with variable phase shifter," in *International Workshop on Antenna Technology (iWAT2013)*, 2013, vol. 2, no. 1, pp. 19–22.

[49] C. B. Dietrich, K. Dietze, J. R. Nealy, and W. L. Stutzman, "Spatial, polarization, and pattern diversity for wireless handheld terminals," *IEEE Trans. Antennas Propag.*, vol. 49, no. 9, pp. 1271–1281, Sep. 2001.

[50] N. Honma, K. Nishimori, Y. Takatori, A. Ohta, and S. Kubota, "Proposal of compact MIMO terminal antenna employing Yagi-Uda array with common director elements," in *IEEE International Symposium on Antennas and Propagation Society*, 2007, pp. 2405–2408.

[51] P. Kyritsi, D. C. Cox, R. a. Valenzuela, and P. W. Wolniansky, "Effect of antenna polarization on the capacity of a multiple element system in an indoor environment," *IEEE J. Sel. Areas Commun.*, vol. 20, no. 6, pp. 1227–1239, Aug. 2002.

[52] P. Y. Qin, Y. J. Guo, and C. H. Liang, "Effect of Antenna Polarization Diversity on MIMO System Capacity," *IEEE Antennas Wirel. Propag. Lett.*, vol. 9, pp. 1092–1095, Nov. 2010.

[53] D. Uchida, "Multi-Antenna Systems Communicating Through Suitable Propagation paths," Yokohama National University, 2011.

[54] K. Miyashita, T. Nishimura, T. Ohgane, Y. Ogawa, Y. Takatori, and K. Cho, "High data-rate transmission with eigenbeam-space division multiplexing (E-SDM) in a MIMO channel," *IEEE 56th Proc. Veh. Technol. Conf.*, vol. 3, pp. 1302–1306, 2002.

[55] H. Arai, "Measurement of Mobile Antenna Systems," Second Edi., Artech House, 2013, p. 27.

[56] Hyper Physics, "Fresnel Equation." [Online]. Available: http://hyperphysics.phy-astr.gsu.edu/hbase/phyopt/freseq.html.

[57] EEM Inc., "EEM-RTM Manual." [Online]. Available: http://www.e-em.co.jp/rtm/eem_rtm.htm.

[58] J. W. Wallace and M. A. Jensen, "Mutual Coupling in MIMO Wireless Systems: A Rigorous Network Theory Analysis," *IEEE Trans. Wirel. Commun.*, vol. 3, no. 4, pp. 1317–1325, Jul. 2004.

[59] J. Sarrazin, Y. Mahé, S. Avrillon, and S. Toutain, "Investigation on Cavity/Slot Antennas for Diversity and MIMO Systems: The Example of a Three-Port Antenna," *IEEE Antennas Wirel. Propag. Lett.*, vol. 7, pp. 414–417, May 2008.

[60] B. N. Getu and J. B. Andersen, "The MIMO cube - a compact MIMO antenna," *IEEE Trans. Wirel. Commun.*, vol. 4, no. 3, pp. 1136–1141, 2005.

[61] M. R. Andrews, P. P. Mitra, and R. DeCarvalho, "Tripling the capacity of wireless communications using electromagnetic polarization," *Nature*, vol. 409, no. 1, pp. 316–318, Jan. 2001.

[62] D. Uchida, H. Arai, Y. Inoue, and K. Cho, "A low-profile dual-polarized directional antenna for enhancing channel capacity in indoor MIMO systems," *IEICE Trans. Commun.*, vol. E93-B, no. 1, pp. 2570–2577, 2010.

[63] A. Suyama, D. Uchida, H. Arai, Y. Inoue, and K. Cho, "A Dual Polarization 8-port MIMO Antenna with Dipole and Slot Antennas," *IEICE Tech. Rep.*, vol. AP2008–234, pp. 113–116, Mar. 2009.

[64] B. Rohani, S. Fuse, H. Arai, Y. Inoue, and K. Cho, "A Low Profile Four-Way Directional

Antenna with Dual Polarization," *J. Electromagn. Anal. Appl.*, vol. 7, no. May, pp. 178–187, May 2015.

[65] Antenna Theory, "The Monopole Antenna." [Online]. Available: http://www.antenna-theory.com/antennas/monopole.php.

[66] I. Stevanovic, A. Skrivervik, and J. R. Mosig, "Smart Antenna Systems for Mobile Communications," Jan. 2003.

[67] R. Jain, S. Katiyar, and N. Agrawal, "Smart Antenna for Cellular Mobile Communication," *VSRD Int. J. Electr. Electron. Commun. Eng.*, vol. 1, no. 9, pp. 530–541, 2011.

[68] C. Peixeiro, "Microstrip patch antennas: An historical perspective of the development," in *SBMO/IEEE MTT-S International Microwave and Optoelectronics Conference (IMOC 2011)*, 2011, pp. 684–688.

[69] Antenna Theory, "Rectangular Microstrip Antenna." [Online]. Available: http://www.antenna-theory.com/antennas/patches/antenna.php.

[70] W. Yang and J. Zhou, "A single layer wideband low profile tooth-like-slot microstrip patch antenna fed by inset microstrip line," *Int. Work. Antenna Technol.*, vol. 1, no. c, pp. 248–251, Mar. 2013.

[71] S. Weigand, G. H. Huff, K. H. Pan, and J. T. Bernhard, "Analysis and design of broad-band single-layer rectangular U-slot microstrip patch antennas," *IEEE Trans. Antennas Propag.*, vol. 51, no. 3, pp. 457–468, Mar. 2003.

[72] T. Huynh and K.-F. Lee, "Single-layer single-patch wideband microstrip antenna," *Electron. Lett.*, vol. 31, no. 16, p. 1310, 1995.

[73] H. F. Pues and A. R. Van de Capelle, "An impedance-matching technique for increasing the bandwidth of microstrip antennas," *Antennas Propagation, IEEE Trans.*, vol. 37, no. 11, pp. 1345–1354, 1989.

[74] C. Barth, K. Van Cackenberghe, and K. Sarabandi, "An embedded broadband impedance matching technique for microstrip patch antennas," in *IEEE International Symposium of Antennas and Propagation Society*, 2005, vol. 2B, pp. 214–217.

PUBLICATIONS

Journal Paper

1. Rohani Bakar, Shumpei Fuse, Hiroyuki Arai, Yuki Inoue, Keizo Cho, "A Low Profile Four-Way Directional Antenna with Dual Polarization," no. 7, pp. 178-187, Journal of Electromagnetic Analysis and Application, May 2015.

International Conference

1. 2013 Asia-Pacific Microwave Conference (APMC2013), Coex, Seoul, Korea, 5~8 Nov 2013, (Attending).
2. Rohani Bakar, Hiroyuki Arai, "Three Layers Switched Multibeam Antenna with Dual-Polarization", pp. 167-168, 2014 IEEE International Workshop on Electromagnetics (iWEM2014), Hokkaido University, Sapporo, 4-6 August 2014.
3. Rohani Bakar, Hiroyuki Arai, "A Low Profile Directional Antenna with Dual Polarization for Channel Capacity Enhancement",2015 IEEE International RF and Microwave Conference (RFM2015), Kuching, Malaysia, 14-16 Dec 2015.

IEICE Technical Report

1. Rohani Bakar, Hiroyuki Arai, “Dual Polarized Switched Multi-Beam Antenna”, 2013 IEICE Society Conference, Fukuoka Institute of Technology, Fukuoka, 17~20 Sept 2013.
2. Rohani Bakar, Hiroyuki Arai, “Dual Polarized Switched Multi-Beam Antenna”, 2014 IEICE General Conference, Niigata University, Niigata, 18~21 March 2014.
3. Rohani Bakar, Hiroyuki Arai, “Enhancing 4 x 4 MIMO Channel Capacity by Dual Polarized Directional Antenna”, 2016 IEICE General Conference, Kyushu University, 15~18 March 2016.